Immune regulation in *Plasmodium berghei* ANKA infected mice either lacking type I interferon signalling or mimicking malaria tolerance

DISSERTATION

zur

Erlangung des Doktorgrades (Dr. rer.nat.)

der

Mathematisch-Naturwissenschaftlichen Fakultat

der

Rheinischen Friedrich-Wilhelms-Universität Bonn
Fach Molekulare Biomedizin

Vorgelegt von

Patricia Jebett Korir

aus Nakuru Kenya

Bonn, Januar 2017

Angefertigt mit Genehmigung der Mathematisch-Naturwissenschaftlichen Fakultät der Rheinischen Friedrich-Wilhelms-Universität Bonn.

1. Gutachter Prof. Dr. med. Achim Hörauf

2. Gutachter Prof. Dr. rer. nat. Sven Burgdorf

Tag der Promotion: 17 Januar 2017

Erscheinungsjahr: 2017

Gedruckt mit Unterstutzung des Deutschen Akademischen Austauschdienstes.

SUMMARY

Malaria is a disease caused by *Plasmodium* parasites and transmitted by female *Anopheles* mosquitoes. Children under the age of five, pregnant women and none-immune individuals are at risk of developing severe malaria such as cerebral malaria (CM), caused only by *P. falciparum*. During *Plasmodium* infection, the parasite and its products are recognised by pattern recognition receptors on myeloid cells and dendritic cells (DCs) in the spleen resulting in the secretion of pro and anti- inflammatory cytokines, which can drive the disease to either a severe outcome or induce tolerance.

Among the secreted cytokines are the type I interferons (IFNs), which signal via the heterodimeric interferon alpha receptor (Ifnar). In the first part of this thesis we show that type I IFN signalling via the receptor on myeloid cells plays a crucial role in the mediation of pathology during infection with *P. berghei* ANKA. Mice that lack the receptor on myeloid cells (LysM^{Cre}*Ifnar1*$^{fl/fl}$) had a phenotype comparable to the full (knockout) ko mice (*Ifnar1*$^{-/-}$). Upon PbA-infection, these mice showed a stable blood brain barrier, had very few cells (such as CD8^{+} T cells, CD4^{+} T cells NK cells and Ly6C^{hi} inflammatory monocytes) present in their brains and low inflammatory mediators in comparison to the wild type (WT) mice and the mice that lack the receptor on DCs (CD11c^{Cre}*Ifnar1*$^{fl/fl}$). Although these mice were protected from ECM, they were able to recognise endogenous parasite-specific antigen and transgenic antigen and to mount a specific cytolytic response in the spleen. Importantly, these effector cytotoxic CD8^{+} T cells were retained/arrested in the spleen. In the absence of Ifnar on myeloid cells or on all cells, the mice had less Ly6C^{hi} inflammatory monocytes in their spleens.

Importantly, the protected mice contained a special subset of macrophages showing an immune-regulatory phenotype. We found in spleens of PbA-infected Ifnar ko alternatively activated macrophages (M2), which expressed *YM-1*, *Relm α / Fizz* and *Arg-1* and produced IL-10 and arginase. However, mice that lacked the receptor specifically on myeloid cells contained very low amount of these cells in their spleens but they had high levels of IL-10 and IL-6, which could have been produced by another form of suppressive/regulatory macrophages. We conclude that these cells contributed to creating a suppressive milieu in the spleens of the protected mice, resulting in retention of immune cells in the spleen. The change in the macrophage phenotype to a suppressive/immunoregulatory phenotype occurred without altering the Th-1 response.

In the second part of this thesis we analysed the changes in the immune response after infection with elevated parasite dose, which resulted in protection from ECM, thereby mimicking malaria tolerance experimentally. This was mediated by complete blockage of IFNγ production and partial suppression of the Th1 response. Also the high parasite dose resulted in suppression of the expression of MHC class II on Ly6C^{hi} inflammatory monocytes. Using mice that are genetically deficient of IL-10 on myeloid cells, we showed that the IL-10 production by myeloid cells had a crucial role in the protection of mice from ECM in this malaria tolerance model. In conclusion; our results showed that during infection with *Plasmodium berghei* ANKA, type I IFN inflammatory signalling and production of IL-10 by myeloid cells, mostly macrophages and monocytes, are crucial in driving the disease to either the severe outcome that is observed in C57BL/6 or tolerance that is observed in the high dose infected mice.

ZUSAMMENFASSUNG

Malaria ist eine Krankheit, die durch eine Infektion mit Parasiten der Gattung *Plasmodium* entsteht und durch weibliche *Anopheles* Mücken übertragen wird. Besonders Kinder unter 5 Jahren, schwangere Frauen und nicht-immune Reisende haben ein hohes Risiko, eine schwere Malaria zu entwickeln, wie zum Beispiel zerebrale Malaria (ZM), die nur durch *P. falciparum* verursacht wird. Während einer *Plasmodium*-Infektion wird der Parasit selbst und von ihm ausgeschiedene Produkte in der Milz durch sogenannte Mustererkennungsrezeptoren auf myeloiden und dendritischen Zellen (DZs) erkannt und lösen in diesen Zellen die Ausscheidung von verschiedenen pro- und anti-entzündlichen Mediatoren aus, die entweder eine schwere Verlaufsform der Krankheit begünstigen oder Immuntoleranz induzieren können. Unter den freigesetzten Zytokinen befinden sich Typ I Interferone (IFNs), die an den heterodimeren Interferon alpha Rezeptor (Ifnar) binden und weitere Schritte der Immunantwort induzieren. Im ersten Teil dieser Arbeit konnten wir zeigen, dass die Typ I IFN Signalkaskade über den Rezeptor auf myeloiden Zellen eine wichtige Rolle in der Pathologie einer *P. berghei* ANKA-Infektion (PbA) spielt, die ein akzeptiertes Mausmodell für die Entstehung von ZM im Menschen darstellt (experimentelle ZM (EZM)). Mäuse, denen der IFN alpha Rezeptor auf myeloiden Zellen fehlt (LysM^{Cre}*Ifnar1*$^{fl/fl}$), zeigen einen ähnlichen Krankheitsverlauf wie Tiere, denen der Rezeptor auf allen Zellen fehlt (*Ifnar1*$^{-/-}$). Nach einer PbA-Infektion zeigten diese Tiere im Vergleich zu Wildtyp (WT) Mäusen und Mäusen, denen der Rezeptor auf Dendritischen Zellen fehlt (CD11c^{Cre}*Ifnar1*$^{fl/fl}$), eine intakte Blut-Hirn-Schranke und geringe Mengen an periphere Immunzellen (wie etwa CD8^{+} T Zellen, CD4^{+} T Zellen, NK Zellen und Ly6C^{hi} inflammatorische Monozyten) und Entzündungsmarkern im Gehirn. Trotz ihres Schutzes vor EZM konnte in LysM^{Cre}*Ifnar1*$^{fl/fl}$ Mäusen endogenes parasiten-spezifisches und transgenes Antigen erkannt werden und eine spezifische zytolytische Immunantwort in der Milz gebildet werden. Interessanterweise verblieben die zytotoxischen CD8^{+} T Zellen aber in der Milz und migrierten nicht ins Gehirn der Tiere. Milzen aus Mäusen, denen Ifnar auf myeloiden oder auf allen Zellen fehlte, hatten allerdings eine geringere Anzahl an Ly6C^{hi} inflammatorischen Monozyten. Von besonderer Bedeutung war, dass in geschützten genetisch defizienten (ko) Mäusen ein besonderer Untertyp von Makrophagen gefunden wurde, der für seine regulatorischen Eigenschaften bekannt ist. Wir konnten in Milzen der PbA-infizierten *Ifnar1*$^{-/-}$ Mäuse sogenannte alternativ aktivierte Makrophagen (M2) nachweisen, die *YM-1*, *Relm α / Fizz* und *Arg-1* exprimierten und außerdem IL-10 und Arginase produzierten. Allerdings konnten wir diese Zellen in LysM^{Cre}*Ifnar1*$^{fl/fl}$ Mäusen nur in geringer Anzahl finden, konnten dafür aber dort erhöhte Mengen an IL-10 und IL-6 nachweisen, die auch von anderen supprimierenden / regulierenden Makrophagen sekretiert werden können. Aus diesen Ergebnissen schließen wir, dass diese Zellen ein regulatorisches Milieu begünstigen, welches zum Verbleib der Immunzellen in der Milz führt. Die Th-1 Antwort nach PbA-Infektion wurde allerdings durch die Änderungen des Phänotyps der Makrophagen in eine supprimierende / regulierende Art nicht beeinflusst.

Im zweiten Teil dieser Arbeit untersuchten wir die Änderungen in der Immunantwort nach einer Infektion mit einer höheren Dosis an Parasiten, die zum Schutz vor EZM in WT Mäusen führte, was einer experimentell induzierten Malariatoleranz entspricht. Diese Toleranz konnte auf die vollständige Verhinderung der IFNγ-Produktion und eine Reduzierung der Th-1

Antwort zurückgeführt werden. Die höhere Parasiten-Dosis resultierte außerdem in einer reduzierten Expression von MHC Klasse II Molekülen auf inflammatorischen Monozyten. Mithilfen von Mäusen, deren myeloide Zellen kein IL-10 produzieren, konnten wir zeigen, dass IL-10 aus diesen Zellen eine entscheidende Rolle in diesem Malria-Toleranz-Modell zukommt. Zusammenfassend zeigen unsere Daten, dass die Signalwirkung von Typ IFN I sowie die Produktion von IL-10 durch myeloide Zellen (hauptsächlich Makrophagen und Monozyten) entscheidend sind, um den Krankheitsverlauf zu beeinflussen: entweder in Richtung einer schwerwiegenden Verlaufsform in PbA-infizierten WT Mäusen (normale Dosis) oder in Richtung einer Toleranzentwicklung nach Infektion mit einer erhöhten Parasitendosis.

List of abbreviations

µ	Micro- (10^{-6})
ACT	Artemisinin-based combination therapy
Ag	Antigen
AMM	Alternatively activated macrophages
APC	Antigen presenting cell
app.	Approximately
ATF	Activating transcription factor
BBB	Blood-brain barrier
BCP	1-bromo-3-chloropropane
BL/6	C57 BL/6 mice
BMDC	Bone-marrow derived dendritic cells
BrdU	Bromodeoxyuridine
BSA	Bovine serum ovalbumin
C	Celsius
Ca	Calcium
CCL	CC chemokine ligand
CCR	CC chemokine receptor
cDC	Conventional dndritic cells
CFSE	Carboxy fluorescein di-amino suyyinimidyl ester
CM	Cerebral malaria
CTL	Cytotoxic T lymphocyte
CXCL	CXC chemokine ligand
CXCR	CXC chemokine receptor
d	Day
DC	Dendritic cell
DMSO	dimethyl sulfoxide
DNA	Desoxyribonucleic acid
dNTP	Deoxyribonucleotide
dpi	Days post infection
e.g.	Exempli gratia (for example)
ECM	Experimental cerebral malaria
EDTA	Ethylendiamintetraacetate dehydrate
ELISA	Enzyme-linked immunosorbent assay
EMP	Erythrocyte membrane protein
et al.	Et alteres (and others)
FACS	Fluorescent activated cell sorter

FCS	Fetal calf serum
Fizz1	Found in inflammatory zone1
FOXP3	Forkhead box P3
g	Gram
GATA	Trans-acting T-cell-specific transcription factor GATA-3
hr	Hour(s)
HSTaq	HotStar Taq DNA Polymerase
i.e.	Id est (that is)
i.p.	Intraperitoneal
i.v.	Intravenous
ICAM	Intracellular adhesion molecule
IFNaR	Interferon alpha receptor (human)
Ifnar	Interferon alpha receptor (Mouse)
IFNγ	Interferon-gamma
IL	Interleukin
iRBC	Infected red blood cell
IRF	Interferon regulatory factors
ISG	Interferon stimulated genes
JAK	Janus kinase
kg	Kilogram
ko	Knock out
LT-α	Lymphotoxin-α
m	Meter, milli (10^{-3})
M	Molar
MACS	Magnetic-activated cell sorting
MCP-1	Monocyte chemo-attractant protein 1
$MgCl_2$	Magnesium chloride
MHC	Major histocompatibility complex
min	Minute(s)
MIP	Monocyte inflamatory protein
MMP	Matrix metalloproteinase
MSP	Merozoite surface protein
MyD88	Myeloid differentiation primary response gene 88 (MYD88)
n	Nano (10^{-9}); number
NaCl	Natrium chloride
NFκB	Nuclear factor kappa B
NK	Natural killer

NLR	Nucleotide-binding oligomerization domain-like receptors
NO	Nitric oxide
NOD	Nucleotide-binding oligomerization domain
OD	Optical densitiy
OVA	Ovalbumin
P.	*Plasmodium*
p.i.	Post infection
PAMP	Pathogen associated molecular pattern
PbA	*Plasmodium berghei* ANKA
PbAMA	*Plasmodium berghei* ANKA-Ama1 expressing ovalbumin (Transgenic parasite)
PBS	Phosphate buffered saline
PbTG	Transgenic strain of *Plasmodium berghei* expressing ovalbumin
PCR	Polymerase chain reaction
PfEMP-1	*Plasmodium falciparum* erythrocyte membrane protein 1
PSGL-1	P-selectin glycoprotein ligand 1
RANTES	Regulated upon activation, normal T-Cell expressed and secreted
RBC	Red blood cell
RMCBS	Rapid murine coma and behavior scale
RORγT	RAR-related orphan receptor gamma (RORγ)
rpm	Rounds per minute
RPMI	Roswell Park Memorial Insitute, cell culture medium
RT	Room temperature
sec	Second(s)
SPF	Specific pathogen free
spp.	*Species pluralis*
STAT	Signal transducer and activator of transcription
Tbet	T-box transcription factor TBX21
TCR	T cell receptor
Th	T helper
TMB	Tetramethylbenzidine
TNF	Tumor necrosis factor
T-reg	T regulatory cell
TRIF	TIR-domain-containing adapter-inducing interferon-β (TRIF)
vs.	Versus
WHO	World Health Organization
WT	Wild type
Zn	Zinc

Table of Contents

List of Figures and Tables

1 Introduction

1.1 Health burden caused by infection with *Plasmodium* parasite

Malaria is still one of the most important tropical infectious diseases of humans, infecting nearly 10% of the world population and causing one to two millions deaths, mostly of children, every year. The greatest burden of Malaria is borne by the poor and developing countries, mainly in sub-Saharan Africa. According to WHO report, in 2015, malaria transmission occurred in 95 countries, with 88% of the cases and 90% deaths occurring in Sub-Saharan African (WHO fact sheet 2016). This burden has a negative impact on the economy and social-economy of the region, as considerable amount of working days are lost due to the disease. Children under the age of 5 are the most affected in populations living in the areas of high transmission, with 70% of disease and death affecting this age group (WHO fact sheet 2016).

Malaria is a vector-borne disease caused by infection with various species of the protozoa *Plasmodium* that are transmitted to the human host by the female Anopheles mosquito. Five different *Plasmodium* species - of which *P. falciparum* is the most virulent and prevalent – cause disease in humans. Serious pathological complications such as severe malarial anemia, metabolic acidosis and cerebral malaria (CM) represent life-threatening risks of infection. CM is multi-factorial and a complex syndrome. It is assumed that CM is a consequence of immune-mediated pathology due to overwhelming inflammatory processes.

1.2 Life cycle of *Plasmodium* parasites

Plasmodium parasites are obligate intracellular blood protozoans of the phylum Apicomplexa, transmitted to vertebrates by infective bite of the female *Anopheles* mosquitoes. Four of the species infecting man are human pathogens, *P. falciparum, P. vivax, P. ovale* and *P. malariae,* while the natural host of *P. knowlesi* is the macaque monkey of Southeast Asia. Infection with *P. falciparum* results in the most severe and life threatening forms of malaria disease.

The malaria parasites require two hosts to complete their life cycle, a vertebrate for the asexual and an arthropod vector for the sexual stages. The female anopheles mosquitoes are the only vectors for the malaria parasite. When the female *Anopheles* takes a blood meal from an infected host, it can pick up gametocytes. The gametocytes exflagellate and develop into macro and microgametes, which fertilize and develop into an ookinetes (White 2014). The ookinetes migrate into the gut of the mosquito and form oocysts, which develop and burst to produce

thousands of sporozoites into the haemolymph (White 2014). The sporozoites will reach the salivary gland of the mosquito, where they develop into mature forms. These will be injected into the vertebrate during the mosquito's next blood meal, depending on *Plasmodium* species and temperatures this part of the cycle lasts 10-35 days (White 2014). During its next blood meal, the infected mosquito will inject and deposit sporozoites, which will actively invade the blood vessels, and of these only 70% manage to enter the blood circulation (Amino et al. 2006). Once in the blood vessels, the sporozoites will be transported to the liver to invade the hepatocytes. Here, the next developmental step called exo-erythrocytic schizogony occurs and results in release of mature merozoites into the blood stream upon bursting of the hepatocytes. Depending on the on the *Plasmodium* species, this takes in *P. falciparum* up to 5.5 days while this step in *P. malariae* lasts 15 days (White 2014). However, in some cases *P. ovale* and *P. vivax* can acquire an inert status known as hypnozoites, and reactivate at an unknown time to cause disease (White 2014). Once the merozoites burst out of the liver into the blood stream, they infect red blood cells (RBC) and begin the erythrocytic schizogony. The parasites will nourish on haemoglobin and develop into trophozoites, this will mature into a schizont, which contains new merozoites. Fully matured schizont will burst and release the merozoites into the blood circulation, repeating the erythrocytic cycle (White 2014). This cycle will be repeated several times and after some cycles the trophozoite will develop into gametocytes, which can be taken up by the mosquito during its blood meal.

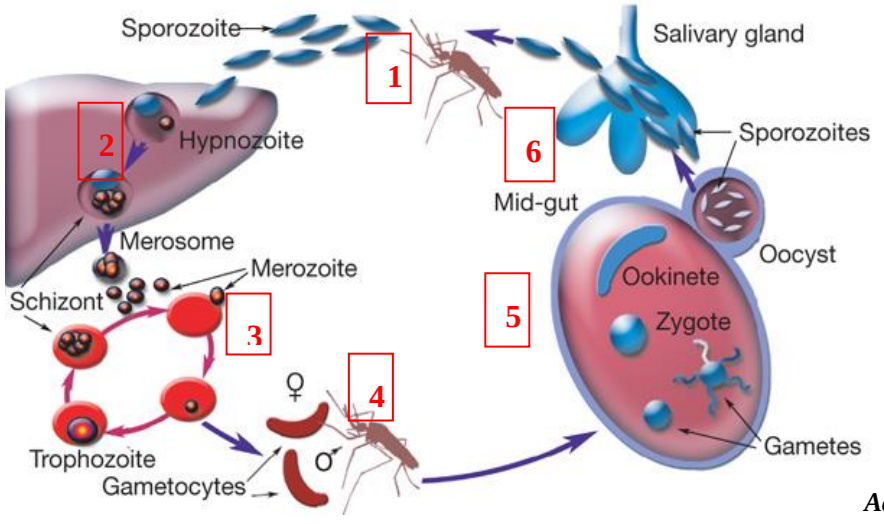

Figure 1 *Plasmodium* life cycle

(**1**) Anopheles injects sporozoites during a blood meal, (**2**) which infect hepatocytes in the liver and develop into merozoites, when mature merozoites will enter the blood circulation (**3**) and infect red blood cells. After several cycles the trophozoites develop into gametocytes, (**4**) which are taken up by the mosquito during its blood meal. (**5**) In the mosquito the gametocyte mate (sexual stage), resulting in production of sporozoites, (**6**) which move to the salivary gland and are injected into humans during the mosquitoes next blood meal.

1.3 Malaria transmission

Malaria transmission is dependent on several factors, among the important ones are the presence of a competent vector, right temperature and humidity and presence of individuals harbouring gametocytes. Transmission occurs in areas where the mosquitoes have a long lifespan and preferentially feed on humans than other animals, these characteristics makes the African vectors competent transmitters (White 2014). Malaria endemic zones are characterized as either stable or unstable, in the stable zone they are also characterised depending on parasite rates in children between the ages of 2-9 years (White 2014). These zones are divided into hypoendemic areas (parasite rates: 0-10%), mesoendemic areas (parasite rates: 10-50%), hyperendemic areas (parasite rates: 50- 75%) and holoendemic areas (parasite rates: >75%) (White 2014).

1.4 Complications due to *Plasmodium* infections

Patients suffering from malaria present with several symptoms, fever being a classical feature of the disease, headache, vomiting, general malaise and flu like symptoms. The disease is categorised into two broad groups, uncomplicated and severe complicated malaria.

1.4.1 Uncomplicated malaria

Uncomplicated malaria can be caused by any of the species that infect humans and is defined by the absence of severe complications in patients who are positive for *Plasmodium* parasites (White et al. 2014).

1.4.2 Severe malaria

Severe malaria is caused mainly by *P. falciparum* parasite and is defined as the presence of complications in patients who are positively tested for parasites and other causes for the complications can be excluded. These complications can be one or more of the following symptoms: Coma, convulsions, acidosis, hypoglycaemia, severe anaemia, pulmonary oedema, renal injury, bleeding, shock and hyperparasitemia (Gachot & Ringwald 2014; White et al. 2014). Although *P. vivax* and P. *knowlesi* can in some cases cause severe malaria, the impact is not as high as that caused by *P. falciparum*. The occurrence of severe malaria is multifactorial, with sequestration, immunopathology and endothelial dysfunction being some of the key factors that are implicated (Cunnington et al. 2013).

1.4.2.1 Cerebral malaria (CM)

CM is the severest outcome of infection with *P. falciparum* with high risk of mortality. Clinical diagnosis is based on peripheral parasitemia accompanied by unarousable coma, neurological symptoms without any other alternative cause, with scores of; <11 for with Glasgow coma scale or <3 Blantyre coma score (Gachot & Ringwald 2014). The cause of CM is multi-factorial, with parasite sequestration in the brain microvascular, inflammatory cytokines, activation of the endothelial, blood brain barrier disruption being some of the key factors proposed (Cunnington et al. 2013; Storm & Craig 2014).

1.4.3 Sequestration of parasitized red blood cells

The expression of the *P. falciparum* erythrocyte membrane protein 1(PfEMP-1) on the surface of infected RBCs (iRBCs) enables the infected cells to attach to the endothelium in order to evade the destruction of the parasitized red blood cells in the spleen. PfEMP-1 is encoded by the *var* genes, which are variant surface antigens (Storm & Craig 2014). This adherence of iRBCs is termed sequestration and is found in the brains, placenta, lungs and other organs during *P. falciparum* infection (Storm & Craig 2014). PfEMP-1 binds to ligands on the endothelial cells like ICAM-1, blocking the capillaries and resulting in hypoxia (Idro et al. 2010). Presence of sequestering parasites in the brain result in activation of the endothelium, leading to inflammatory responses, however, sequestration alone as a cause of cerebral malaria has been questioned and host immune response thought to also play a part in CM (Cunnington et al. 2013).

1.5 Immune responses towards *Plasmodium* parasites

The immune system is a complex and organised system, whose main aim is to protect the body from pathogens. A successful immune system is one that is able to recognise harmful agents and defend the body accordingly. Pathogens, toxins, cancer cells and allergens are some of the triggers for an immune response. The first line of defence is made up of physical and chemical barriers. Once pathogens have successfully penetrated these barriers, the second line of defence is the innate immunity, which is comprised mainly of phagocytic cells and those which are able to respond rapidly to the pathogens due to pattern recognition receptors. This does not require previous knowledge of the invading organism and hence the response is almost immediate. The innate system will try and control the infection until the adoptive immunity is activated. The adoptive immunity is very specific and is also the source of immune memory, for initiating a faster response in case of re-infection. The innate and adoptive immune responses are carried

out by leukocytes and products of the leukocytes. Leukocytes originate from the bone marrow from the pluripotent hematopoietic stem cell and develop into lymphocytes or myeloid cells. The myeloid cells develop from the common myeloid progenitor, these are the macrophages, monocytes, dendritic cells, neutrophils, eosinophils, basophils and mast cells. The lymphocytes develop from the common lymphoid progenitor into: natural killer cells, B- lymphocytes or T-lymphocytes (Murphy et al. 2012) and allow the specific elimination of pathogens.

1.5.1 The spleen in malaria

Once the malaria- causing *Plasmodium* parasites have successfully managed to evade the immune response in the liver, the parasites reach by taking up residence in the erythrocytes the next step of their life cycle: the so-called blood stage marks the entry into a systemic infection and involves mainly the spleen. Located on the upper left side of the abdomen, the spleen is important for the removal of senescent red blood cells, recycling of haem, clearing blood-borne pathogens and the initiation of immune response against blood pathogens (Murphy et al. 2012). Structurally the spleen has a unique architecture, it is made up of the white pulp, which is separated from the red pulp by the marginal zone. The red pulp is mostly composed of red pulp macrophages (RPM), which have a role in the filtration of the blood to remove pathogens, as well aged RBCs for iron recycling (Mebius & Kraal 2005; Davies et al. 2013). The marginal zone separates the white pulp from the red pulp, and it is composed of specialized cells such as marginal zone macrophages, marginal metallophillic macrophages, marginal zone B cells, immature DCs and few T cell (Mebius & Kraal 2005). The white pulp has an inner layer, which is populated with T cells and an outer layer with B cells. Immature DCs and B cells in the marginal zone filter for blood pathogens and antigens, after which they migrate to the T cell zone, where they present Ag to the T cells and initiate the adoptive immunity (Mebius & Kraal 2005). Since *Plasmodium* parasites infect the red blood cells, the spleen is therefore the most important organ in the immune response against these parasites. During the process of blood filtration and haem recycling, the red pulp macrophages are among the early immune cells to interact with the parasite (Yadava et al. 1996).

1.5.2 Recognition *of Plasmodium* parasite by pattern recognition receptors (PRRs)

PRRs on the surface, cytosol and endosome of innate cells recognise antigen, resulting in signalling via the recognition pathways, leading to the production of cytokines, chemokines and other signals. When blood flows into the spleen loaded with infected red blood cells (iRBCs), pathogen associated molecular patterns (PAMPs), parasites ligands are sensed by the

(PRR) being expressed on the surface of macrophage and DCs, majorly in the spleen (Gazzinelli et al. 2014). TLRs are key sensors in malaria, since in *P. berghei ANKA* infection, a well-established and accepted experimental model of CM (ECM) - using genetically deficient mice, Coban et al. demonstrated the role of TLR2 and TLR9 involvement in the pathogenesis of ECM via TLR-MYD88 pathway (Coban et al. 2007). *Plasmodium*-derived gylycosyl-phosylphatidylinositol (GPI) is sensed by TLR1/TLR2 or TLR2/TLR6 on macrophages and dendritic cells, resulting in production of pro-inflammatory cytokines TNF, IL-1β, IL-12 and nitric oxide (NO) (Schofield & Hackett 1993; Schofield & Grau 2005; Zhu et al. 2011).

Hemozoin crystals are a by-product occurring during the degradation of haemoglobin by the parasite and are recognised –in a complex coupled with parasitic DNA -by the endosomal TLR-9 and NOD-like receptors NLRP3 and NLRP12 in the cytoplasm (Parroche et al. 2007; Gazzinelli et al. 2014). The *Plasmodium* AT-rich genome is recognised by an unknown cytosolic sensor and signals via stimulator of IFN genes (STING) –IRF3-IRF7 pathway, inducing the production of type I IFN (Sharma et al. 2011).

Haem, microvesicals and urate crystals are recognized as danger associates molecular patterns (DAMPs); haem is sensed by TLR4, while urate and microvesicals are sensed by cytosolic sensors (Gazzinelli et al. 2014). These sensing pathways results in production of massive amounts of type I IFNs, IL-1β and other cytokines, in order to eliminate the infection, thus intended to be beneficial, but harbour the risk of overwhelming inflammation, therefore may also be detrimental.

1.6 Studying immune responses leading to CM with the help of experimental models: experimental cerebral malaria (ECM)

To enable an effective study of the basis of cerebral malaria, animal models are valuable and necessary due to ethical limitations in infected humans. There is plenty of valuable information that has been learnt from these models, even if ECM differs in some aspects from human CM. In a review by Hunt and Grau, comparing similarities in cerebral malaria between human and mouse, several outcomes were found to be comparable: presence of neurological symptoms, inflammatory changes in the brain of infected individuals, increased expression of pro-inflammatory cytokines and some changes of biochemical and metabolic markers (Hunt & Grau 2003). There are some factors that are still under investigations, for example, whether leukocytes play a role in hCM or whether parasite sequestration in the mouse model is as important as in humans (Hunt & Grau 2003). Nevertheless, the short and rapid breeding cycle

of the rodent model, and their ability to mimic CM features, makes them suitable for studying the immune process and pathology of ECM.

During ECM, different cells, cytokines and chemokines are involved, which are assumed /partically proven to drive the disease to the severe outcome. Next to $CD8^+$T cells, which are the major effectors of ECM pathology, also DCs, macrophages, NK cells and $CD4^+$ T cells have been shown to play key roles in driving the disease to the severe outcome (Villegas-Mendez et al. 2012; Lundie et al. 2008; Hansen et al. 2007; Schumak et al. 2015; Schofield & Grau 2005; Piva et al. 2012).

1.6.1 Antigen-presenting cells in *Plasmodium* infection

DCs are the most important APCs, they ingest pathogens and degrade them into peptides, which they then present via the MHC molecules to T cells. DCs are largely grouped into two groups, plasmacytoid DC (pDC) and conventional DCs (cDC). The cDCs are further characterized into $CD8\alpha^+$DCs and $CD8\alpha^{neg}$DCs. The main role of cDCs is presentation of Ag to T cells and priming them, which has been elegantly shown for the infection with *P. chaubaudi* and *P. berghei,* (Lundie et al. 2008; deWalick et al. 2007; Sponaas et al. 2006), while pDCs are the major interferon producers (Murphy et al. 2012:77).

Although pDCs produced more type I IFNs than cDCs during *P.berghei* infection, their role in ECM was ruled out as their deletion did not protect mice from development of ECM (deWalick et al. 2007; Piva et al. 2012). In *P. chabaudi* infection, both $CD8\alpha^+$DCs and $CD8\alpha^{neg}$DCs were able to present Ag to $CD4^+$T cells, as the disease progressed, the $CD8\alpha^{neg}$DCs became more efficient presenters than $CD8\alpha^+$DCs (Sponaas et al. 2006). Not only are DC important in Ag presentation during PbA infection, they also induce production of IFNγ by activated $CD4^+$ and $CD8^+$ T cells (deWalick et al. 2007; Lundie et al. 2008; Sponaas et al. 2006; Piva et al. 2012). The key role of $CD8\alpha^+$DCs in pathogenesis of ECM is via the priming of the effectors $CD8\alpha^+$T cell (Lundie et al. 2008), the deletion of cDCs in mice resulted high survival and ECM protection (deWalick et al. 2007).

Macrophages originate from the bone marrow as blood monocytes and differentiate in the tissue into resident macrophages, depending on the tissue where they are found, they have different names (Davies et al. 2013). In the liver, macrophages known as Kupffer cells are present, in the brain we find microglia and alveolar macrophages are found in the lungs (Davies et al. 2013; Murray & Wynn 2011). In the spleen, diverse subtypes of macrophages are named depending on their function or specific localization. The microglia, unlike most

macrophages, do not originate from the blood monocytes, but are formed during the early embryonic formation from primitive cells (Ginhoux et al. 2010). Macrophages have several roles in the induction of specific immune response, since they phagocytise and kill pathogens, they recognise pathogens via immune sensing PRR, through which they detected Ag and produce chemokines and cytokines, and they are also able to act as antigen presenting cells (Franken et al. 2016; Davies et al. 2013; Murray & Wynn 2011).

Monocytes can be identified as $Ly6C^{low}CX_3CR1^{hi}$ and $Ly6C^{hi}CX_3CR1^{low}$, and exist as either patrolling or inflammatory monocytes, respectively (Franken et al. 2016; Shi & Pamer 2011). The $Ly6C^{hi}$ inflammatory monocytes express the chemokine receptor CCR2 and are recruited in a CCR2/CCL2 dependent manner to the site of inflammation (Shi & Pamer 2011). Migration and recruitment of monocytes is not limited to CCR2, other receptors CCR1 and CCR5 and their ligands CCL3/MIP1α, CCL5/Rantes are also found to be involved depending on specific diseases (Shi & Pamer 2011).

During infection, macrophages can be polarized into different phenotypes depending on the signals that they receive. In an inflammatory environment and in the presence of inflammatory cytokines like IFNγ or inflammatory stimuli like LPS, macrophages acquire a classical activated status (Mills et al. 2000; Mulder et al. 2014). In the presence of anti-inflammatory Th2 cytokines IL-4 and or IL-13, macrophages acquire an alternative activated phenotype (AAM) (Mulder et al. 2014). The classically activated macrophages are also known as M1 macrophages and AAM are known as M2 macrophages (Mills et al. 2000). M1 are typically found in Th1-driven diseases and are characterized by production of pro-inflammatory cytokines, such as TNF, IL-12, IL-1β and release nitric oxide (Chávez-Galán et al. 2015; Mills et al. 2000; Mulder et al. 2014). M2 macrophages are found in Th2 driven diseases like helminth infections and are characterized by production of anti-inflammatory cytokines IL-10, TGF-β, expression of Relmα/ Fizz , YM1 and arginase-1 (Mills et al. 2000; Raes et al. 2002; Chávez-Galán et al. 2015). M2 macrophages have been further divided into the subclasses M2a, M2b, M2c and M2d, the table below (adopted from Rőszer 2015), summaries some of the molecules associated with these subsets.

Table 1 Alternative activated macrophages subtypes

	Stimulators	**Markers expressed**	**Cytokines produced**
M2a	IL4, IL13, helminths infection	Arginase-1, YM-1, Fizz, CD163, CD206	IL10, TGF-β
M2b	immune complexes	CD86, MHC-II	IL-6, IL-1, TNF-α, IL-10
M2c	IL-10, TGF-β, and glucocorticoides	CD163, CD206	IL-10, TGF-β
M2d	IL-6, adenosine	VEGF-A	IL-10, IL-12, TNFα, TGF-β
Adopted with modification from Rőszer et al. 2015).			

In *Plasmodium* infection, macrophages and monocytes are among the most important cell populations. The encounter with the iRBC and parasite Ag in the spleen results in activation of several PRR pathways, making them the greatest source of the inflammatory cytokines and pro-inflammatory signals (Gazzinelli et al. 2014). As discussed above, TLRs, cytosolic and endosomal sensors in macrophages have been shown to recognise the parasite and its derived antigens. During ECM, inflammatory monocytes have been shown to infiltrated into the brain and to have a crucial role in T cell recruitment into the brain, thereby strongly contributing to ECM pathology (Pai et al. 2014; Schumak et al. 2015). The crucial role of monocytes and macrophages in ECM was further confirmed by Schumak et al., where early depletion of monocytes and macrophages was shown to protect mice from severe disease, in contrast to neutrophils (Schumak et al. 2015). Neutrophils belong to the class of granulocytes, as also do eosinophils and basophils. Of these, neutrophils constitute the major population with a role in infection control, whereas eosinophils and basophils are important in allergy and helminth infections (Murphy et al. 2012). As mentioned above, our lab could show that neutrophils do not have a role in ECM pathogenesis as their depletion did not protect mice from severe disease (Schumak et al. 2015).

1.6.2 Effector cells and mediators relevant in ECM

Malaria is generally considered as a Th-1 disease, which has been clearly demonstrated in murine PbA infection with detrimental roles of CD8 T cells and interferon gamma.

1.6.2.1 T cells in Plasmodium infection

CD8 T cells recognise Ag presented via MHC class I. Upon activation, $CD8^+$ T cells differentiate into cytotoxic T lymphocytes, which kill their target cells by release of cytotoxic effector proteins; granzyme-B, perforin and granulysin (Murphy et al. 2012; 372-377). They

also release cytokines IFNγ, TNF and LT-α which helps to further control the infection by increasing the expression of MHC class-I and activation of macrophages (Murphy et al. 2012; 372-377).

Using murine models, cytotoxic $CD8^+$T cells have been shown to be the key mediators of pathology in the brain. The role of $CD8^+$ T cells in the pathology of ECM was demonstrated upon specific depletion of these cells or the use of ko mice which led to protection from ECM (Belnoue et al. 2002; Yañez et al. 1996). It was also shown that these brain infiltrating $CD8^+$ T cells are primed by $CD8\alpha^+$ DCs in the spleen before migrating to the brain (Lundie et al. 2008). In the brain, the endothelial cells cross present Ag to these $CD8^+$T cells resulting in pathology (Howland et al. 2013). Brain-infiltrated $CD8^+$ T cells cause pathology by the release of cytotoxic granules granzyme B and perforin (Nitcheu et al. 2003; Haque et al. 2011). The cytotoxic brain-infiltrated $CD8^+$T cells also express CD11c, which is read as an indication of cytotoxicity and activation, some of these cells are producers of IFNγ (Tamura et al. 2011; Zhao et al. 2014; Haque et al. 2011). Although $CD8^+$ T cells are important in the development of ECM, it has been demonstrated that their ability to cause pathology is dependent on the amount of parasite antigen present in the brain (Baptista et al. 2010; Howland et al. 2013; Haque et al. 2011).

T cell activation is antigen specific and occurs after the T cell receptor on its surface recognises antigen displayed as peptide by APC on the MHC molecules. $CD4^+$ T cells recognises Ag mounted on MHC class II while $CD8^+$ T cells recognised peptides mounted on MHC class I (Murphy et al. 2012; 148). Depending on the cytokines present $CD4^+$ T cells polarize to differentiate T-helper (Th) subsets. In the presence of high levels of IL-12, type I IFNs and IFNγ, $CD4^+$ T cells polarize to a Th1 phenotype, this is characterised by the expression of transcriptional factor T-bet and production of high amounts of IFNγ (Swain et al. 2012). In the presence of IL-4, $CD4^+$T cells polarizes to a Th-2 phenotype which is characterised by the expression of transcriptional factor GATA3 and production of high levels of IL-4, IL-5 and IL-13 (Swain et al. 2012). Regulatory T cells (T-reg) polarization occurs in the presence of cytokines IL-2 and TGFβ, and is characterised by expression of transcriptional factor Foxp3 and production of high levels of IL-10 (Swain et al. 2012). In the presence of IL-6 and TGFβ, $CD4^+$T cells are polarized to the Th-17 phenotype, which is characterised by the expression of the transcriptional factor RORγt and production of IL-17A, IL-17F and IL-22 (Swain et al. 2012). In the presence of cytokines IL-6 and IL-21, $CD4^+$ T cells are polarized to T-follicular

(Tfh) phenotype, and they are characterised by the expression of transcription factor BCL-6 and production of IL-4 and IL-21(Swain et al. 2012).

As stated above, ECM is marked by increased production of the pro-inflammatory cytokine IFNγ, which is the only member of type II interferons and is produced by lymphoid cells. IFNγ signals via the **i**nterferon **g**amma **r**eceptor (IFNGR) activating the JAK-STAT pathway resulting in the transcription of ISGs (Platanias 2005). IFNγ is produced by NK cells at the early stages of in *Plasmodium* infection and later by $CD4^+$ T cell and $CD8^+$ T cells (Gazzinelli et al. 2014). Mice lacking the *IFNγ* gene or the receptor $Ifn\gamma r^{-/-}$ are highly protected from ECM (Yañez et al. 1996; Amani et al. 2000). During *Plasmodium* infection, IFNγ has roles in parasite control, activation of macrophages to increase phagocytosis (Stevenson & Riley 2004) and trafficking of T cells into the brain (Belnoue et al. 2008) and is one of the key mediators involved in ECM pathology.

During the blood-stage infection, cDCs, particularly $CD8^{neg}$ DCs and $CD4^+$DCs were shown to be the key cells presenting Ag to $CD4^+$ T cells, activating them and inducing production of IFNγ (Lundie et al. 2008; deWalick et al. 2007; Sponaas et al. 2006). Depletion of $CD4^+$ T cells in early stages of infection or use of knockout mice resulted in protection of mice from development of ECM (Yañez et al. 1996; Belnoue et al. 2002). The Th-1 (T bet^+ $CD4^+$T cell) population has been shown to be the $CD4^+$ T-cell subset with a key role in driving pathology, this was shown using knockout mice lacking T-bet transcriptional factor (Oakley et al. 2013). The control of parasite load by $CD4^+$ T cell was also shown to be performed mostly by T-bet^+CD4^+ T cell subset (Oakley et al. 2013). The other $CD4^+$ T cells subset involved in ECM are the natural occurring T-regs, since mice lacking $Foxp3^+CD4^+CD25^+$ T cells are protected from ECM (Haque et al. 2010; Amante et al. 2007). However, the Th17 subset was shown not to have a role in ECM (Ishida et al. 2010).

NK cells are lymphoid cells that form part of the innate immunity and are not Ag specific, they kill the target cells by production of cytotoxic granules granzyme B and perforin, they are also producers of interferon gammy (IFNγ) (Murphy et al. 2012;113). In efforts to analyse the role of NK cells in ECM, depletion of these cells by two groups using different antibodies showed different results, in one group they showed protection (Hansen et al. 2007) and in another no protection (Yañez et al. 1996). Moreover, the Hansen group showed that the role of NK cells in ECM was by the recruitment of effector $CD8^+$ T cells into the brains in a CXCR3 dependant manner (Hansen et al. 2007).

1.6.2.2 TNF and chemokine signaling in ECM

Tumor necrosis factor alpha (TNF) is another strong inflammatory mediating cytokine secreted mainly by monocytes, macrophages and T cells, although other cells can also be producers. It is important in homeostasis, monocyte/macrophage differentiation, chemo-attraction and induction of production of cytokines and chemokines (Sedger & McDermott 2014). TNF has been found elevated during severe *Plasmodium* infection and it is strongly linked with CM and other forms of severe malaria, while it is found reduced in mild and asymptomatic malaria (Grau et al. 1987; Hunt & Grau 2003; Othoro et al. 1999). However, recent study demonstrated the relevance of other members of the TNF superfamily, such as LTα, LTβ rather than TNF (Engwerda et al. 2002; Randall et al. 2008).

CXCR3 is a chemokine receptor that has been strongly associated with ECM development, and its role in the migration of effector $CD8^+$ T and NK cells into the brain, it is highly expressed on $CD8^+$ T cells and NK cells that have infiltrated the brain (Hansen et al. 2007; Van den Steen et al. 2008). Its ligands CXCL9 and CXCL10/IP-10 have been found increased in the brains of ECM positive mice and knockout mice have some levels of protection (Coban et al. 2007; Van den Steen et al. 2008; Campanella et al. 2008). Furthermore, CCR5 is important in leukocytes trafficking into the brains of mice that develop ECM, receptor ko mice are protected up to 80% from ECM, with reduced brain infiltrates (Belnoue et al. 2003; Coban et al. 2007). CCR5 has several ligands MIP1α/CCL-3, MIP-1βCCL-4 and RANTES/CCL-5. CCL3 gene expression was found up-regulated in ECM positive mice and was suggested to be involved in the recruitment of T cells, NK cells and CD11c DCs into the brain (Coban et al. 2007). Interestingly, the expression of CCR7 was found to be crucial only on $CD8a^+$DC for activation of $CD8^+$ T cells but was not required for migration of $CD8^+$ T cell to the brain (Zhao et al. 2014).

1.6.3 Inflammatory and anti-inflammatory cytokines in *Plasmodium* infection

The sensing PRR systems on macrophages and DCs trigger the production of several cytokines IL-1β, TNF, type I IFNs, IL-6, and IL-12, while NK cells, $CD4^+$ T cells and $CD8^+$ T cell produce IFNγ (Gazzinelli et al. 2014).

1.6.3.1 Type I interferons

Type I Interferons (IFNs) were first described by their ability to interfere with the spread of viruses (Murphy et al. 2012; 111). IFNα, IFNβ, are the main type I IFNs, although there are others IFNε, IFNκ and IFNω (McNab et al. 2015). Type I IFNs are produced by cells after

recognition of pathogens, PAMP and DAMPs by PRRs (McNab et al. 2015) and although a lot of cells can produce type I IFN, pDCs are the strongest producer and are also known as interferon-producing cells (Murphy et al. 2012; 111). Recognition of pathogens via TLR3 and TLR4 and signalling via adaptor molecule TRIF (TIR- domain-containing adoptor rotein inducing IFNβ), or TLR7, TLR8 and TLR9 signalling via adaptor protein MyD88 (Myeloid differentiation primary response protein 88), leads to activation of IRF3 and subsequent production of IFNα and IFNβ (McNab et al. 2015). Stimulation of cytosolic sensors such as NOD2, RIG-I and MDA-5 signalling via adaptor molecule MAVs also results in production of type I IFNs (McNab et al. 2015). During *Plasmodium* infection, recognition of haemozoin, parasite RNA, and AT-rich motifs of DNA by PRRs results in the production of type I IFNs (Gazzinelli et al. 2014).

Type I IFNs bind and signal via the heterodimeric receptor, **I**nterferon **a**lpha **R**eceptor (IFNaR), located on cell surfaces. On binding of type I IFNs to the receptor, Janus activated kinase (JAK) and tyrosine kinase-2 (TYK2) are activated and lead to phosphorylation of Signal transducer and activator of transcription (STAT) (Platanias 2005).

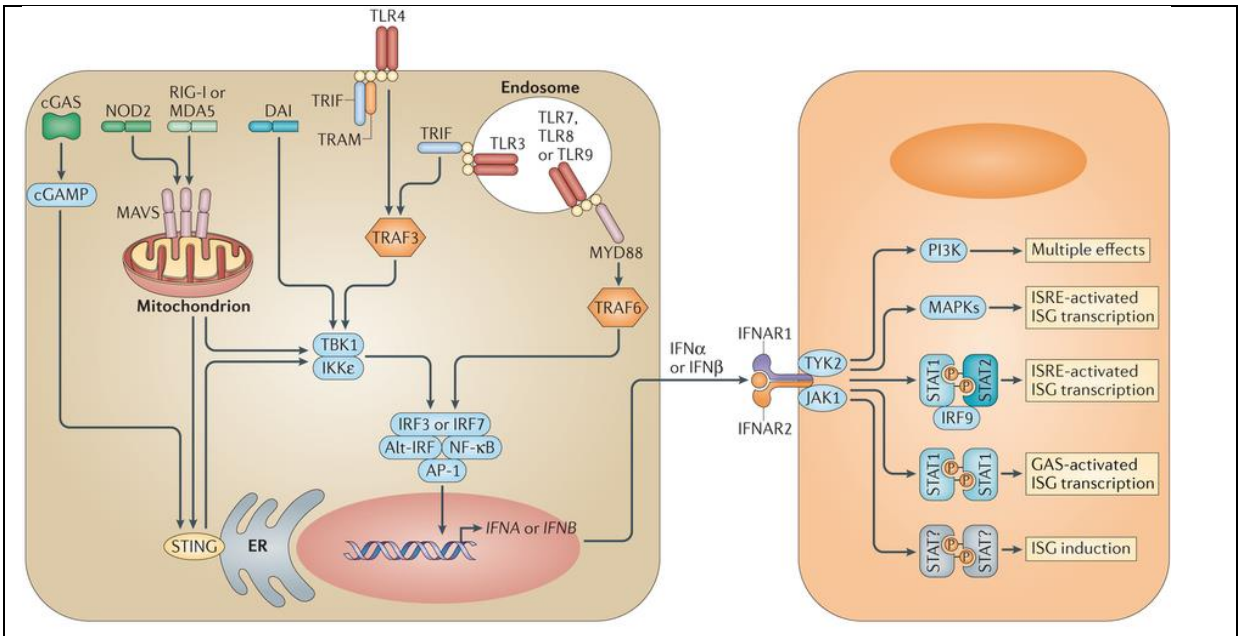

Figure 2 Type I IFNs production and signalling.

The PRRs on the cell surface, endosome and cytosol recognise pathogen, PAMPs and DAMPs and signal via their adaptor molecules and bind to either IRF3/7 or STING, which results in production of type I IFNs. These Type I IFNs then bind to the receptor IFNAR1/2 and signal via the JAK/STAT pathway, MAPK or P13K resulting in production of ISGs. (Adopted from McNab et al. (2015), *Nat Rev Immunology.*

The activated and phosphorylated STATs form homodimers STAT1-STAT1, STAT3-STAT3, STAT4-STAT4, STAT6-STAT6 or heterodimers STAT1-STAT2, STAT1-STAT3, STAT2-STAT3 that translocate to the nucleus (Platanias 2005). Binding of type I IFNs to the receptor

and signalling via the JAK STAT pathway leads to transcription of **I**nterferon **s**timulated **g**enes (ISG) (Platanias 2005). The most common pathway is the STAT1-STAT2 heterodimers, which form together with IRF9 a so-called ISGF3 complex, this binds to Interferon stimulated response element (ISRE), leading to production of specific ISGs (Platanias 2005). STAT homodimers and other heterodimers bind to interferon gamma activated sites (GAS), resulting also in production of ISGs (Hervas-Stubbs et al. 2011).

Although the JAK-STAT signalling pathway is the classical pathway and mostly used, alternative pathways exist, these include the mitogen activated protein kinase (MAPK) pathway and NFκB pathway (Hervas-Stubbs et al. 2011). These ISG control cytokine production, the upregulation of chemokines and their receptors, they enhance detection of pathogens by upregulation of PRRs, they regulate the functions of NK cells, T cells, monocytes and macrophages (Hervas-Stubbs et al. 2011; McNab et al. 2015).

During *Plasmodium* infection, ISG linked to type I IFNs have been found to be upregulated in both blood and liver stages (Aucan et al. 2003; Sharma et al. 2011; Liehl et al. 2014). Polymorphisms of the IFNaR due to mutation was shown to protect children from development of severe malaria (Aucan et al. 2003). Using mice that are genetically deficient in expression of the Ifnar, *Ifnar1*$^{-/-}$ mice, it was shown that signalling via this receptor had a role in the pathogenesis of ECM (Ball et al. 2013; Palomo et al. 2013; Sharma et al. 2011).

1.6.3.2 Interleukin 10 (IL-10)

IL-10 is an anti-inflammatory cytokine produced by cells of both innate and adoptive immunity (Saraiva & O'Garra 2010). IL-10 is highly produced by macrophages when they polarize to an AAM phenotype (Rőszer 2015). Mice lacking IL-10 are prone to developing inflammatory bowel syndrome and are also more susceptible to microbial infections (Saraiva & O'Garra 2010). Parasitic diseases like *Leishmania major*, *Trypanosoma cruzii*, *Toxoplasma gondii* and *Schistosoma mansonii* among others, stimulate production of IL-10 by macrophages and T-regs (Couper et al. 2008). *Plasmodium* infection induces the production of IL-10 by T-regs, macrophages and other cells (Couper et al. 2008). Increased level of IL-10 has been found in asymptomatic pregnant women and children with mild malaria in Africa (Wilson et al. 2010; Othoro et al. 1999; Guiyedi et al. 2015).

1.7 Aims and Objectives of the study

Cerebral malaria is a complex disease, with several interplays between the parasite and the host immune system trying to control and to terminate the infection. The first part of the study was based on the observation that type I IFN signalling was important in ECM pathology (Aucan et al. 2003; Ball et al. 2013; Palomo et al. 2013). However, in those studies they did not show the mechanisms that resulted in prevention of the disease or as to whether the lack of the receptor impaired the priming and activation of the effector cells. Thus, we addressed here the following questions:

- Was the protection of PbA-infected Ifnar ko due to impaired parasite-specific CTL responses?
- Could we identify a specific cell population that was responsible for transmitting the Ifnar signals and /or is also relevant for disease?

In the second part of this thesis, we worked on a "Malaria tolerance" mouse model that was established in our lab. This bases on the observation that mice infected with elevated parasite dose were protected from the development of ECM, in IL-10 dependent manner. In this part of the study, we addressed the following questions;-

- Was the tolerance = protection from ECM due to impaired inflammatory /adaptive immune response in these mice?
- Would we be able to localize to a specific cell population that were providing the IL-10 that was mediating survival?

2 Materials and Methods

2.1 Materials

2.1.1 Anaesthesia

Anaesthesia route of admin.	Drug	Company
Inhalation	Isofluran	Abbott (Wiesbaden, Germany)
Intramuscular	Rompun 2% Ketamin 50mg/ml	Bayer (Leverkusen, Germany) Ratiopharm GmbH (Ulm, Germany)

2.1.2 Buffers

FACS buffer; PBS supplemented with 1% FCS, stored at 4°C.

MACS buffer; PBS supplemented with 1% FCS and 2mM EDTA, stored at 4°C.

2.1.3 Cell culture medium

For cell culture RPMI 1640 medium was supplemented with 10 % FCS, 1% Penicillin/Streptomycin or Gentamicin and 2mM L-Glutamine was used, stored at 4^0C.

2.1.4 CFSE stock

5,6-carboxy-succinimidyl-fluoresceine-ester (CFSE) was dissolved in DMSO to 5mM and stored at -20°C.

2.1.5 FarRed stock

CellTrace Far Red DDAO-SE (FarRed) was dissolved in DMSO to 1mM and stored in aliquots at -20°C.

Reagents	**Manufacturer**
Antibiotics; Penicillin, Streptomycin and Gentamicin	Lonza, (Wuppertal, Germany)
CFSE (carboxy-succinimidyl-uoresceine-ester)	Invitrogen (Darmstadt, Germamy)
DMSO (Dimethyl sulfoxide)	Merck KGaA (Darmstadt, Germany)
EDTA (Ethylendiamintetraacetatedehydrate)	Roth (Karlsruhe, Germany)
FarRed (CellTrace Far Red DDAO-SE)	Invitrogen (Darmstadt, Germamy)
FCS (Fetal calf serum)	PAA, (Cölbe, Germany)
L-Glutamine	PAA, (Cölbe, Germany)
PBS (Phosphate-buffered saline)	PAA, (Cölbe, Germany)
RPMI 1640 medium	Sigma, (Munich, Germany)

2.1.6 Machines

Machine & Manufacturer	Location
autoMACS® Pro Separator Miltenyi Biotec GmbH	Bergisch Gladbach, Germany
BD FACS Canto. I® BD Biosciences	Heidelberg, Germany
BD FACS Canto. II® BD Biosciences	Heidelberg, Germany
BD LSRFortessa® BD Biosciences	BD, San Jose, USA
CASY® TT Cell Counter, Schaerfe Systems	Reutlingen, Germany
Rotorgene RG-3000®, Corbett Research Qiagen	Hilden, Germany
Spectra Max 340pc384m, Photometer Molecular Devices	Sunnyvale, USA

2.1.7 Analysis software

FlowJo® TreeStar Software	Ashland, USA
Prism 5 GraphPad Software® (Statistics)	La Jolla, USA
Rotor-Gene 6.1®, Corbett Research Qiagen	Hilden, Germany
SoftMax® Pro 3.0 Pro Molecular Devices	Sunnyvale, USA

2.2 Methods

2.2.1 Animals

Six (6) week old female C57BL/6N mice were purchased from Janvier or Charles River. *Ifnar1*$^{-/-}$, LysM^{Cre}*Ifnar1*$^{fl/fl}$, CD11c^{Cre} *Ifnar1*$^{fl/fl}$, *IL-10*$^{-/-}$, LysM^{Cre}*IL-10*$^{fl/fl}$, *Irf1*$^{-/-}$ and *Irf3*$^{-/-}$ mice were breed in the House of Experimental Therapy (HET), University Hospital Bonn. Mouse studies were approved by local regulatory agencies (LandesamtfuerNatur, Umwelt und Verbraucherschutz Nordrhein-Westfalen (LANUV NRW) §84-02.04.2012.A264). Water and food were provided ad libitum.

Conditional floxed Ifnar and IL-10 mice were crossed with Cre expressing mice leading to deletion of the gene on the cells expressing Cre. Conditional knockout Ifnar$^{fl/fl}$ LysM^{Cre} have deletion of the Ifnar on CD11b^{+} populations, resident monocytes CD11b^{+}Ly-6C^{lo}, inflammatory monocytes CD11b^{+}Ly-6C^{hi} and granulocytes (Prinz et al. 2008). Conditional knockout Ifnar$^{fl/fl}$ CD11c^{Cre} have deletion of the Ifnar on conventional dendritic cells (Cervantes-Barragan et al. 2009). Conditional knockout, *IL-10*$^{fl/fl}$ LysM^{Cre} have deletion of the IL-10 on CD11b^{+} populations.

2.2.2 Parasites, infection and disease

Plasmodium berghei transgenic parasite (PbAMA) containing MHC class I restricted epitopes from chicken ovalbumin were kindly provided by Dr. Ann Kristin Mueller, University of Heidelberg. *Plasmodium berghei* ANKA expressing OVA parasitized red blood cells (RBC) were injected intravenously (i.v). Before infection of the test animals, two animals were first injected with parasite stock-stabilates intra-peritoneally, the stock contained $1x10^7$ iRBCs in glycerine that had been stored in liquid nitrogen. At d+4 post infection (dpi) blood was collected and analysed for parasitemia and RBC count. The iRBCs was calculated and diluted to an infective dose of $5x10^4$ iRBC, which was then injected into the study animals. From d+5p.i animals were observed for symptoms of ECM using the RMCBS score.

2.2.3 Determination of ECM related symptoms

Mice were analysed for symptoms related to ECM using RMCBS score described by (Carroll et al. 2010). Ten parameters were analysed and for each a score of two was given. These parameters are analysed in three minutes; in the first ninty secs, the mice are assessed for hygiene by how the fur was groomed and movements which was assessed by its gait, exploration of the cage. In the next ninty seconds the reflexes of the mice and aggression were measured. The maximum score for a healthy mouse in twenty, due to ethical consideration and as required by the animal grant, animals with a score of five or less were sacrificed.

2.2.4 Harvesting and preparation of organs

Mice were anaesthetized, and blood collected either from the orbital-vein or the heart. The mice were then perfused intra-cardially with 1x PBS for 5 minutes. Spleens and brains were isolated, brains were cut into small pieces, while spleens were first injected with collagenase A (Roche (Basel, Switzerland), then cut into small pieces. The organs were then and digested with 0.5 mg/ml collagenase A by incubation at $37^{\circ}C$ for 30 min. The organs were then gently pressed through a metal sieve to obtain single cells and washed with MACs buffer at 1500rpm for 5 minutes as $4^{\circ}C$.

Spleens; the supernatant was discarded and the cells resuspended in 5ml medium and counted using CASY® TT Cell counter, the cells were then adjusted to $1x10^7$ cell per ml.

Blood; collected blood was kept on ice and centrifuges at 8000rpm for 5 minutes and the serum or plasma collected.

Brains; To enrich for lymphocytes in the brain, after centrifugation the homogenates were resuspended in 5 ml of 30% Percoll (GE Healthcare, Freiburg, Germany), which was carefully underlayed with 5 ml of 70 % Percoll. Cells were centrifuged for 25 min at room temperature at 2000 rpm without brake. The leucocytes were collected from the interphase of the two percoll solution, by aspiration. The cells were then resuspended in 30ml MACs buffer, centrifuged at 1500rpm for 5 minutes at 4°C and counted using CASY® TT Cell counter.

2.2.5 Parasitemia determination

Blood was collected from the tail vein and thin blood smears made. The blood slides were air dried and fixed in absolute methanol. Giemsa staining solution was made by mixing 1:20 Giemsa stock (Merck KGaA (Darmstadt Germany)) and Giemsa buffer pH 7.2. Slides were stained for 20 minutes followed by rinsing in tap water for 1 minute, after which they were left to airdry. Approximately 800 red blood cells were counted and the infected cells noted, and percentage of iRBCs calculated (=(iRBCs/counted RBCs)*100).

2.2.6 Evans Blue Assay:

Mice were infected as described above and on d+6p.i injected intravenously with 200μl of 2% Evans Blue in 0.95% NaCl. After 1 hour mice were sacrificed and the brains removed, photographed and weighed, thereafter they were placed in falcon tubes containing 2 ml formamide and incubated for 48 hours at 37°C. Quantification of Evans Blue extravasation was done by taking 100µl of the incubated Formamide/brain solution in 96 well plates in triplicates. The standard curve was prepared by diluting Evans Blue to 200µg/ml with 0.95% NaCl (starting concentration), and diluted 1:2 in duplicates with Formamide. The concentration of Evans Blue was measured sprectophotometrically at 620nm. The amount of infiltrated dye was calculated as µg Evans Blue/ g brain tissue *2.

2.2.7 Antibodies for FACS

Directly conjugated monoclonal antibodies that were used for FACS analysis (anti-mouse CD3, CD4, CD8α, CD11b, CD11c, CD19, CD45, CD54, CD206, CCR2, CCR5, CCR7 CXCR3, FOXP3, F4/80, GATA3, Granzyme B, I-Ab, Ly6C, Ly6G, NK1.1, Relm-α, RORγT, Tbet and 1A8) were bought from Biolegend (Fell,Germany), BD Pharmingen (Heidelberg, Germany) or eBioscience (Frankfurt, Germany).

2.2.8 Flow cytometry

For analysis by flow cytometry, either $2x10^6$ spleen cells or all cells collected from the brain were stained in sterile 1x PBS containing 1% FCS for 20 min on ice. Intracellular staining was performed without stimulation using Fix-Perm and Perm Buffer protocol from eBioscience (eBioscience, Heidelberg, Germany) according to the manufacturer´s protocol. Acquisition was performed on a FACS Canto II® flow cytometer and LSR Fortessa® (BD, San Jose, USA). Data were analysed with FlowJo® Software (Treestar Inc., Ashland, USA).

2.2.9 In vivo cytotoxicity assay and peptide restimulation

CTL activity in PbAMA infected animals was determined in vivo on day 6 p.i.. *In vivo* cytotoxicity assay was used to measure the ability of $CD8^+$ T cells to recognise antigens presented on MHC-I by APCs and lyse them. Splenocytes from syngenic donor mice were pulsed with 1µM of the specific H-$2k^b$ peptide SIINFEKL (Ovalbumin) and MSP1 peptides for 30 min at 37°C and subsequently with 1µM of CFSE for 15 min ($CFSE^{high}$, specific target cells) for SIINFEKL, and 1µM of FarRed for MSP1 peptides. Reference cells were not pulsed with peptide and labeled with 0.1µM CFSE for 15 min ($CFSE^{low}$, reference cells). After fluorochromelabeling, the cells were washed and the cell number was determined. The cell populations were mixed at a 1:1:1 ratio ($CFSE^{high}$/$CFSE^{low}$/FarRed). Each recipient received $5x10^5$ cells per 50µl of each population mixed with 50µl on NaCl to a final solution 200 µl of cells into the tail vein on day 5. Mice were sacrificed 18 hours later on day 6 after infection and spleens were isolated and single-cell suspensions prepared as described above. Lysis of peptide-loaded cells was quantified by measuring the ratio of $CFSE^{high}$/ $CFSE^{low}$ cells via flow cytometry (Canto II, BD Biosciences). The percentage of specific lysis, termed SL8-specific lysis, was calculated using the following equation:

$100 - [(CFSE^{high}/CFSE^{low})_{immunized}/(CFSE^{high}/CFSE^{low})_{naïve}] \times 100$ and

$100 - [(FarRed/CFSE^{low})_{immunized}/(FarRed^{high}/CFSE^{low})_{naïve}] \times 100$.

2.2.10 Cytokine ELISA

Organs from experimental animals were isolated on day 6 p.i. and single cell suspensions were prepared as described above. 10^6 splenocytes or $1.25x10^6$ cells from brain homogenates were cultured in triplicates in 200µl RPMI medium over night. The supernatant were analysed for cytokines by sandwich ELISA according to the manufacture's guide.

CCL2	R&D (Minneapolis USA)
CCL3	R&D (Minneapolis USA)
CCL5	R&D (Minneapolis USA)
Granzyme-B	R&D (Minneapolis USA)
IFN-γ	eBioscience (Frankfurt, Germany)
IL-4	BD Pharmingen (Heidelberg, Germany)
IL-6	eBioscience (Frankfurt, Germany)
IL-10	BD Pharmingen (Heidelberg, Germany)
TNF	eBioscience (Frankfurt, Germany)

2.2.11 Magnetic beads cell sorting

Spleen cells $4x10^7$ were taken into sterile falcon tubes, centrifuged at 1500 rpm for 5 min 4°C and the supernatant discarded. Cells were then re-suspended in 300µl sterile MACS buffer, and anti $CD11b^+$ or anti $CD8^+$ beads added (10µl beads per 10^7 cells). The cells were then incubated for 15 mins at 4°C, followed by washing the cells 2x. The cells were then resuspended in 5ml MACS buffer, filtered through sterile gaze immediately before separation step at the autoMACS. Eluted cells were counted and stained to check purity.

2.2.12 Real Time PCR

Whole brain tissues were removed after perfusion and immediately frozen in liquid nitrogen, then stored at -80 till further use. MACS sorted cells $CD11b^+$ cells were stored in -20 overnight. The next day the samples were homogenized with 1ml of TRIzol® (Thermo Fisher Scientifics, WA, USA) in BashingBeads tubes (Zymo Research, Freiburg, Germany). PeqGOLD HP Total RNA Kit was used for purification according to the manufacturer's instructions. Thereafter, on-membrane DNase I digestion (peqGOLD, Erlangen, Germany) was performed. For qPCR, TaqMan® RNA-to-Ct™ 1-Step Kit (Life Technologies, Darmstadt, Germany) was used with 2 µg total RNA in a reaction volume of 20µl.

2.2.12.1 Primer sequence

Gene	Primer FWD	Reverse
Brain 18sRNA	5' ctaacatggctttgacgggta 3'	5' ctgctgccttccttagatgtg 3'
IL-10	5' ggttgccaagccttatcgga 3'	5'acctgctccactgccttgct 3'
YM1	5' gcccttattgagaggagcttta 3'	5' tacagcagacaagacatcc 3'
Relm	5' actgctactgggtgtgcttgt 3'	5' gggttctccacctcttcatt 3'

iNOS	5’ cagctgggctgtacaaaccctt 3’	5’ cattggaagtgaagcctttcg 3’
TNF	5’ catcttctcaaaattcgagtgacaa 3’	5’ tgggagtagacaaggtacaaccc 3’
Arginase	5’ cctatgtgtcatttgggtgga 3’	5’ caggagaaaggacacaggttg 3’
Beta actin	5’ agagggaaatcgtgcgtgac 3’	5’ caatagtgatgacctggcggt 3’

2.2.12.2 qRT-PCR master mix

Master-mix were prepared using the dilutions listed below and the samples analysed in triplicates.

	β- actin	**18sRNA**
H_2O	10.8 µl	10.4 µl
10x buffer	2 µl	2 µl
$MgCl_2$ (25 mM)	2.4 µl	1.2 µl
dNTPs (40 mM)	0.1 µl	0.1 µl
Forward primer (5 µM**)**	1.2 µl	2 µl
Reverse primer (5 µM)	1.2 µl	2 µl
Sybr green (1:1000)	0.2 µl	0.2 µl
HSTaq (250 U)	0.1 µl	0.1 µl
DNA	2 µl	2 µl

	Arg1, IL10 &YM-1	***iNOS &Relm-α***	***TNF***
H_2O	13.6	13	12.4
10x buffer	2	2	2
$MgCl_2$ (25 mM)	0.4	0.8	1.2
dNTPs (40 mM)	0.1	0.2	0.1
Forward primer (10 µM**)**	0.8	0.8	1
Reverse primer (10 µM)	0.8	0.8	1
Sybr green (1:1000)	0.2	0.2	0.2
HSTaq (250 U)	0.1	0.1	0.1
DNA	2	2	2

2.2.12.3Formula for fold change

Fold change was calculated using the formula below from (Pfaffl 2001), samples were normalised to *beta actin* which was used as the housekeeping gene

Fold change = $\frac{(\mathbf{E}p-target)^{\Delta CT-target}}{(\mathbf{E}p\ housekeeping)^{\ \Delta CT-housekeeping}}$

- $C_{T\text{-}target}=(C_{\ T\ Naive}-C_{T\text{-}PbAMA\ infected})$
- $C_{T\text{-}housekeeping}=(C_{\ T\ naive\ housekeeping}-C_{T\text{-}housekeeping\ PbAMA\ infected})$.

2.2.13 Arginase assay

Arginase reagents (Abnova, Taiwan) were brought to room temperature and buffers preheated to 37°C. MACS sorted $CD11b^+$ cells (described above) were counted and $1x10^6$ cells plated into 96 well plates and centrifuged at 1000g at $4^{\circ}C$ for 10 mins. Cells were then lysed for 10 mins with 100µl of 10mM Tris-HCl pH 7.4 (Sigma-Aldrich, Munich, Germany), containing 1 µM pepstatinA (Sigma-Aldrich, Munich, Germany), 1µM leuppeptin (Sigma-Aldrich, Munich, Germany), and 0.4% (w/v) Triton X-100 (Sigma-Aldrich, Munich, Germany). Lysates were centrifuges at 14,000g at 4^0C for 10 mins. Supernatant was taken and used for arginase assay. Analysis for urea quantity was then performed according to manufacturer's instructions (Abnova, Taiwan). The amount of arginase activity was calculated was denoted as units per liter of sample (U/L).

2.2.14 CD11b+ adoptive transfer to LysM^{Cre} *Ifnar1*$^{fl/fl}$ mice

Twenty WT mice and twenty LysM^{Cre} *Ifnar1*$^{fl/fl}$ mice were infected with PbA. On d+3p.i ten of the PbA-infected WT mice were sacrificed and spleens harvested. $CD11b^+$ cells were sorted from the spleen cells as described above. These cells were counted and $5x10^6$ cells were injected into ten of the PbA infected LysM^{Cre} *Ifnar1*$^{fl/fl}$ mice, the other ten ko mice were used as controls. The Mice were scored from d+5p.i for survival and ECM related symptoms using RMCBS score.

2.2.15 Statistical analysis

Survival experiments were performed with 10 mice per group and analysed with Log-rank (Mantel-Cox) test. *Ex vivo* analyses experiments were performed with 3-5 mice per group and statistical analysis was performed using non-parametrically One-way analysis of variance (ANOVA) test with Bonferroni post-test when comparing more than 2 groups. If not otherwise stated, mean and standard error of the means are shown. Significant differences are indicated by the stars in brackets between the groups (*$p<0.05$; **$p<0.01$, ***$p<0.001$). All statistics were performed in GraphPad Prism®.

3 RESULTS

3.1.1 Type I IFN signalling plays a role in the pathogenesis of ECM

During infection with *Plasmodium* parasites, infected red blood cells (iRBC), Pathogen associated molecular patterns (PAMP) and damage associated molecular patterns (DAMP) related to the parasite are recognised by pattern recognition receptors (PRR) on innate cells mainly in the spleen. These cells trigger a cascade of immune responses leading to production of pro- and anti-inflammatory cytokines. Among the cytokines produced are the type I interferons, which bind to the heterodimeric surface cell receptor (interferon alpha/beta receptor IFNaR1 and IFNaR2), thereby leading to signalling and production of interferon-stimulated genes.

This study bases on the observation that mice deficient of the receptor (*Ifnar1*$^{-/-}$) were partially protected from experimental cerebral malaria (ECM) (our own obserations, Ball et al. 2013; Palomo et al. 2013). Since detailed analysis of the adaptive immune responses have not been performed, we addressed the question of whether the protection of Ifnar ko mice resulted from impaired CTL responses towards the parasites. To first confirm whether using our transgenic parasites, PbAMA-OVA, would also result in an absence of ECM in the transgenic mice, we performed a survival experiment on WT and *Ifnar1*$^{-/-}$ mice using these parasites. We observed a survival rate of less than 10% among the infected WT mice, with 90% of the mice dying by d+7p.i. In contrast, 75% of the infected *Ifnar1*$^{-/-}$ mice, survived past the ECM phase (Figure 3). The *Ifnar1*$^{-/-}$ mice that survived past the ECM phase, later on developed symptoms related to anaemia and high parasitemia and were sacrificed.

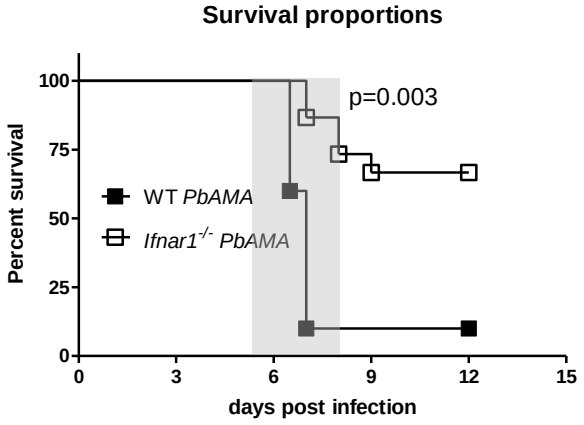

Figure 3 PbA-infected *Ifnar1*$^{-/-}$ are protected from experimental cerebral malaria (ECM).

C57BL/6 (WT ■ and *Ifnar1*$^{-/-}$ □) mice were inoculated with 5x10^4 red blood cells infected (iRBC) with *P. berghei ANKA-Ama1* (PbAMA) i.v. and monitored from d+5 p.i for survival. The shaded area indicates the ECM phase. n=8 per group. Statistics: Log-rank (Mantel-Cox) test.

Taken together, the survival rate of the *Ifnar1*$^{-/-}$ mice shown here correlates with what had been shown by others (Ball et al. 2013; Palomo et al. 2013). As it has not yet been addressed

whether the protection from ECM in PbA-infected *Ifnar1*$^{-/-}$ mice was due to impaired parasite-specific CTL responses and /or impaired inflammation in the brain of the mice or whether it can be localized to a specific cell population that is responsible for transmitting the type IFN signals, we proceeded with a detailed characterization of the infected and protected mice versus the ECM-positive WT mice.

3.1.2 Type I IFN signalling in myeloid cells is crucial for ECM development

As shown above using the *Ifnar1*$^{-/-}$ mice, type I IFN signalling has a role in the development of ECM. However, as the receptor is widely expressed (on almost all nucleated cells), we were interested in the role of type I IFN signalling in myeloid cells and its role in the pathogenesis of ECM. To this end, we employed the use of cell-specific conditional knockout mice. When LysM^{Cre} mice are crossed with *Ifnar1*$^{flox/flox}$ (LysM^{Cre}*Ifnar1*$^{fl/fl}$), there is deletion of the *Ifnar1* gene on LysM expressing cells, in particular on macrophages, monocytes and granulocytes (Clausen et al. 1999; Prinz et al. 2008). Similarly when CD11c^{Cre} mice are crossed with *Ifnar1*$^{flox/flox}$ (CD11c^{Cre}*Ifnar1*$^{f/fl}$), specifically conventional dendritic cells lack this receptor (Caton et al. 2007; Cervantes-Barragan et al. 2009).

We infected WT, *Ifnar1*$^{-/-}$, LysM^{Cre}*Ifnar1*$^{fl/fl}$ and CD11c^{Cre}*Ifnar1*$^{fl/fl}$ mice with 5x10^4 PbAMA iRBCs and analysed the mice from d+5p.i for survival, parasitemia using Giemsa stain and evaluation of the specific neurological score upon PbA infection using "rapid murine coma and behaviour scale" (RMBCS), a health score for quantitative assessment of ECM described by Carroll et al (Carroll et al. 2010).

As before, 90% of PbA-infected WT mice developed ECM by day 7, while the PbA-infected *Ifnar1*$^{-/-}$ had a survival rate of 75%. We observed that mice lacking Ifnar1 on LysM$^+$ expressing cells were protected against the development of ECM syndromes and had a survival comparable to that of the full receptor ko (Figure 4A). These mice did not develop neurological symptoms associated with ECM, as was demonstrated by a high RMBCS (Figure 4B). In contrast, lack of the IFN receptor on cDCs (CD11c^{cre}*Ifnar1*$^{fl/fl}$) did not provide protection and the mice developed neurological symptoms and succumbed to ECM with only one day delay in comparison to the infected WT (Figure 4A). It was important to observe that the survival occurred independently of the peripheral parasitemia, since the percentage of infected RBCs on d+6p.i was comparable among the infected groups (Figure 4C). This indicated that there was equal antigen load among all the infected groups and therefore the protection observed was not due to reduced antigen load. Taken together; our observation showed type I IFN signalling on

LysM expressing cells was more relevant for the pathogenesis of ECM, than signalling on DCs.

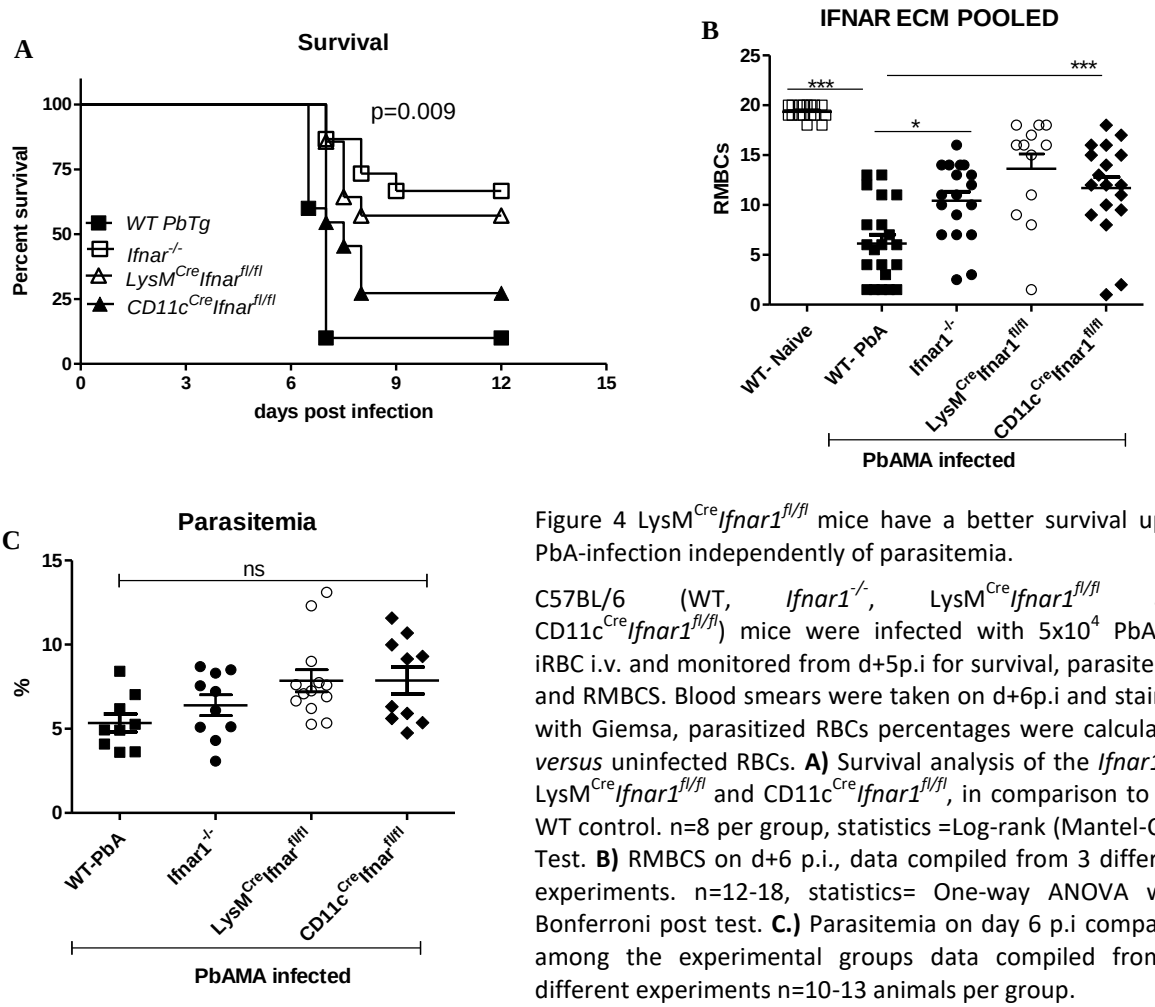

Figure 4 LysM^{Cre}*Ifnar1*$^{fl/fl}$ mice have a better survival upon PbA-infection independently of parasitemia.

C57BL/6 (WT, *Ifnar1*$^{-/-}$, LysM^{Cre}*Ifnar1*$^{fl/fl}$ and CD11c^{Cre}*Ifnar1*$^{fl/fl}$) mice were infected with 5x10^4 PbAMA iRBC i.v. and monitored from d+5p.i for survival, parasitemia and RMBCS. Blood smears were taken on d+6p.i and stained with Giemsa, parasitized RBCs percentages were calculated *versus* uninfected RBCs. **A)** Survival analysis of the *Ifnar1*$^{-/-}$, LysM^{Cre}*Ifnar1*$^{fl/fl}$ and CD11c^{Cre}*Ifnar1*$^{fl/fl}$, in comparison to the WT control. n=8 per group, statistics =Log-rank (Mantel-Cox) Test. **B)** RMBCS on d+6 p.i., data compiled from 3 different experiments. n=12-18, statistics= One-way ANOVA with Bonferroni post test. **C.)** Parasitemia on day 6 p.i compared among the experimental groups data compiled from 3 different experiments n=10-13 animals per group.

3.1.3 Stabile blood brain barrier in PbA-infected Ifnar ko

Breakdown of the BBB is one of the hallmarks of ECM and is demonstrated with the appearance of neurological symptoms in ECM positive mice. We assessed whether the survival we had observed in PbA-infected Ifnar ko was due to a stable BBB, by performing an Evans blue assay. Evans Blue dye binds to serum albumin, which is not able to permeate the BBB due to its size, however, upon disruption of the barrier, infiltration of the albumin- bound dye into the brain is facilitated resulting in blue brains.

We observed strong coloration of the brains of infected WT mice (Figure 5A) which could be quantified with the help of a colorimetric assay (Figure 5B), reflecting a disrupted BBB and significant leakage of the dye into the tissue. In contrast, samples from naïve controls remained completely bright (Figure 5A) and contained only background levels of the dye (Figure 5B), thus demonstrating a stable BBB (Figure 5A&B). Importantly, brains of PbA-infected *Ifnar1*$^{-/-}$,

LysM^{Cre}*Ifnar1*$^{fl/fl}$ and CD11c^{Cre}*Ifnar1*$^{fl/fl}$ mice, showed a reduced amount of infiltrated dye, as compared to samples from PbA-infected WT mice (Figure 5A&B). This confirms the link between stable BBB and ECM, whereas brains of non-ECM mice lacked any dye infiltration. This observation further supported our hypothesis on the role of type I IFN signalling in the pathogenesis of ECM and indicated a role in BBB disruption.

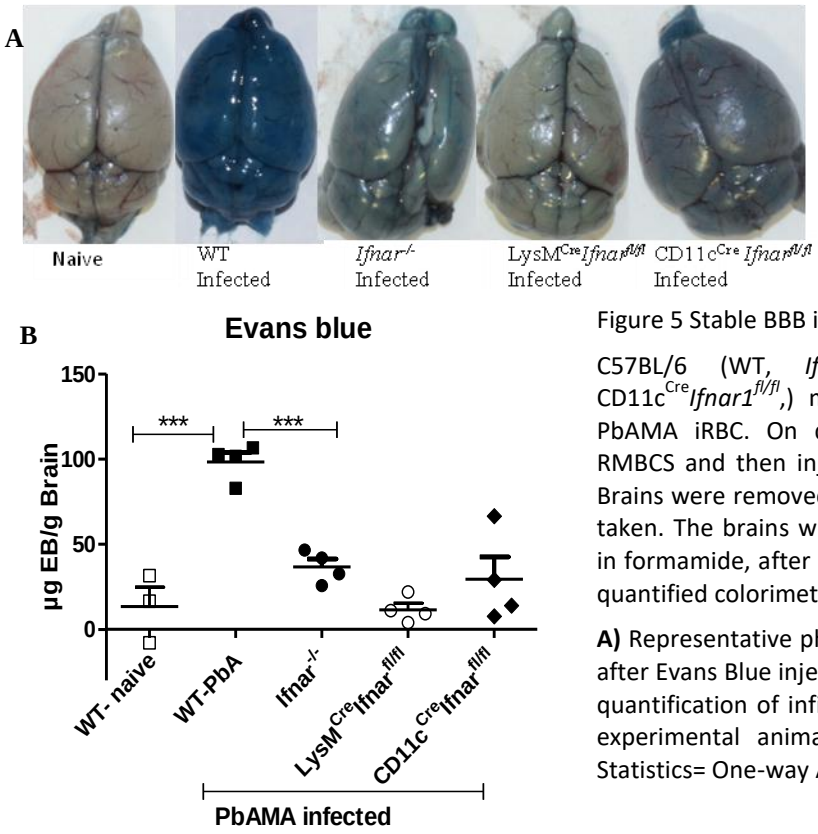

Figure 5 Stable BBB in PbA-infected Ifnar ko

C57BL/6 (WT, *Ifnar1*$^{-/-}$, LysM^{Cre}*Ifnar1*$^{fl/fl}$ and CD11c^{Cre}*Ifnar1*$^{fl/fl}$,) mice were infected with 5x10^4 PbAMA iRBC. On d+6p.i., mice were scored for RMBCS and then injected i.v. with Evans blue dye. Brains were removed after 1hr, weighed and photos taken. The brains were incubated at 37^{0}C for 48hrs in formamide, after which the extravasated dye was quantified colorimetrically.

A) Representative photos of the brains taken 1 hour after Evans Blue injection. **B)** Spectrophotometrically quantification of infiltrated dye in the brains of the experimental animals. n=3/4 animals per group, Statistics= One-way ANOVA, Bonferroni post test.

3.1.4 Brain of PbA-infected Ifnar ko mice contained parasites

Several factors are attributed to the breakdown of the BBB during ECM, among them are the presence of effector CD8$^+$ T-cells and sequestration of iRBCs in the brains of infected mice. In ECM models, these iRBCs are shown to adhere to the endothelial cells (Shaw et al. 2015). Howland *et al.* showed that iRBC present in the brains provided antigen, which is cross-presented to cytotoxic CD8$^+$T cells by endothelial cells and thereby contributed to the destruction of the BBB (Howland et al. 2013). Parasite-load due to sequestration of iRBCs in the brain was also shown to be important for ECM development (Baptista et al. 2010). We next addressed the question whether the protection and stable BBB we had observed was due to reduced numbers of parasites in the brain. We therefore quantified the parasite load in the brains of WT and Ifnar ko PbA-infected mice by qPCR using *P.b*A-specific 18s rRNA primers. Our results show that all infected mice contained sequestered iRBCs in the brain tissue as

measured by copy numbers. We observed a non-significant difference in the parasite load in brain tissue of PbA-infected *Ifnar1*$^{-/-}$ and PbA-infected LysM^{Cre}*Ifnar1*$^{fl/fl}$ mice (Figure 6), but sample numbers were too low to reach significant differences. Furthermore, we could not distinguish between parasites that were still present in the blood circulation and others that had passed the BBB, providing parasite Ag in these brains that was probably contributing to pathology.

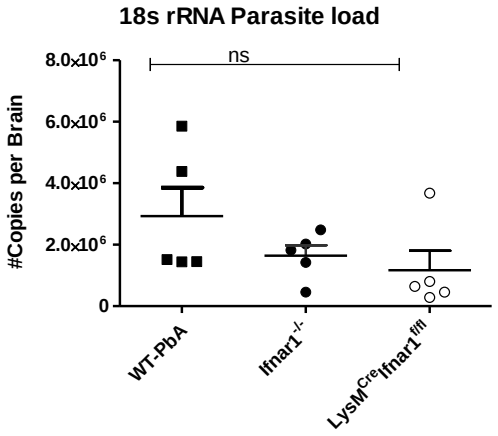

Figure 6 All PbA-infected mice contained parasites in their brain

C57BL/6 mice (WT, *Ifnar1*$^{-/-}$, LysM^{Cre}*Ifnar1*$^{fl/fl}$ and CD11c^{Cre}*Ifnar1*$^{fl/fl}$) were infected with 5x10^4 PbAMA, iRBC. i.v. On d+6p.i, mice were scored for RMBCS and perfused with PBS, the brains were removed and placed in liquid nitrogen. RNA was isolated using the Trizol-chloroform protocol. RNA was reverse transcribed into cDNA. Parasite 18s rRNA was quantified using qPCR. n=5 animals per group, Statistics = One-way ANOVA with Bonferroni post test. p = 0.2096.

3.1.5 Lack of type I IFN signalling resulted in reduced brain infiltrates

Infiltration of immune cells from the periphery into the brain is another important factor that is associated with the breakdown of the BBB during ECM. We have demonstrated above the presence of parasite = Ag in the brains of the ECM protected mice (Figure 6); however the presence of effector CD8$^+$ T-cells and other leukocytes are also required for brain pathology to occur (Lundie et al. 2008; Baptista et al. 2010; Howland et al. 2013; Haque et al. 2011).

We therefore questioned whether the protection from ECM in PbA-infected *Ifnar1*$^{-/-}$ and LysM^{Cre}*Ifnar1*$^{fl/fl}$ mice was due to the lack of infiltrating peripheral immune cells into their brains. To quantify infiltrating cells, single suspensions were prepared and lymphocytes were enriched via percoll gradient as described in the methods section, then the total cell count was calculated. Cells were first gated according to their expression of CD45 and CD11b, since cellular infiltrates from the periphery can be identified via flow cytometry by high expression of the surface marker CD45 and thus easily differentiated from brain resident cells such as microglia, which express low levels of CD45 but high levels of CD11b (Schumak et al. 2015). The CD45^{pos} were defined as peripheral immune cells and separated from the CD11b^{hi}CD45^{int} microglia. Next, they were further categorized into infiltrated leukocytes (CD11b^{low}CD45^{hi}) and mononuclear cells (CD11b^{hi}CD45^{hi}) as shown in schematic Figure 7A. The gating strategy contained three populations of interest-; P1= infiltrated lymphocytes and other CD11b

negative/low populations, P2= infiltrated inflammatory monocytes and neutrophils and P3= resident microglia cells.

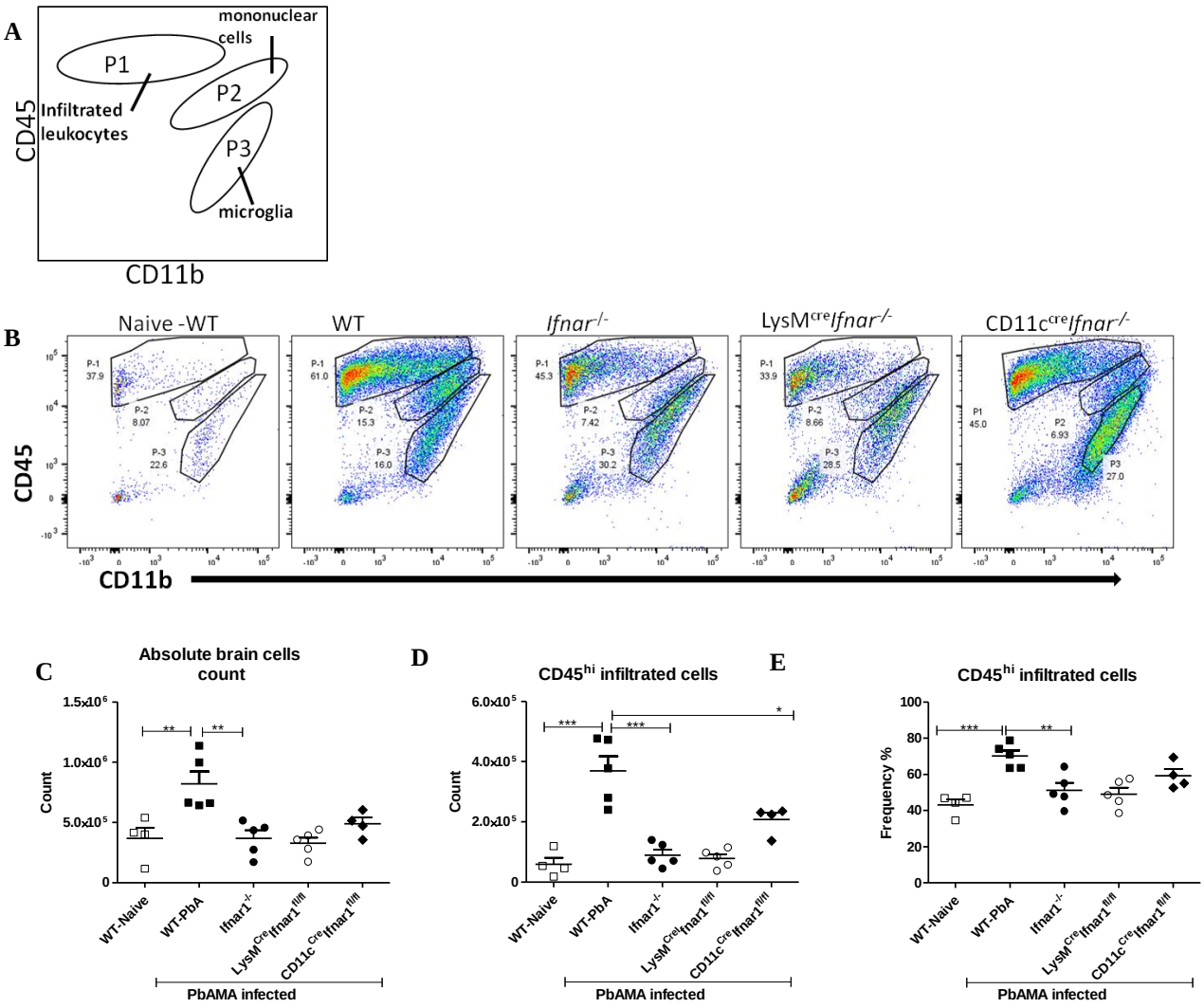

Figure 7 Type I IFN signalling was important for infiltration of cells into the brain

C57BL/6 mice (WT, *Ifnar1*$^{-/-}$, LysM^{Cre}*Ifnar1*$^{fl/fl}$, CD11c^{Cre}*Ifnar1*$^{fl/fl}$) were infected with 5x10^4 PbAMA, iRBC i.v. On d+6p.i, mice were scored for RMBCS and perfused with PBS, the brains were then collagenase-digested. Single cell suspensions were prepared and counted, cells were stained, then analysed by flow cytometry. **A)** Scheme showing the gating to discriminate CD45^{hi} cells populations infiltrated to the brain from brain-resident CD11b^{hi} CD45^{lo} microglia. **B)** Raw data from representative samples from all experimental groups **C)** Total brain count **D**) Total infiltrated cell counts according to CD45^{hi} expression. **E**) Frequency of infiltrated cell counts according to CD45^{hi} expression. Statistical analysis= One-way ANOVA with Bonferroni's post test. p.value= 0.008. Data representative of more than 4 independent experiments. n=4/5 per group.

The processing of brain tissue of naïve mice resulted only in an average yield of <5x10^5 cells per sample and minor cell fractions in the CD11b vs CD45 staining, whereas the recovery of lymphocytes from brain tissue of infected WT, resulted in a significantly elevates number of both total cell count and CD45^{hi} positive population indicating strong infiltration of cells from the periphery into the brains (Figure 7C & D).

The total count of brain infiltrated cells was 2.3 fold higher in the PbA-infected WT in comparison to the samples of the naïve mice. The same trend was observed in comparison to the brain samples of the infected Ifnar ko mice, with the infected WT having fold increase of 2.2 x to *Ifnar1*$^{-/-}$, 2.5 x to LysM^{Cre}*Ifnar1*$^{fl/fl}$ and 1.3x to CD11c^{Cre}*Ifnar1*$^{fl/fl}$ (Figure 7C).

We observed in brains of the infected WT mice a significant increase of the CD45^{hi} population, with multiple increases in comparison to the samples of the other groups (6.2x to naïve, 4.1x to infected *Ifnar1*$^{-/-}$, 4.6 x to LysM^{Cre}*Ifnar1*$^{fl/fl}$ and 1.8x to CD11c ^{Cre}*Ifnar1*$^{fl/fl}$) (Figure 7D). No significant differences were observed between the infected *Ifnar1*$^{-/-}$ and LysM^{Cre}*Ifnar1*$^{fl/fl}$ in comparison to brains of the naïve mice. However, CD11c^{Cre}*Ifnar1*$^{fl/fl}$ had a 3.5 fold increase compared to the samples of naïve control mice (Figure 7D). Also the comparison of the CD45^{hi} population in the brains of the infected WT mice and the other experimental groups revealed differences regarding the counts and frequencies (Figure 7B & E). Brains of PbA-infected WT mice contained on average, 27.3% more cells than the brains of the naïve, 17% more cells than brains of PbA-infected *Ifnar1*$^{-/-}$ and LysM^{Cre}*Ifnar1*$^{fl/fl}$, but only 10% more cells than the brains of the CD11c^{Cre}*Ifnar1*$^{fl/fl}$ mice (Figure 7E). There were no significant difference in the frequency of CD45^{hi} between the naïve and the PbA-infected *Ifnar1*$^{-/-}$, LysM^{Cre}*Ifnar1*$^{fl/fl}$ and CD11c^{Cre}*Ifnar1*$^{fl/fl}$ mice (Figure 7E). Taken together, our data show an important role of type I IFN signalling in the accessibility of peripheral immune cells to the brain during ECM.

3.1.6 Infiltration of lymphocytes from the periphery into the brain was dependent on type I IFN signalling

We have shown above a significant difference in the amount of brain-infiltrated cells, between PbA-infected WT and *Ifnar1*$^{-/-}$ mice (Figure 7B-E). We next characterized the composition of the infiltrated cell populations, to see which different cell populations had infiltrated into the brains. T cells were gated from population P-1, shown in Figure 7 A, as CD3^{+}CD45^{hi}CD11b^{neg}, and from this group, CD8^{+} and CD4^{+} T cells.

We looked for effector CD8^{+} T cells, as these cells have an undisputed role in mediating the pathology observed during ECM. CD8^{+}T cells have been proven to be the effector cells during ECM, as deletion of CD8^{+} T cells prior to the onset of ECM or use of T cell deficient mice conferred protection from fatal outcome. Furthermore, these brain recruited cells have been shown to be parasite-specific (Belnoue et al. 2002; Haque et al. 2011; Howland et al. 2013; Lundie et al. 2008; Shaw et al. 2015). The CD8^{+}T-cells mediated pathology involves several effector molecules, granzyme-B, perforin and IFNγ (Belnoue et al. 2008; Haque et al. 2011;

Nitcheu et al. 2003; Rénia et al. 2006; Howland et al. 2013). In contrast, CD4^{+}T-cells have been show to exhibit relevant functions only in early phases of infection but their presence is not required in late stage for pathology (Belnoue et al. 2002; Yañez et al. 1996).

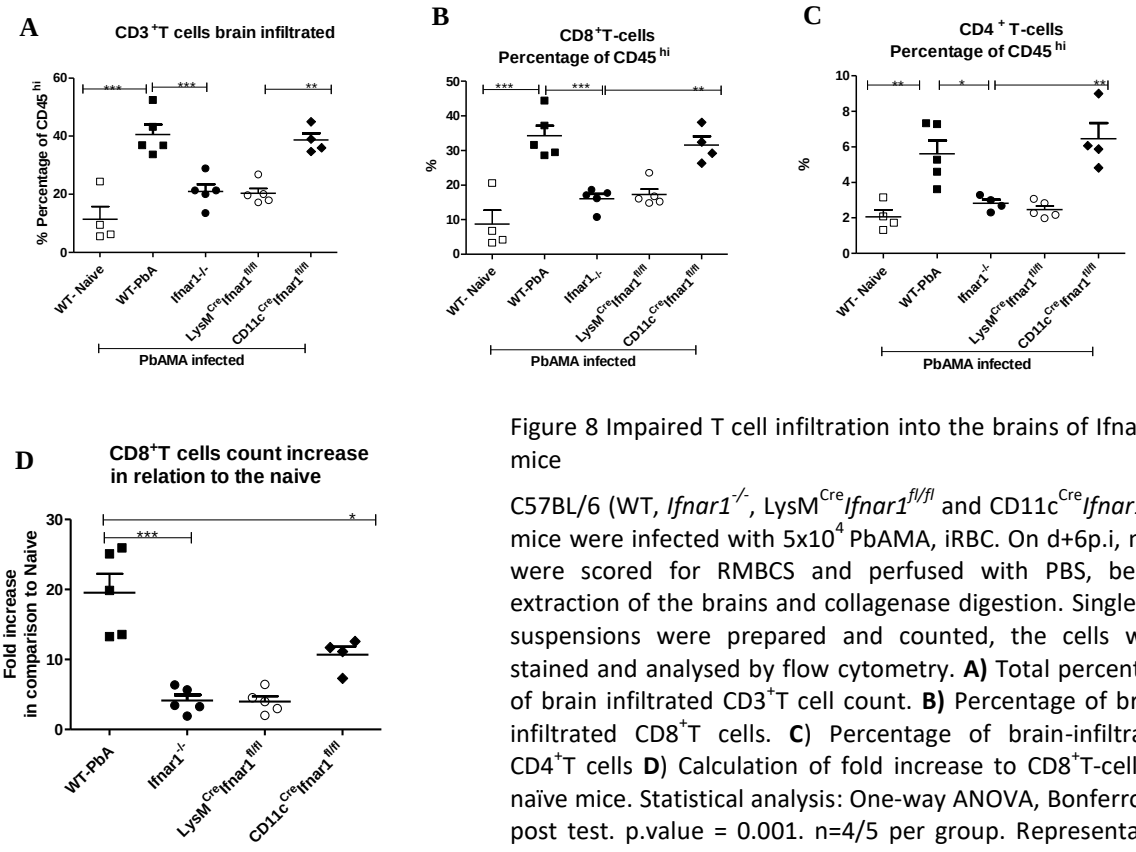

Figure 8 Impaired T cell infiltration into the brains of Ifnar ko mice

C57BL/6 (WT, *Ifnar1*$^{-/-}$, LysM^{Cre}*Ifnar1*$^{fl/fl}$ and CD11c^{Cre}*Ifnar1*$^{fl/fl}$) mice were infected with 5x10^{4} PbAMA, iRBC. On d+6p.i, mice were scored for RMBCS and perfused with PBS, before extraction of the brains and collagenase digestion. Single cell suspensions were prepared and counted, the cells were stained and analysed by flow cytometry. **A)** Total percentage of brain infiltrated CD3^{+}T cell count. **B)** Percentage of brain-infiltrated CD8^{+}T cells. **C**) Percentage of brain-infiltrated CD4^{+}T cells **D**) Calculation of fold increase to CD8^{+}T-cells of naïve mice. Statistical analysis: One-way ANOVA, Bonferroni's post test. p.value = 0.001. n=4/5 per group. Representative data of more than 4 independent experiments.

We observed in brains of PbA-infected WT mice a massive infiltration of T cells (Figure 8A), which is in agreement with what has been previously reported. CD8^{+} T cells composed more than 80% of the brain infiltrated cells, which resulted in them accounting for ~56% (±4%) of the total brain infiltrated cells (Figure 8B). These cells were not present in the brains of the naïve animals, indicating that they had infiltrated into the brains of the infected mice. When we compared samples from PbA-infected WT with those from infected *Ifnar1*$^{-/-}$ mice, the samples from the infected WT and CD11c^{Cre}*Ifnar1*$^{fl/fl}$ mice contained the highest frequencies of infiltrated T cells (Figure 8A). Furthermore, they both had 20% more infiltrates in their samples than brain samples from PbA-infected *Ifnar1*$^{-/-}$ and LysM^{Cre}*Ifnar1*$^{fl/fl}$ mice (Figure 8A). PbA-infected WT and CD11c^{Cre}*Ifnar1*$^{fl/fl}$ had comparable frequencies of CD4^{+}T cells in their brains, which was twice as much as that determined in brains from PbA-infected *Ifnar1*$^{-/-}$ and LysM^{Cre}*Ifnar1*$^{fl/fl}$ mice (Figure 8C). Here, the LysM^{Cre}*Ifnar1*$^{fl/fl}$ continued to show a phenotype similar to that of the full Ifnar ko with very few CD8^{+} T cells and CD4^{+} T cells infiltrating into

their brains (Figure 8B & C). However, PbA-infected WT and CD11c^{Cre}*Ifnar1*$^{fl/fl}$ displayed equally high percentages in both CD8$^+$ and CD4$^+$ T-cells that had infiltrated into the brains (Figure 8A-C). When we calculated the fold increase of CD8$^+$ T cells in relation to the results from brains of the naïve control mice, we observed the highest fold increase in the WT with a mean fold increase factor of 19.5, followed by CD11c^{Cre}*Ifnar1*$^{fl/fl}$ with factor of 10.7, while *Ifnar1*$^{-/-}$ and LysM^{Cre}*Ifnar1*$^{fl/fl}$ had each a mean factor of 4 (Figure 8D). Taken together, we observed that PbA-infected *Ifnar1*$^{-/-}$ or LysM^{cre}*Ifnar1*$^{fl/fl}$ showed strongly impaired infiltration of effector CD8$^+$ T-cell into the brain, thus indicating that the protection we observed was due to reduced number of effector CD8$^+$T cells that had infiltrated into the brains of *Ifnar1*$^{-/-}$ and LysM^{Cre}*Ifnar1*$^{fl/fl}$ and which was probably not sufficient to induce pathology, since it was possible that they did not pass the BBB.

3.1.7 *Ifnar1*$^{-/-}$ and LysM^{Cre}*Ifnar1*$^{fl/fl}$ contained less infiltrated cytotoxic CD8$^+$Tcells in their brains

As shown above, PbA-infected mice deficient of the type I IFN receptor had an intact BBB (Figure 5) and less infiltration of cells into the brain (Figure 7D), in particular less CD8$^+$T cells (Figure 8B). However, there was a small number of infiltrated CD8$^+$T-cells that has infiltrated into the brains, therefore we further analysed these infiltrated CD8$^+$T-cells for cytotoxicity by analysing for the expression of granzyme-B and expression of CD11c. Pathology in the brains of ECM positive mice was shown to be mediated via production of cytotoxic molecules, granzyme-B and perforin (Haque et al. 2011; Nitcheu et al. 2003), with Ag specific cytotoxic CD8$^+$T cells expressing CD11c (Tamura et al. 2011; Zhao et al. 2014).

As expected, there was no expression of granzyme-B in brain derived CD8$^+$ T cells of naïve mice (Figure 9 A&B). Importantly, we detected in brain samples from PbA-infected WT mice elevated levels of granzyme B expression in CD8$^+$ T cells by gMFI as well as absolute cell numbers of granzyme-B$^+$CD8$^+$T-cells population (Figure 9A & B). In comparison to the naïve mice, CD8$^+$ T cells in brain samples from PbA-infected *Ifnar1*$^{-/-}$ and LysM^{Cre}*Ifnar1*$^{fl/fl}$ mice showed increased granzyme-B expression (Figure 9A), although the absolute cell number of CD8$^+$ T-cells expressing granzyme-B was reduced in comparison to the PbA-infected WT mice (Figure 9B).

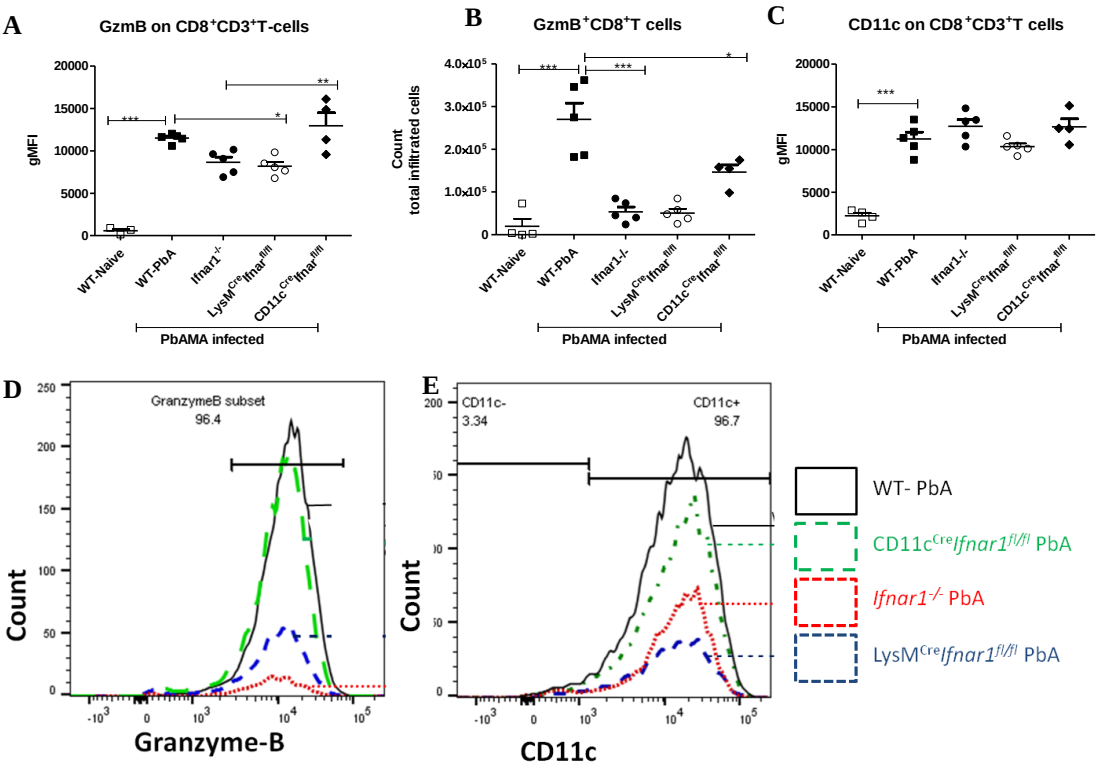

Figure 9 Lack of Ifnar led to reduced presence of cytotoxic CD8$^+$T cells in the brain.

C57BL/6 mice (WT, *Ifnar1*$^{-/-}$, LysM^{Cre}*Ifnar1*$^{fl/fl}$ and CD11c^{Cre}*Ifnar1*$^{fl/fl}$) were infected with 5x10^4 PbAMA-iRBC i.v. On d+6p.i single cell suspensions from perfused and digested brains were prepared. The cells were counted, stained first for surface markers and followed by intracellular markers, then analysed by flow cytometry. **A)** gMFI of granzyme-B in gated brain infiltrated CD8$^+$T cells. **B**) Total count of brain infiltrated granzyme B$^+$ CD8$^+$T cells. **C**) gMFI of CD11c in gated brain infiltrated CD8$^+$T cells. **D**) Count overlay of granzyme B$^+$CD8$^+$ T cells. **E**) Count overlay of CD11c$^+$CD8$^+$T cells. Statistical analysis = One-way ANOVA with Bonferroni's post test. n=4/5 per group. Data representative of 2 independent experiments.

This observed difference in gMFI and cell count can be explained by Figure 9D, since we observed that although few CD8$^+$T cells had infiltrated into the brain, all the infiltrated CD8$^+$T cells were expressing granzyme-B (Figure 9D). PbA-infected CD11c^{Cre}*Ifnar1*$^{fl/fl}$ mice contained a similar expression of granzyme-B (gMFI) by CD8$^+$T-cells as the infected WT mice, however, the cell count was slightly different (Figure 9A, B &D). Furthermore, we observed in the brain samples from all the infected groups of mice (both WT and ko), but not in samples from naïve mice that >95% of the CD8$^+$ T cells highly expressed CD11c (Figure 9 C &E). Taken together these results suggest that the protection against ECM we observed among *Ifnar1*$^{-/-}$ and LysM^{Cre}*Ifnar1*$^{fl/fl}$ was probably due to reduced/low numbers of cytotoxic CD8$^+$T-cell infiltrating into the brains. Finally, we cannot exclude that these few cells did not infiltrate but maybe rather were on the other side of the (intact) BBB.

3.1.8 Increased expression of ICAM-1, CCR5 and CXCR3 on brain infiltrated CD8+T of PbA-infected Ifnar ko

We have shown above less infiltration of $CD8^+$T-cells in the brains of ECM protected mice, however, more than 95% of those cells showed still signs of cytotoxicity (Figure 9D & E). We then next evaluated the activation status of these $CD8^+$ T cells in the brain samples by analysing expression of intercellular adhesion molecule ICAM-1, chemokine receptors CCR2, CCR5, CXCR3, CCR7 and the activation marker CD69.

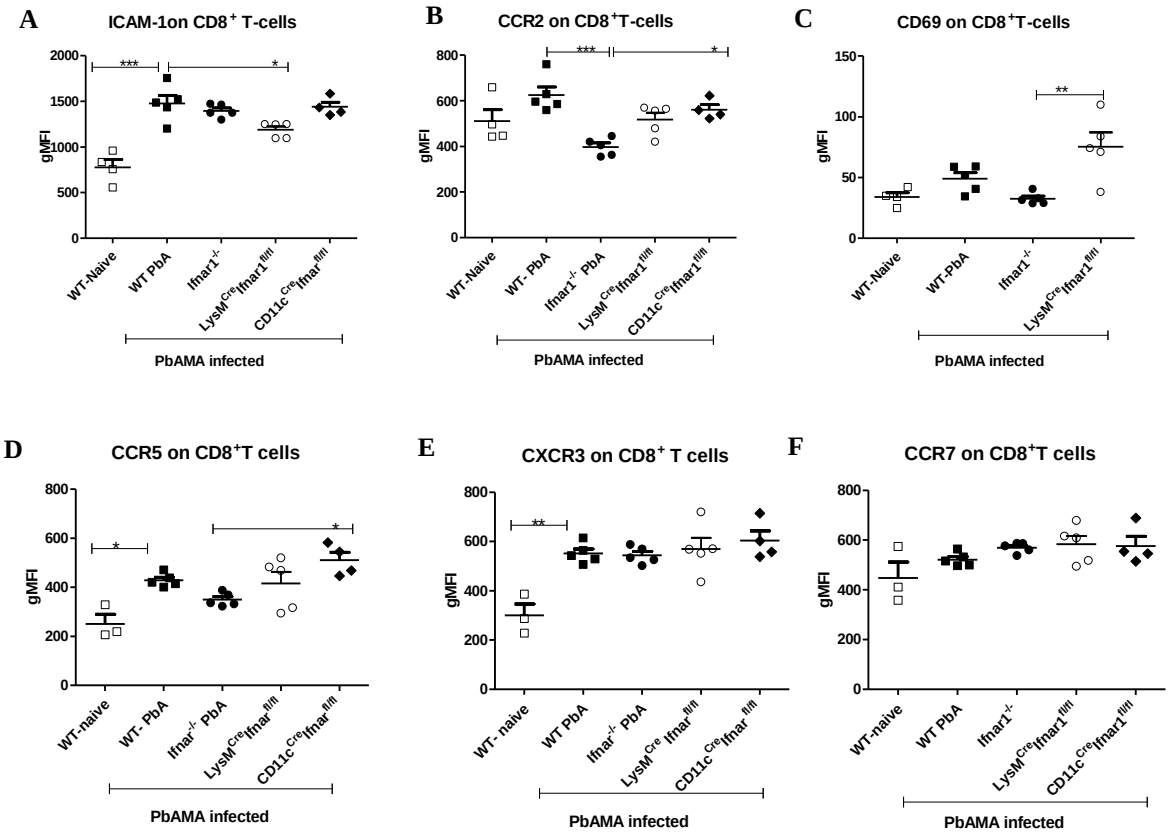

Figure 10 ICAM-1, CCR-2 and CD69 on infiltrated $CD8^+$T cells.

C57BL/6 mice (WT, *Ifnar1*$^{-/-}$, LysM^{Cre}*Ifnar1*$^{fl/fl}$ and CD11c^{Cre}*Ifnar1*$^{fl/fl}$) were infected with 5x10^4 PbAMA, iRBC i.v. On d+6p.i, single cell suspensions from brains were prepared, stained and analysed by flow cytometry. **A**) ICAM-1 expression on brain infiltrated $CD8^+$T cells. **B**) Expression of CCR2 on brain infiltrated $CD8^+$T cells. **C**) Expression levels of CD69 on brain infiltrated $CD8^+$T cells. **D**) Expression of CCR5 on brain infiltrated $CD8^+$T cells. **E**) Expression of CXCR3 on brain infiltrated $CD8^+$T cells. **F**) Expression of CCR-7 on brain infiltrated $CD8^+$T cells. Statistical analysis = One-way ANOVA with Bonferroni post test. n=3/4/5 animals per group.

We detected elevated ICAM-1 levels on $CD8^+$ T cells from brains of all infected groups of mice in comparison to samples of the naïve mice, although the expression levels in samples from PbA-infected LysM^{Cre}*Ifnar1*$^{fl/fl}$ were slightly reduced in comparison to the infected WT mice (Figure 10A). CCR-2 expression levels on $CD8^+$ T cells were similar among most of the PbA-infected mice in comparison to the samples from naïve mice, but importantly, we

observed decreased CCR-2 expression on $CD8^+$ T cells of PbA-infected *Ifnar1*$^{-/-}$ in comparison to those of PbA-infected WT and infected $CD11c^{Cre}$*Ifnar1*$^{fl/fl}$ mice (Figure 10B). We did not observe a difference in CD69 expression between naïve mice, PbA-infected WT and infected *Ifnar1*$^{-/-}$ mice, whereas $CD8^+$T cells from $LysM^{Cre}$*Ifnar1*$^{fl/fl}$ mice showed increased levels of CD69 in comparison to infected *Ifnar1*$^{-/-}$ mice (Figure 10C). Brain samples from all infected animals showed elevated expression levels of CCR5 and CXCR3 on $CD8^+$T cells, here, infected $CD11c^{Cre}$*Ifnar1*$^{fl/fl}$ presented the highest expression of CCR5 (Figure 10D & E). Expression levels of CCR7 were comparable between all the brain samples (Figure 10F). These data show variation in the expression of activation markers on brain infiltrated $CD8^+$ T cells, and partially impaired expression of CCR2 and CCR5 on effector T cells from ECM negative mice, which might explain /contribute their protection from brain inflammation due to less signals from T cells that are required for brain infiltration.

3.1.9 Increased expression of ICAM-1 and CXCR3 on brain infiltrated $CD4^+$ T cells

We next addressed the question whether also the few infiltrated $CD4^+$ T cells observed in brains of infected Ifnar ko mice had a different phenotype than those of the PbA-infected WT mice. Therefore, similarly to the $CD8^+$ T cells, we evalutated the expression levels of adhesion molecule ICAM-1, activation marker CD69, chemokine receptors CCR5 and CXCR3 on $CD4^+$ T cells found among brain infiltrated lymphocytes. As $CD4^+$ T cells have been described in some conditions to exert also cytotoxic functions, we also analysed their production of granzyme B.

We observed an increased expression of ICAM-1 on brain infiltrated $CD4^+$ T cells of all the infected mice in comparison to the $CD4^+$ T cells in the samples from the naïve mice (Figure 11A). Although $CD4^+$ T cells from infected WT showed elevated CD69 expression on $CD4^+$ T cells in comparison to the $CD4^+$ T cells from the naïve mice, this was not statistically significant (Figure 11B). Expression of CD69 on brain infiltrated $CD4^+$ T cells from PbA-infected *Ifnar1*$^{-/-}$ mice was reduced in comparison to the $CD4^+$ T cells of infected WT mice (Figure 11B). $CD4^+$ T cells from brains of $LysM^{Cre}$*Ifnar1*$^{fl/fl}$ mice had more CD69 in comparison to the naïve and *Ifnar1*$^{-/-}$, however comparable to the PbA-infected WT mice (Figure 11B). Importantly, brain-infiltrated $CD4^+$ T cells of infected WT mice showed the highest expression of granzyme B, whereas $CD4^+$ T cells from naïve did not express any granzyme B (Figure 11C). However, it is important to bear in mind here, that the level of granzyme B expressed by $CD4^+$T cells was 4.5 times lower than that expressed by $CD8^+$T cells of the same mice (Figure 9A). We observed significantly less granzyme-B^+CD4^+ T-cells in

brain samples from *Ifnar1*$^{-/-}$ and LysM^{Cre}*Ifnar1*$^{fl/fl}$ mice in comparison to infected WT mice (Figure 11C). CD4^{+} T cells from brain samples derived from CD11c^{Cre}*Ifnar1*$^{fl/fl}$ showed similar high granzyme production as those from the infected WT mice (Figure 11C), which both suffered from ECM.

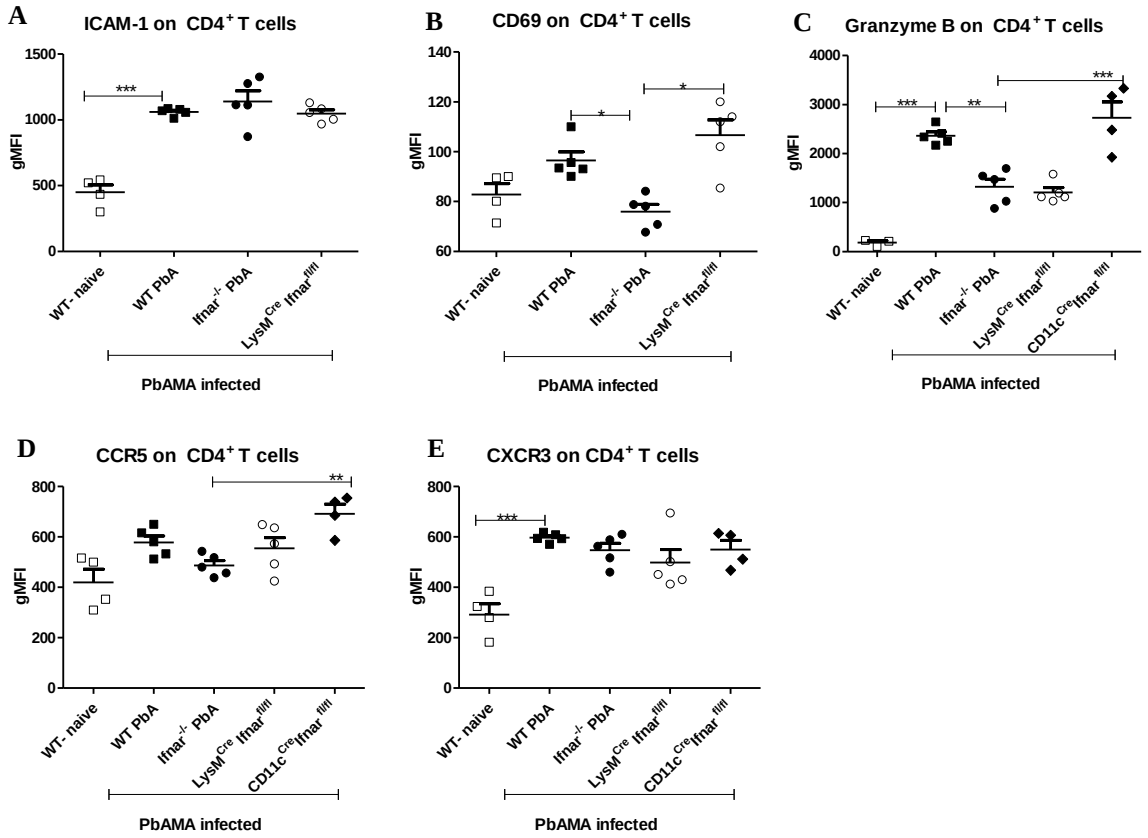

Figure 11 CD4^{+}T cells from *Ifnar1*$^{-/-}$ are less activated

C57BL/6 mice (WT, *Ifnar1*$^{-/-}$, LysM^{Cre}*Ifnar1*$^{fl/fl}$ and CD11c^{Cre}*Ifnar1*$^{fl/fl}$) were infected with 5x10^{4} PbAMA, iRBC i.v. On d+6p.i, Single cell suspensions were prepared from brains, counted and analysed by flow cytometry. **A)** Expression of ICAM-1 on brain infiltrated CD4^{+}T cells. **B)** Expression of CD69 on brain infiltrated CD4^{+}T cells. **C)** Expression of Granzyme B by brain infiltrated CD4^{+}T cells. **D)** Expression of CCR5 on brain infiltrated CD4^{+}T cells. **E)** Expression of CXCR3 on brain infiltrated CD4^{+}T cells. Statistical analysis = One-way ANOVA with Bonferroni post test. n=3/4/5.

Expression of the chemokine receptor CCR5 was significantly elevated only in brain samples from CD11c^{Cre}*Ifnar1*$^{fl/fl}$ in comparison to the naïve control and *Ifnar1*$^{-/-}$ mice (Figure 11D), whereas expression of CXCR3 on CD4^{+}T cells was elevated on all the brain samples from PbA-infected mice in comparison to the naïve control mice (Figure 11E).

Taken together, our data show that brain infiltrated CD4^{+}T-cells from infected *Ifnar1*$^{-/-}$ mice were less activated and also produced less effector molecules (grz B) than from infected WT mice. Lack of type I IFN signalling did not interfere with the expression of ICAM-1 and CXCR3 on CD4^{+} T cells during PbA infection.

3.1.10 Reduced levels of brain infiltrated natural killer cells in PbA-infected LysM^{Cre}*Ifnar1*$^{fl/fl}$ mice

Natural killer (NK) cells are innate lymphocytes with the ability to kill target cells by release of cytotoxic granules. Their role during ECM is still unclear, the Hansen group showed a role for NK cells in the recruitment of T cells into the brain, but not in performing effector functions (Hansen et al. 2007). Therefore, we next analysed whether there was a difference in the proportions of NK cells that had infiltrated into the brains of PbA-infected WT suffering from ECM and Ifnar ko mice that were protected from ECM.

We did not observed any differences in frequencies of NK cells in the brains of the infected WT mice in comparison to those of the naïve mice (Figure 12A). But it is important to note that the absolute cell counts calculated per brain were higher in the infected WT mice. The frequencies of NK cells among the PbA-infected *Ifnar1*$^{-/-}$ and CD11c^{Cre}*Ifnar1*$^{fl/fl}$ mice were comparable to the results from naive and WT infected mice, but importantly, significantly decreased in brains of PbA-infected LysM^{Cre}*Ifnar1*$^{fl/fl}$ mice (Figure 12A).

NK cell are also able to produce granzyme B, another important effector molecule in ECM. We observed the strongest signals of intracellular granzyme B in NK cells within brain samples from the infected WT, in comparison to the naïve mice (Figure 12B). Although there was an increase in the expression levels of granzyme-B in NK cells among *Ifnar1*$^{-/-}$ and LysM^{Cre}*Ifnar1*$^{fl/fl}$ mice in comparison to the naïve control mice, this increase was not as high as that observed among the infected WT mice (Figure 12B). NK cells from brains of PbA-infected CD11c^{Cre}*Ifnar1*$^{fl/fl}$ mice had increased levels of granzyme-B, which were comparable to the infected WT mice (Figure 12B), which both suffered from ECM. Similar to the trend observed with T cells, these data indicate a role of type I IFN signalling in myeloid cells in recruitment of NK cells into the brain during PbAMA infection, and subsequent production of effector molecules, since the ECM protected ko mice showed impaired NK cell presence and also less granzyme B production, thereby contributing to less brain inflammation.

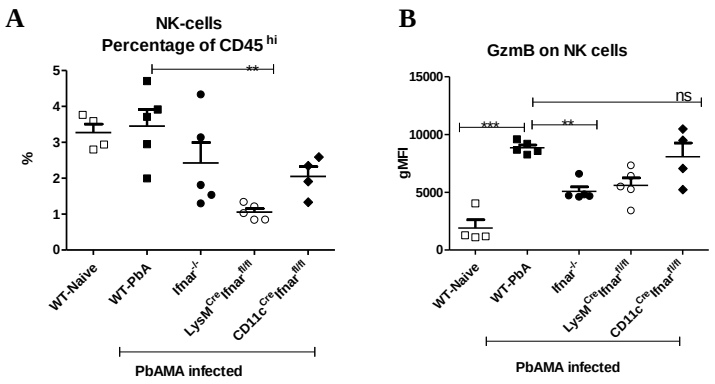

Figure 12 Less infiltration of NK cells into brains of PbA-infected Ifnar ko

C57BL/6 mice (WT, *Ifnar1*$^{-/-}$, LysM^{Cre}*Ifnar1*$^{fl/fl}$ and CD11c^{Cre}*Ifnar1*$^{fl/fl}$) were infected with 5x10^4 PbAMA iRBC i.v. On d+6p.i, Single cell suspensions were prepared from the brain, counted, stained and analysed by flow cytometry. **A**) Percentage of brain infiltrated NK cells. **B**) Expression of granzyme-B on brain infiltrated NK cells. Statistical analysis = One-way ANOVA with Bonferroni post test. n=4/5 animals per group.

3.1.11 Insignificant amounts of brain infiltrated B cells during PbAMA infection

So far, the role of B cells in the pathogenesis of ECM is not well understood. Published experimental studies with mice, did not indicate the presence of B cells within the brain infiltrated cells (Belnoue et al. 2002). In our experiments, we did not detect relevant amounts of B cells in the brains of infected WT, *Ifnar1*$^{-/-}$ and CD11c^{Cre}*Ifnar1*$^{fl/fl}$ mice (Figure 13). Although there was some B cell population in brain samples from infected LysM^{Cre}*Ifnar1*$^{fl/fl}$ and naïve mice the difference between all the groups was not statistically significant. We did not pursue the role of B cells in the brain any further.

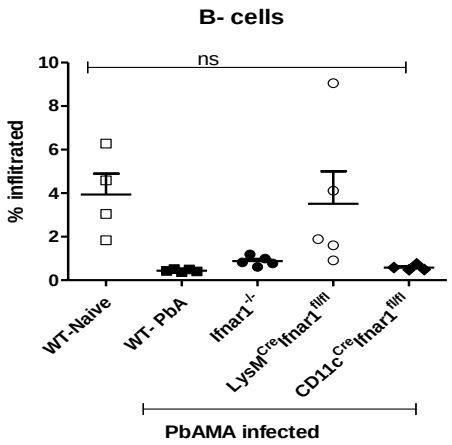

Figure 13 Non-significant amount of B cells in the brains of experimental mice

C57BL/6 mice (WT, *Ifnar1*$^{-/-}$, LysM^{Cre}*Ifnar1*$^{fl/fl}$ and CD11c^{Cre}*Ifnar1*$^{fl/fl}$) were infected with 5x10^4 PbAMA, iRBC i.v. On d+6p.i, Single cell suspensions from the brain were prepared, counted, stained and analysed by flow cytometry for the presence of B cells as determined by CD19 expression. Statistical analysis= One-way ANOVA with Bonferroni's Multiple Comparison test. n=4/5 animals per group.

3.1.12 Low counts of infiltrated CD8α$^+$DCs in brains of Ifnar ko mice

CD8α$^+$ dendritic cells (DCs) from the periphery have been shown to infiltrate into the brain during ECM; however, effector CD8$^+$ T cells do not require a second priming from DCs in the brain (Shaw et al. 2015). To address the question whether the ECM negative *Ifnar1*$^{-/-}$ mice showed differences in the composition of antigen-presenting cells that had migrated to the brains, we analysed them by flow cytometry. DCs were gated from population P1 (Figure 7A)

and characterized as CD11c^{+}CD45^{hi}CD11b^{low}CD3^{neg}. The DCs were then further characterised as CD8α^{+} DCs or CD8α^{neg} DCs.

We did not observe a significant difference in the frequency of infiltrated CD8α^{+} DCs among the infected WT, *Ifnar1*$^{-/-}$ and CD11c^{Cre}*Ifnar1*$^{fl/fl}$ mice in comparison to the naïve mice (Figure 14A). We observed a decrease in the percentage of CD8α^{+} DCs in brain samples of infected LysM^{Cre}*Ifnar1*$^{fl/fl}$. However when we calculated the absolute cell count, there were very few CD8α^{+} DCs that could be detected in the brains samples of infected Ifnar ko, with cell counts being similar to those of the naïve mice (Figure 14B).

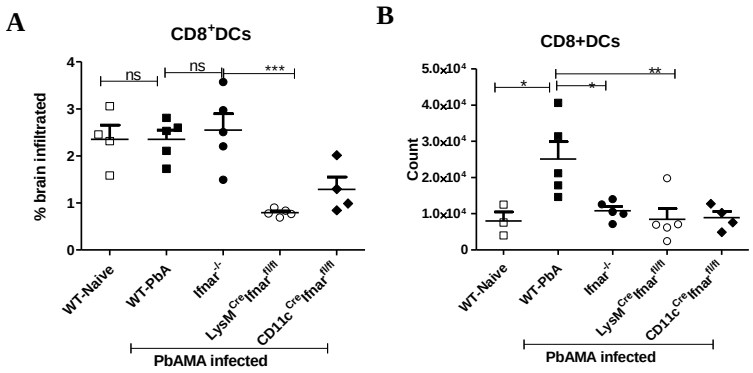

Figure 14 Ifnar ko had low numbers of brain infiltrated CD8^{+}DCs

C57BL/6 mice (WT, *Ifnar1*$^{-/-}$, LysM^{Cre}*Ifnar1*$^{fl/fl}$ and CD11c^{Cre}*Ifnar1*$^{fl/fl}$) were infected with 5x10^{4} PbAMA, iRBC i.v. On d+6p.i, single cell suspensions from the brain were prepared, counted, stained and analysed by flow cytometry. **A)** Frequency of CD8α^{+} DCs (brain) **B)** Total cell count of CD8α^{+} DCs (brain). Statistical analysis = One-way ANOVA with Bonferroni's Multiple Comparison test. n=4/5 animals per group.

3.1.13 Infiltration of inflammatory monocytes into the brain was dependent on type I IFN signalling on macrophages

Infiltrated CD8^{+} T cells and inflammatory monocytes have been found to compose the bulk percentage of brain infiltrated cells during ECM. Infiltrated monocytes were shown to play a role in recruitment of effector CD8^{+} T cells into brains of mice during ECM (Pai et al. 2014; Schumak et al. 2015). We have shown the relevance of Ly6C^{hi} inflammatory monocytes rather than neutrophils in ECM development (Schumak et al. 2015). We have shown above, that there were less lymphocytes infiltrating into the brains of *Ifnar1*$^{-/-}$ and LysM^{Cre}*Ifnar1*$^{fl/fl}$ mice in comparison to the infected WT mice during PbA infection. To further confirm the role of type I IFN signalling in brain inflammatory processes during ECM, we evaluated the infiltration of inflammatory monocytes and neutrophils into the brain. We defined infiltrated inflammatory monocytes as Ly6C^{hi}CD11b^{hi}CD45^{hi}Ly6G^{neg} and neutrophils as Ly6G^{hi}Ly6C^{int}CD11b^{hi}CD45^{hi}, these cells were gated from P-2 as indicated in (Figure 15A).

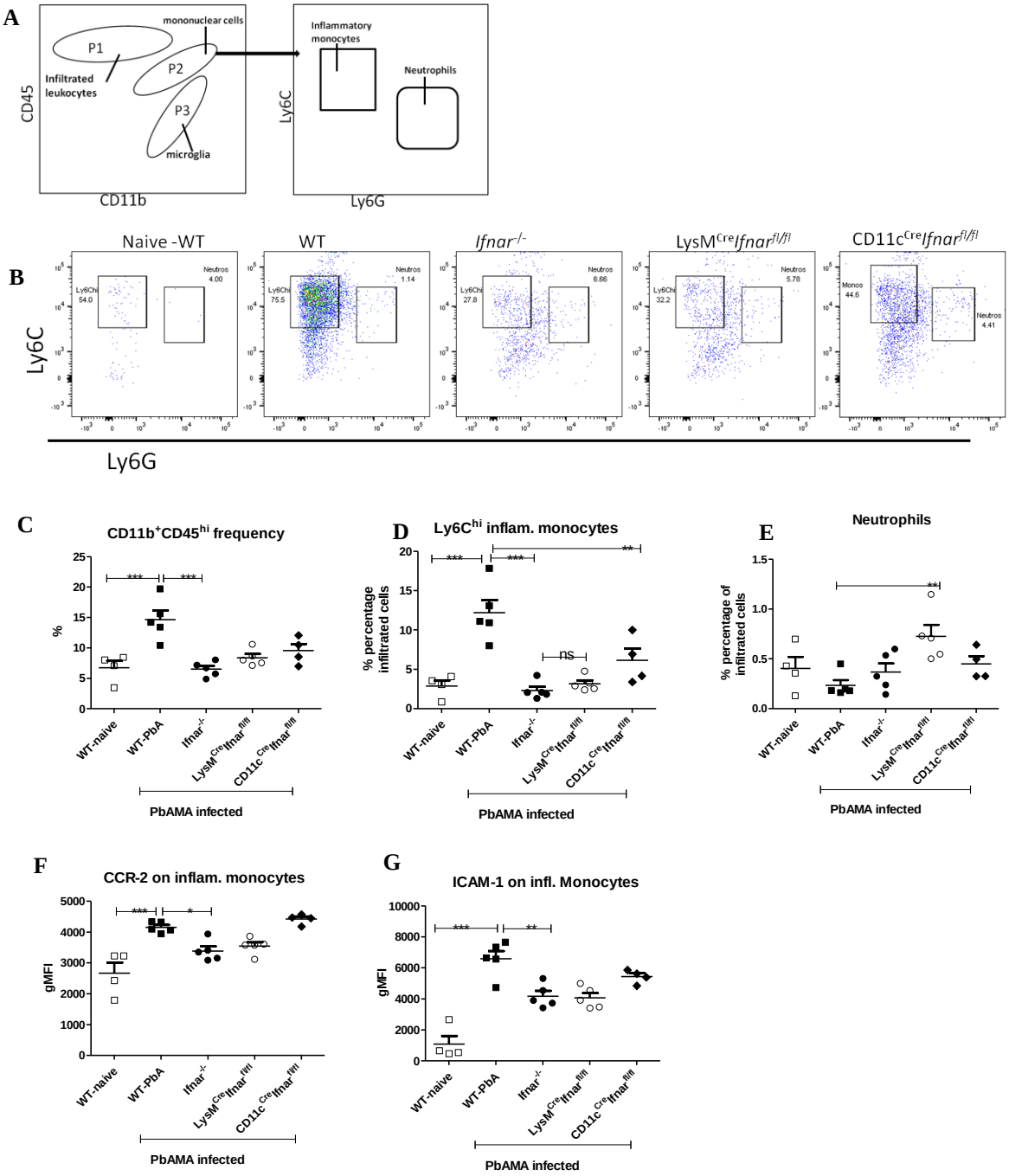

Figure 15 Type I IFN signalling has a crucial role in recruitment of inflammatory monocytes into the brain

C57BL/6 mice (WT, *Ifnar1*$^{-/-}$, LysM^{Cre}*Ifnar1*$^{fl/fl}$ and CD11c^{Cre}*Ifnar1*$^{fl/fl}$) were infected with 5x10^4 PbAMA, iRBC i.v. On d+6p.i, Single cell suspensions from the brain were prepared, counted, stained and analysed by flow cytometry **A**) Gating schematic for infiltrated monocytes and neutrophils. **B**) FACS picture of inflammatory monocytes and neutrophils from representative groups. **C**) Total percentage of brain infiltrated CD11b$^+$ population. **D**) Total percentages of Ly6C^{hi} inflammatory monocytes in the brain **E)** Total percentages of neutrophils in the brain **F**) Expression of CCR2 on Ly6C^{hi} inflammatory monocytes (brain). **G**) ICAM-1 expression levels on Ly6C^{hi} inflammatory monocyte. Statistical analysis = One-way ANOVA with Bonferroni's post test. n=4/5 per group. Data is representative of 4 independent experiments.

Brains of infected WT mice contained significantly increased frequency regarding CD11b$^+$CD45^{hi} cells, compared to the naïve mice (Figure 15C). Ly6C^{hi} inflammatory monocytes composed more than 75% of the CD11b^{hi}CD45^{hi} population among the brain

samples from the infected WT (Figure 15B). We detected >4x more inflammatory monocytes in brains samples from infected WT in comparison to the naïve (Figure 15D). All groups of infected Ifnar ko mice had approximately half the frequencies of infiltrated $CD11b^{hi}CD45^{hi}$ cells in their brains compared to the brain samples from the infected WT mice (Figure 15C&D). The infected Ifnar ko mice showed a phenotype similar to the naïve mice with very few inflammatory monocytes in their brain samples (Figure 15D). We did not observe any significant difference in the frequency of infiltrated neutrophils between samples from the PbA-infected mice and the naïve mice, however, $LysM^{Cre}$*Ifnar1*$^{fl/fl}$ mice had a higher frequency of neutrophils in their brains in comparison to brain samples of the infected WT (Figure 15E).

We further analysed the phenotype of the $Ly6C^{hi}$ inflammatory monocytes in the brain samples by examining the expression of CCR2 and ICAM-1 on their surface. CCR2 and ICAM-1 have important roles in the recruitment of monocytes to the site of inflammation during infection. We observed an elevated CCR2 expression on $Ly6C^{hi}$ inflammatory monocytes from brains of all infected animal, in comparison to those of the naïve mice (Figure 15F). Also, we detected increased levels of ICAM-1 expression on $Ly6C^{hi}$ inflammatory monocytes from brain samples of all the infected animals in comparison to the monocytes in brain samples from naïve mice (Figure 15G). However, in comparison to the samples from infected WT mice, monocytes in brain samples from both infected *Ifnar1*$^{-/-}$ and $LysM^{Cre}$*Ifnar1*$^{fl/fl}$ mice had significantly lower ICAM-1 levels (Figure 15G). This observation further supports the role of type I IFN signalling on recruitment of $Ly6C^{hi}$ inflammatory monocytes to the brain during ECM upon PbA infection, whereas ECM negative mice contained decreased levels of monocytes and less adhesion markers.

3.1.14 Brains of PbA-infected *Ifnar1*$^{-/-}$ and $LysM^{Cre}$*Ifnar1*$^{fl/fl}$ lacked inflammatory cytokine TNF, chemokines CCL3 and CCL5

Cytokines are another important factor considered to contribute in the disruption of the BBB. Members of the TNF family, which belong to the inflammatory cytokines, have been found in increased levels in the brains of both human malaria patients and mice during (experimental) cerebral malaria. Chemokine are a group of cytokines mediating chemotaxis. CCL3 and CCL5 are inflammatory chemokines secreted during inflammation, with a central role in the recruitment of T cells, NK cells and monocytes to the site of infection.

Here, we observed significant TNF production in supernatants from brain samples of infected WT and $CD11c^{Cre}$*Ifnar1*$^{fl/fl}$ mice in comparison to the naïve control (Figure 16A). Analysis of

supernatants from brain samples of infected *Ifnar1*$^{-/-}$ and LysM^{Cre}*Ifnar1*$^{fl/fl}$ mice, did not reveal any TNF production and showed comparable values as the samples from naïve mice (Figure 16A). Elevated levels of secreted chemokines CCL3 and CCL5 were measured from supernatants of brain samples of infected WT and CD11c^{Cre}*Ifnar1*$^{fl/fl}$ mice in comparison to supernatants from naïve mice (Figure 16B &C). Importantly, supernatants from brain samples of infected *Ifnar1*$^{-/-}$ and LysM^{Cre}*Ifnar1*$^{fl/fl}$ mice contained very low levels of secreted CCL3 and CCL5 with comparable results to samples from naïve mice (Figure 16B &C). This low levels in secreted inflammatory chemokines, matches with the observation made earlier, where we detected very low numbers of infiltrated T cell and inflammatory monocytes in the brains of the *Ifnar1*$^{-/-}$ and LysM^{Cre}*Ifnar1*$^{fl/fl}$ mice. The lack of TNF production observed in supernatants from brain samples of the PbA-infected *Ifnar1*$^{-/-}$ and LysM^{Cre}*Ifnar1*$^{fl/fl}$ mice correlated to the lack of inflammatory monocytes in the brains of these mice, thus indicating the protective effect of impaired monocyte migration and subsequent reduction of effector molecules.

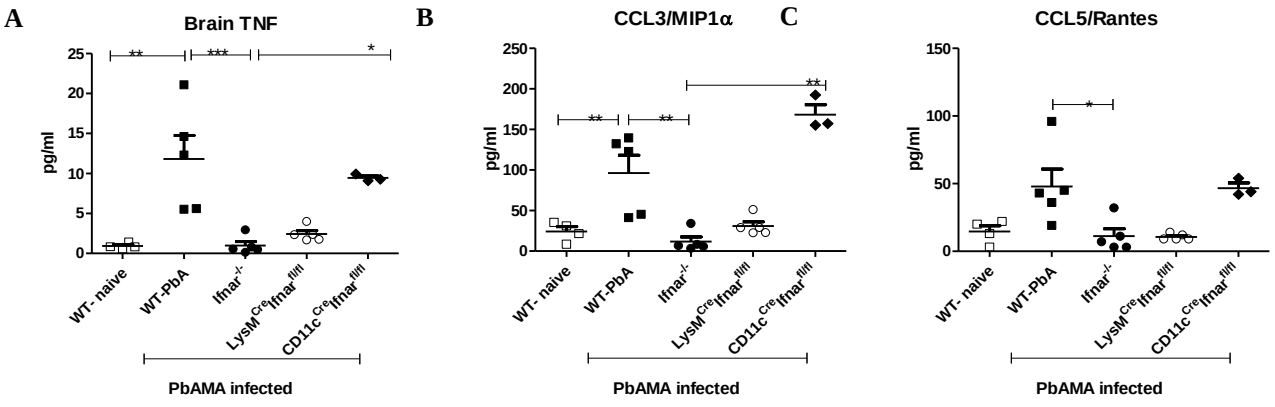

Figure 16 No TNF in brains of PbA-infected and ECM negative *Ifnar1*$^{-/-}$ and LysM^{Cre}*Ifnar1*$^{fl/fl}$ mice

C57BL/6 mice (WT, *Ifnar1*$^{-/-}$, LysM^{Cre}*Ifnar1*$^{fl/fl}$ and CD11c^{Cre}*Ifnar1*$^{fl/fl}$) were infected with 5x10^4 PbAMA, iRBC i.v. On d+6p.i. Brains were perfused, colagenase digested and homogenised, the cells were counted and 1.5x10^6 cells were cultured in triplicates in 96 well plates overnight at 37^{0}C for 24 hrs supernatant were collected and ELISA performed as described in methods. **A**) Levels of TNF production in the brain **B**) Levels of CCL3/MIP1α production in the brain **C**) Levels of CCL5/RANTES production in the brain. Statistical analysis = One-way ANOVA with Bonferroni post test. n=3/4/5 animals per group.

3.1.15 Summary of brain results

Taken together, the results from the brains of the experimental PbA-infected animals described above indicate a crucial role of type I IFN signalling (on LysM expressing cells) in causing ECM pathology due to brain inflammation. Intact signalling via Ifnar in PbA- infected WT mice resulted in infiltration of granzyme B producing effector $CD8^+$T cell and TNF producing $Ly6C^{hi}$ inflammatory monocytes into the brain of C57Bl/6 during infection with *P. berghei* ANKA, whereas PbA-infected Ifnar ko mice were protected from ECM and showed markedly decreased amounts of effector cells and soluble mediators. The table below summarises our major observations in the brain.

Table 2 Summary of results from the brain of PbA-infected mice

	Naïve	WT	*Ifnar*$^{-/-}$	LysM^{Cre}*Ifnar*$^{fl/f}$	CD11c^{Cre}*Ifnar*$^{fl/fl}$
Develop ECM	-	Positive	Negative	Negative	Positive
Breakdown of BBB		Yes	No	No	No
Infiltration of cells into the brain	-	High	Low	Low	Intermediate
$CD8^+$T cell presence	-	High	Low	Low	High
$GzmB^+CD8^+$T cell	-	High	Low	Low	High
$CD11c^+$CD8+T cells	-	High	Low	Low	High
Infl. Monocytes	-	High	Low	Low	Intermediate
TNF	-	Positive	Negative	Negative	Positive
CCL3	-	Positive	Negative	Negative	Positive
CCL5	-	Positive	Negative	Negative	Positive

3.2 Analysis of peripheral immune responses in the spleen of PbA infected Ifnar ko mice in comparison to WT mice

The spleen is a vital organ during infection with *Plasmodium* parasites, as this is the organ where immune induction against blood-borne pathogen occurs. We have shown above that the *Ifnar1*$^{-/-}$ and LysM^{cre} *Ifnar1*$^{fl/fl}$ mice were protected from ECM, characterized by a stable BBB with few cells infiltrating into their brains independently of parasitemia. We next addressed the question whether the protection from ECM we had observed among the *Ifnar1*$^{-/-}$ and LysM^{cre} *Ifnar1*$^{fl/fl}$ mice was due to altered immune responses in the spleen.

3.2.1 Ifnar ko mice had marked splenomegaly

First we performed a general analysis of the spleen. We measured the weight, size and determined the total cell count of the spleen.

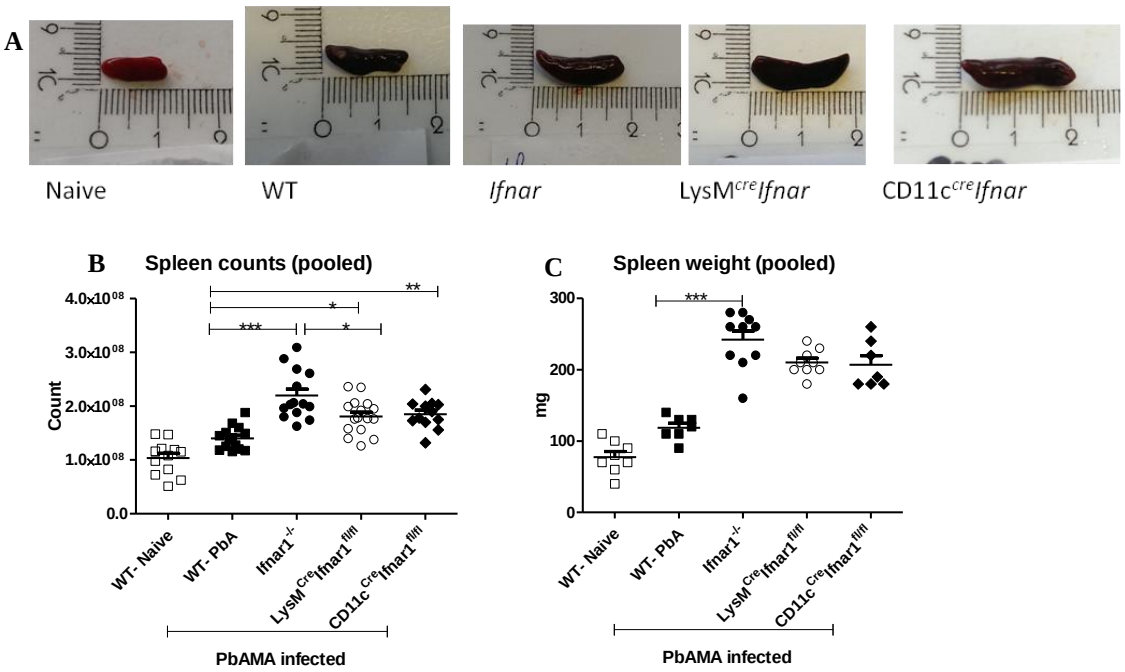

Figure 17 Splenomegaly among the Ifnar ko mice.

C57BL/6 mice (WT, *Ifnar1*$^{-/-}$, LysM^{Cre}*Ifnar1*$^{fl/fl}$ and CD11c^{Cre}*Ifnar1*$^{fl/fl}$) were infected with 5x10^4 PbAMA, iRBC i.v. On d+6p.i, Mice were perfused using PBS, spleens were photographed, weighed, then collagenase-digested. Single cell suspensions were prepared and cells counted **A**) Representative photos of the spleen. **B**.) Total spleen cell count, data pooled from 3 independent experiments n=12/16. **C**) Spleen weights, data pooled from 2 independent experiments n=7/10 per group. Statistical analysis = One-way ANOVA with Bonferroni post test.

Although we observed an increase in the size of the spleen upon PbA infection, in comparison to the naïve (Figure 17A), there was no statistical difference in both the weight of the spleen and the total cell count of splenocytes between the infected WT and the naïve control mice (Figure 17B & C). Interestingly, we observed a remarkable increase in the size, weight and total number of splenocytes in the infected Ifnar ko mice compared to those of the infected WT

and naïve mice (Figure 17A-C). The increase in splenocytes number and size was highest in the infected *Ifnar1*$^{-/-}$, in comparison to the infected WT (Figure 17B&C).

3.2.2 Unimpaired CD8^{+}T cells immune induction in the spleens of Ifnar ko

We questioned whether the protection among the ECM negative mice was due to impaired CD8^{+}T cell priming and cytotoxicity. Parasite-specific CD8^{+}T cells are primed in the spleen by CD8α^{+}DCs (Lundie et al. 2008; Shaw et al. 2015), these CD8^{+}T effector cells then migrate into the brain where they cause pathology (Haque et al. 2011; Howland et al. 2013; Lundie et al. 2008). Brain-infiltrated CD8^{+}T-cells do not require a second activation in the brain after activation in the spleen (Shaw et al. 2015). We therefore investigated whether the CD8^{+}T cells in the spleen of the PbA-infected Ifnar ko were cytotoxic and able to recognize parasite-specific antigen presented via MHC class I and to mount an Ag specific response. To this end, we performed an *in vivo* cytotoxic lysis assay, where we infected mice with transgenic PbAMA expressing ovalbumin. On day 5p.i., we injected defined amounts of fluorochrome-labelled splenocytes pulsed with MHC class I peptides SIINFEKL derived from ovalbumin and also from the parasite-endogenous antigen merozoite-surface protein 1 (MSP-1) and non-pulsed reference cells into PbA-infected mice and naïve control animals. After additional 18 hrs, the mice were sacrificed and splenocytes were isolated to determine the fluorescent signals via flow cytometry, which enabled us to calculate the specific cytolytic activity of peptide-specific T cells that were generated in immunized animals, but not in non-immune naïve control mice.

Importantly we measured in both PbAMA infected WT and Ifnar ko mice comparable parasite specific CTL activity, which was demonstrated by a specific lysis of peptide-loaded target cells presenting OVA and MSP-1 peptides (Figure 18C&D). Figure 18A shows the summary of the experiment layout and the cells were gated as indicated in Figure 18B. The CTL activity was calculated against naïve control that also received target cells but should not be able to recognise or lyse these cells as they have not yet encountered the Ag.

These data demonstrated that there was efficient parasite specific priming and cytotoxic CD8^{+} T-cells lytic activity in the spleen of all the infected mice. This was further confirmed by granzyme-B expression and production by splenocytes of only infected animals and not by naïve mice (Figure 18E-G). The expression levels of granzyme-B on CD8^{+}T cells was comparable among almost all the infected groups, with the mice having the comparable frequencies of granzyme-B^{+}CD8^{+} T cell population, (Figure 18 E&F).

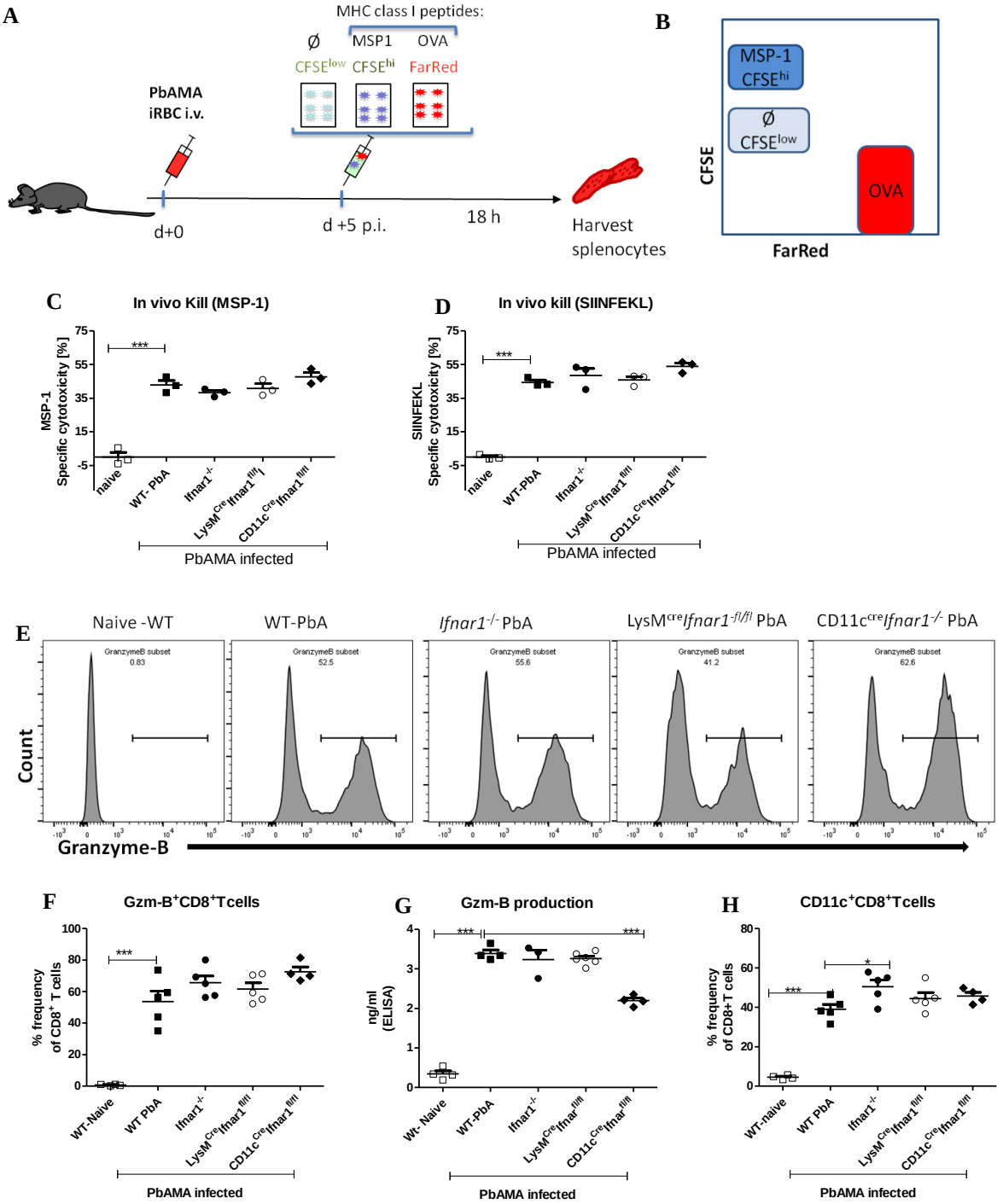

Figure 18 CD8$^+$T-cells in the spleen of Ifnar ko were able to recognise and mount an Ag specific response

C57BL/6 mice (WT, *Ifnar1*$^{-/-}$, LysM^{Cre}*Ifnar1*$^{fl/fl}$ and CD11c^{Cre}*Ifnar1*$^{fl/fl}$) mice were infected with 5x10^4 transgenic PbAMA expressing OVA. On d+5p.i., target cells were prepared from syngeneic naive donor mice by pulsing them with MHC- class I peptides SIINFEKL and peptides from MSP-1, labelled with fluorochromes FarRed and CFSE respectively, and were then injected i.v into the naïve uninfected and PbAMA infected mice. Another 18 h later, cytolytic activity was measured and calculated against naïve controls. **A)** Experiment layout **B**) Schematic of how cells were gated. **C&D**) Measurement of *in vivo* kill of MSP-1 and SIINFEKL loaded target cells. **E**) Representative histograms of granzyme-B expression on CD8$^+$T cells. **F**) Frequency of granzyme-B$^+$CD8$^+$ T cells. **G**) ELISA analysis of granzyme–B production by splenocytes. Statistics= One way ANOVA with Bonferroni post test. n=4/5 animals per group.

Granzyme-B was not only being expressed, but was also being released as shown by ELISA assay, except for PbA-infected CD11c^{Cre}*Ifnar1*$^{fl/fl}$ mice, which showed decreased granzyme-B levels, the other infected groups were comparable (Figure 18G).

Expression of CD11c on CD8^{+} T cells was observed among all infected mice, but not among the naïve mice (Figure 18H), interestingly, infected *Ifnar1*$^{-/-}$ mice had more CD11c^{+}CD8^{+}T-cells in their spleen than the infected WT mice (Figure 18H). Taken together, these results show that lack of type I IFN signalling was dispensable in induction of CTL response in the spleen, as splenic parasite-specific CD8^{+}T cell were efficiently generated. However, there were more cytotoxic CD8^{+}T-cells in the spleens of *Ifnar1*$^{-/-}$ mice, which could be a result of inefficient activation or rather active retention in the spleen.

3.2.3 Lack of type I IFN signalling did not change time points of innate and adoptive immune response during PbA infection

Furthermore, we addressed the question, whether the lack of type I IFN signalling might influence the immune milieu already during the early phases of PbA infection. Therefore, we next compared two different time points of infection; we examined d+2 post infection to analyse the innate immune responses and d+5 before the exit of the primed effector cells from the spleen. In addition, we analysed naïve WT and naïve ko mice to define the baseline.

We observed on d+2 p.i. an increase of splenic DCs among all the infected groups when compared to the non-infected control animals. Although the increase in DCs was observed in both infected WT and Ifnar ko in comparison to the naïve, infected WT had the highest increase of splenic DC populations on d+2 in comparison to the infected Ifnar ko, with significant difference to LysM^{Cre}*Ifnar1*$^{fl/fl}$ and CD11c^{Cre}*Ifnar1*$^{fl/fl}$ mice (Figure 19A). However, a sharp decline in the number of DCs was observed on d+5 among the infected WT in comparison to d+2, with decline resulting in the values at d+5 being comparable to the naïve (Figure 19A). The increase in the total DCs cell counts resulted in elevated amounts of CD8α^{+}DCs and CD8α^{neg}DCs on d+2, with the highest increase being observed among the infected WT mice (Figure 19B &C). We detected similar amounts of CD8α^{+}DCs on d+2 among infected *Ifnar1*$^{-/-}$ and LysM^{Cre}*Ifnar1*$^{fl/fl}$ mice, however, this population was decreased in splenic samples from CD11c^{Cre}*Ifnar1*$^{fl/fl}$ mice (Figure 19B), whereas the population of CD8α^{neg} DCs was increased comparably on day 2 among all the groups (Figure 19C). On day 5p.i, the total cell counts of CD8α^{+}DCs and CD8α^{neg}DCs were strongly reduced among all the infected groups (Figure 19B&C).

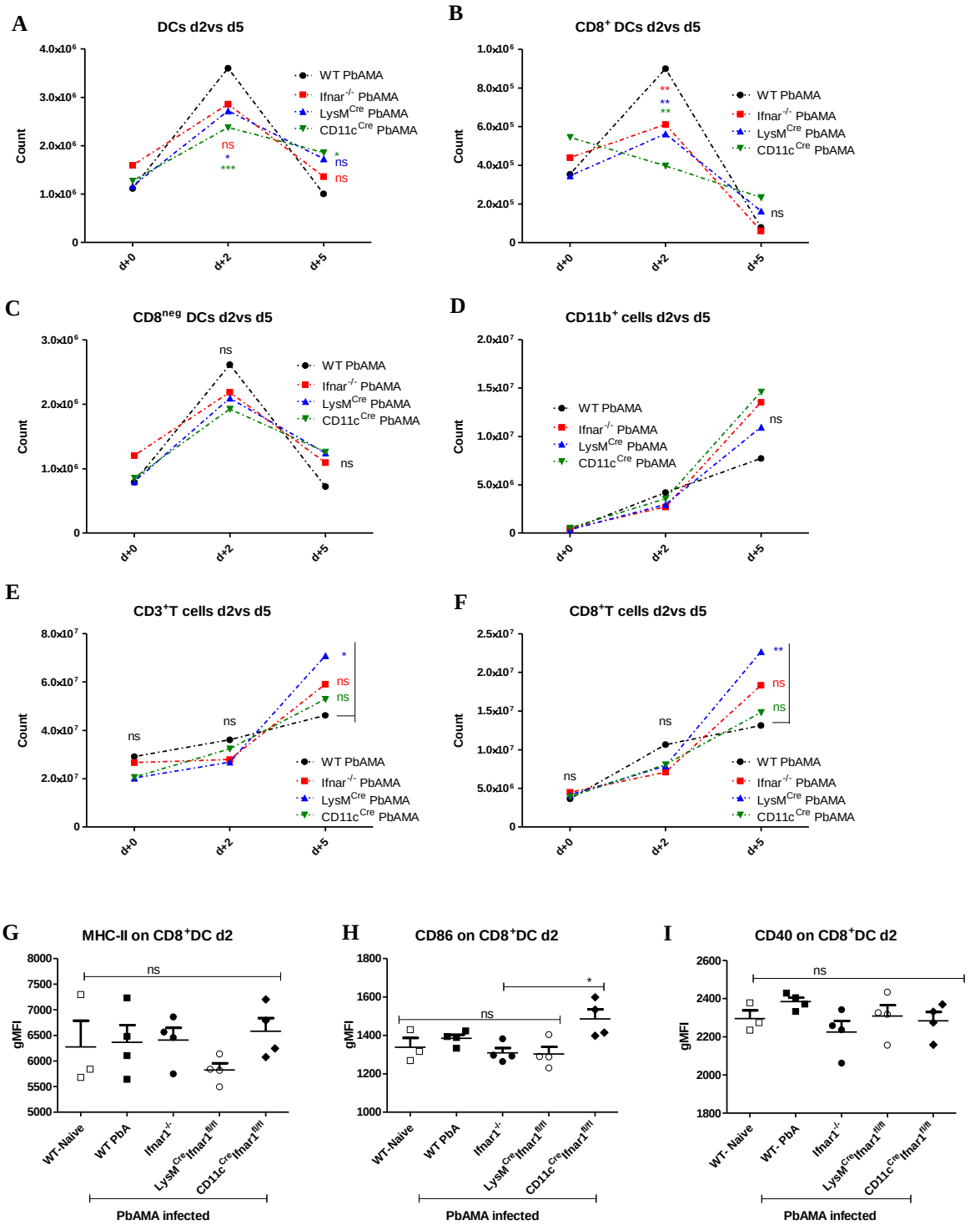
A
DCs d2vs d5
Count
WT PbAMA
Ifnar-/- PbAMA
LysMCre PbAMA
CD11cCre PbAMA
d+0
d+2
d+5
B
CD8+ DCs d2vs d5
C
CD8neg DCs d2vs d5
D
CD11b+ cells d2vs d5
E
CD3+T cells d2vs d5
F
CD8+T cells d2vs d5
G
MHC-II on CD8+DC d2
gMFI
WT-Naive
WT PbA
Ifnar1-/-
LysMCreIfnar1fl/fl
CD11cCreIfnar1fl/fl
PbAMA infected
H
CD86 on CD8+DC d2
I
CD40 on CD8+DC d2

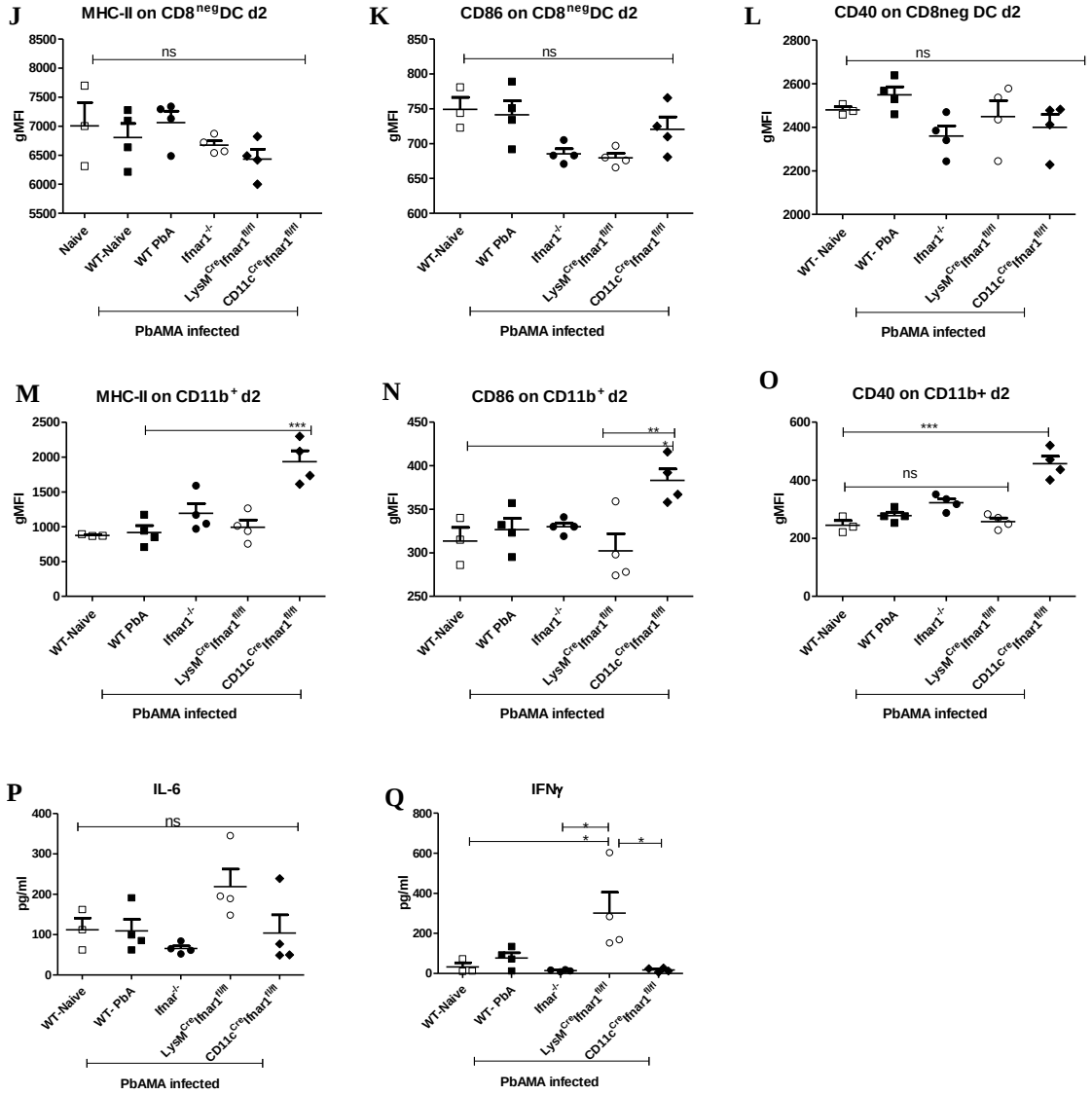

Figure 19 Ifnar ko were not delayed in induction of both innate and adoptive immune response

C57BL/6 mice (WT, *Ifnar1*$^{-/-}$, LysM^{Cre}*Ifnar1*$^{fl/fl}$ and CD11c^{Cre}*Ifnar1*$^{fl/fl}$) were infected with 5x10^4 PbAMA iRBCs i.v. On d+2 p.i and d+5 p.i., spleens were harvested, digested, and single cell suspensions prepared. The cells were counted, stained and analysed using flow cytometry. (**A-F**) Compares cells counts between (d+0) un-infected naive, d+2 and d+5, for total DCs, CD8$^+$DCs, CD8^{neg}DCs, CD11b$^+$, total T cells and CD8$^+$T cells, (**G-O**) Shows expression levels of co stimulatory molecules and MHC class-II on APC populations (**P-Q**) Production of IL-6 and IFNγ measured by ELISA from supernatants of spleen cells from d+2. Statistics= One-way ANOVA with Bonferroni post test analysis, n=3/4 animals per group.

We observed at first a slow increase in the total cell count of CD11b$^+$ on d+2p.i. in relation to the counts of the naïve in all the infected mice (Figure 19D). But by d+5p.i, the CD11b population had increased significantly as compared with d+2 p.i, with 2x fold increase in infected WT, 5x in infected *Ifnar1*$^{-/-}$, and 3.8x in LysM^{Cre}*Ifnar1*$^{fl/fl}$ and CD11c^{Cre}*Ifnar1*$^{fl/fl}$ mice (Figure 19D).

Total T cell count cells and its CD8$^+$ T cells fraction were comparable between the infected groups and the naïves on d0 and d2, but importantly, with an increase being observed on d5

(Figure 19E & F). We observed slightly elevated numbers of $CD8^+$ T cells among the infected WT on d+2 compared to the infected Ifnar ko mice, however, this difference was not statistically significant (Figure 19F). On d+5 p.i., PbA-infected Ifnar ko mice contained the strongly elevated numbers of $CD8^+$ T cells in comparison to the infected WT, with the highest increase being observed among the $LysM^{Cre}$*Ifnar1*$^{fl/fl}$ mice (Figure 19 F).

The expression levels of MHC class-II molecule and co stimulatory molecules CD86 and CD40 on DCs on d+2 were comparable among all the animals, with the exception of $CD11c^{Cre}$*Ifnar1*$^{fl/fl}$ mice, which had increased expression of CD86 on $CD8\alpha^+$DCs (Figure 19G-L). We detected enhanced expression of CD40, CD86 and MHC class-II molecule by $CD11b^+$ cells in samples from the infected $CD11c^{Cre}$*Ifnar1*$^{fl/fl}$ mice in comparison to the naïve control mice and to all the other infected groups (Figure 19M-O). Interestingly, we observed early production of IL-6 and IFNγ in the supernatant from $LysM^{Cre}$*Ifnar1*$^{fl/fl}$ mice; here, IFNγ was statistically significant from naïve and other infected ko group, but not to the infected WT mice (Figure 19P & Q). Taken together our data show that induction of innate and adoptive immune response was not impaired or delayed in ECM protected mice. Also, we observed early production of pro-inflammatory cytokines among the infected $LysM^{Cre}$*Ifnar1*$^{fl/fl}$ mice, which could have had a role in their observed protection ECM.

3.2.4 Splenocytes of *Ifnar1*$^{-/-}$ and $LysM^{Cre}$*Ifnar1*$^{fl/fl}$ produced both pro and anti-inflammatory cytokines at balance.

Plasmodium infection is characterised by the production of both pro- and anti-inflammatory cytokines. Next, we evaluated whether differences in cytokine production might have a role in the ECM protection that we had observed among PbA-infected *Ifnar1*$^{-/-}$ and $LysM^{Cre}$*Ifnar1*$^{fl/fl}$ mice. We analysed on day 6 p.i. the production of the pro-inflammatory cytokines TNF, IFNγ and IL-6, as well as the anti- inflammatory cytokine IL-10 in splenocyte cultures from the different experimental groups.

We measured increased levels of IFNγ in splenocytes cultures prepared from PbA-infected WT and Ifnar ko mice in comparison to the naïve mice, which - as expected - did not produce any IFNγ, while cells from PbA-infected $CD11c^{Cre}$*Ifnar1*$^{fl/fl}$ produced higher amounts in comparison to the samples of PbA-infected WT mice (Figure 20A). In contrast to our observation in the brain-derived primary cells, TNF was highly produced by splenocytes from infected *Ifnar1*$^{-/-}$ and $LysM^{Cre}$*Ifnar1*$^{fl/fl}$ mice in comparison to samples from the naïve control mice (Figure 20B). Samples from infected WT and $CD11c^{Cre}$*Ifnar1*$^{fl/fl}$ mice contained increased

TNF levels, however, when compared to the splenocyte cultures from naïve mice, infected *Ifnar1*$^{-/-}$ and LysM^{Cre}*Ifnar1*$^{fl/fl}$ mice, no statistical significance was observed (Figure 20 B). We were surprised to observe strong production of IL-6 by splenocytes of infected *Ifnar1*$^{-/-}$ and LysM^{Cre}*Ifnar1*$^{fl/fl}$ mice, as their levels were significantly higher than the PbA-infected WT mice, whose values were comparable to the naive control mice (Figure 20 C).

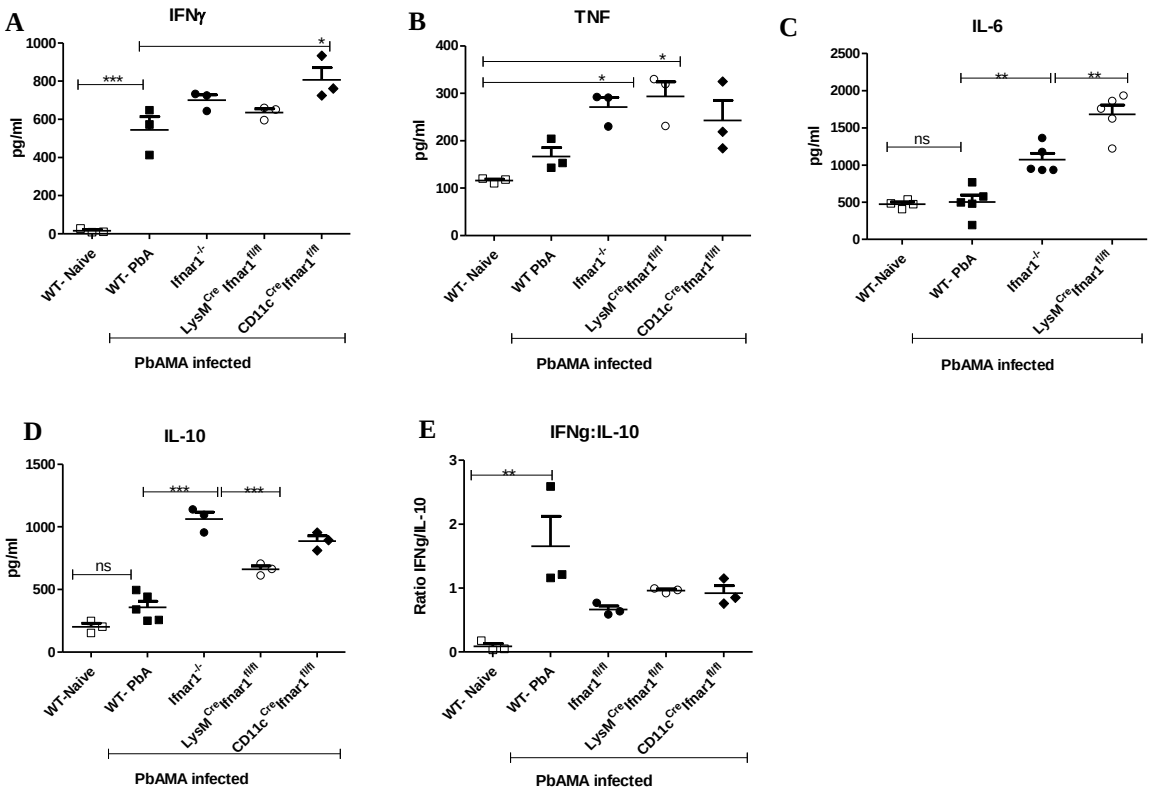

Figure 20 Splenocytes from Ifnar ko produced both pro- and anti- inflammatory cytokines

C57BL/6 (WT, *Ifnar1*$^{-/-}$, LysM^{Cre}*Ifnar1*$^{fl/fl}$ and CD11c^{Cre}*Ifnar1*$^{fl/fl}$) mice were infected with 5x10^4 PbAMA iRBCs i.v. On d+6 p.i., spleens were harvested, digested, and single cell suspensions prepared. The cells were counted and 1x10^6 cells plated in triplicates in 96 well plates, the cultures were then incubated for 24hrs at 37^{0}C. Supernatants were collected and ELISA performed as described in methods. (**A**) IFNγ Production (**B**) TNF production. (**C**) IL-6 production.(**D**) IL-10 production (**E**) Ratio of IFNγ:IL-10 . Statistics = One-way ANOVA with Bonferroni post test analysis. n=3/4/5 animals per group.

Splenocytes from PbA-infected LysM^{Cre}*Ifnar1*$^{fl/fl}$ produced almost twice as much IL-6 as cells from infected *Ifnar1*$^{-/-}$ mice and thrice as much as the splenocytes from PbA-infected WT and the naïve mice (Figure 20C). We did not observe a significant induction of IL-10 production in the splenocyte cultures of infected WT mice compared to the naïve mice (Figure 20D). but importantly, splenocytes from infected *Ifnar1*$^{-/-}$ mice produced the highest amounts of IL-10, which was 5x more than the splenocytes from naïve, 3x more than those of the infected WT and 1.5x times more than the infected LysM^{Cre}*Ifnar1*$^{fl/fl}$ (Figure 20D). Splenocytes from PbA-infected LysM^{Cre}*Ifnar1*$^{fl/fl}$ produced three and two times more IL-10 than those from naïve and

those from PbA-infected WT mice respectively, while splenocytes from CD11c^{Cre}*Ifnar1*$^{fl/fl}$ produced four times more than from naïve and 2x more than from infected WT, respectively (Figure 20D). This increase resulted in a distinct shift of the ratio of IFNγ vs IL-10 in ECM-negative groups of mice (Figure 20E). Taken together, this data suggest a role of IL-10 produced by splenocytes of PbA-infected *Ifnar1*$^{-/-}$ and LysM^{Cre}*Ifnar1*$^{fl/fl}$ mice in counteracting IFNγ, and probably controlling inflammation that occurs during PbAMA infection.

3.2.5 Altered CD4^{+}:CD8^{+} T-cell ratio in the spleens of infected Ifnar ko mice

We have shown that upon PbA infection, the priming of effector CD8^{+}T cells in the spleens of Ifnar ko was apparently unimpaired and comparable to that of the infected WT mice, since the infected groups of Ifnar ko mice were able to recognise and lyse peptide-loaded target cells (Figure 18C&D). Interestingly, Ifnar ko mice presented pronounced splenomegaly and increased total cell counts (Figure 17A-C). We next evaluated splenocyte populations in details; first we analysed the T cells as these are the major effector cell population during ECM and made responsible for pathology.

We did not observe a difference between the cells from infected WT mice and the naïve in the total number of splenic CD3^{+} T cell, CD8^{+} T cells or CD4^{+}T cells (Figure 21A-C). But, importantly the infected Ifnar ko presented with an increase in splenic cell counts of CD3^{+}T cell, CD8^{+}T cells and CD4^{+}T cells in comparison to the naïve and WT infected mice (Figure 21A-C). Infected *Ifnar1*$^{-/-}$ mice had increased CD3^{+}T cells counts in their spleen samples, this was an average fold increase of; 2.4x to the naïve, 2.2x to the infected WT, 1.4x to the infected LysM^{Cre}*Ifnar1*$^{fl/fl}$ mice but comparable to the CD11c^{Cre}*Ifnar1*$^{fl/fl}$ (Figure 21A). This increase in total T cell counts resulted in a significant increase in CD8^{+}T cells counts in spleens of *Ifnar1*$^{-/-}$ mice, with fold increase of; 2.8x to the naïve, 2.5x to the infected WT and 1.4x to the infected LysM^{Cre}*Ifnar1*$^{fl/fl}$ mice (Figure 21B). We also measured increased cell counts of CD4^{+}T on splenocytes from *Ifnar1*$^{-/-}$ mice, with fold increase of ~1.7% ($\pm$0.2%) to the naïve and infected WT mice, whereas, the counts were comparable to the infected LysM^{Cre}*Ifnar1*$^{fl/fl}$ and CD11c^{Cre}*Ifnar1*$^{fl/fl}$ mice (Figure 21C). Splenocytes samples of infected LysM^{Cre}*Ifnar1*$^{fl/fl}$ mice had increased CD3^{+}T cells counts, resulting in high CD8^{+}T cells count, with a fold increase; of ~1.86% ($\pm$0.1%) to the naïve and infected WT mice (Figure 21B). The CD4^{+}T cell counts from the spleen samples of infected LysM^{Cre}*Ifnar1*$^{fl/fl}$ mice were equally increased in comparison to the naïve and the infected WT with fold increase of ~1.5% ($\pm$0.15%) to the naïve and infected WT mice (Figure 21C). While infected CD11c^{Cre}*Ifnar1*$^{fl/fl}$ had comparable values of CD3^{+} T cells, CD8^{+} T cells and CD4^{+} T cells to the infected *Ifnar1*$^{-/-}$ mice (Figure 21A-C).

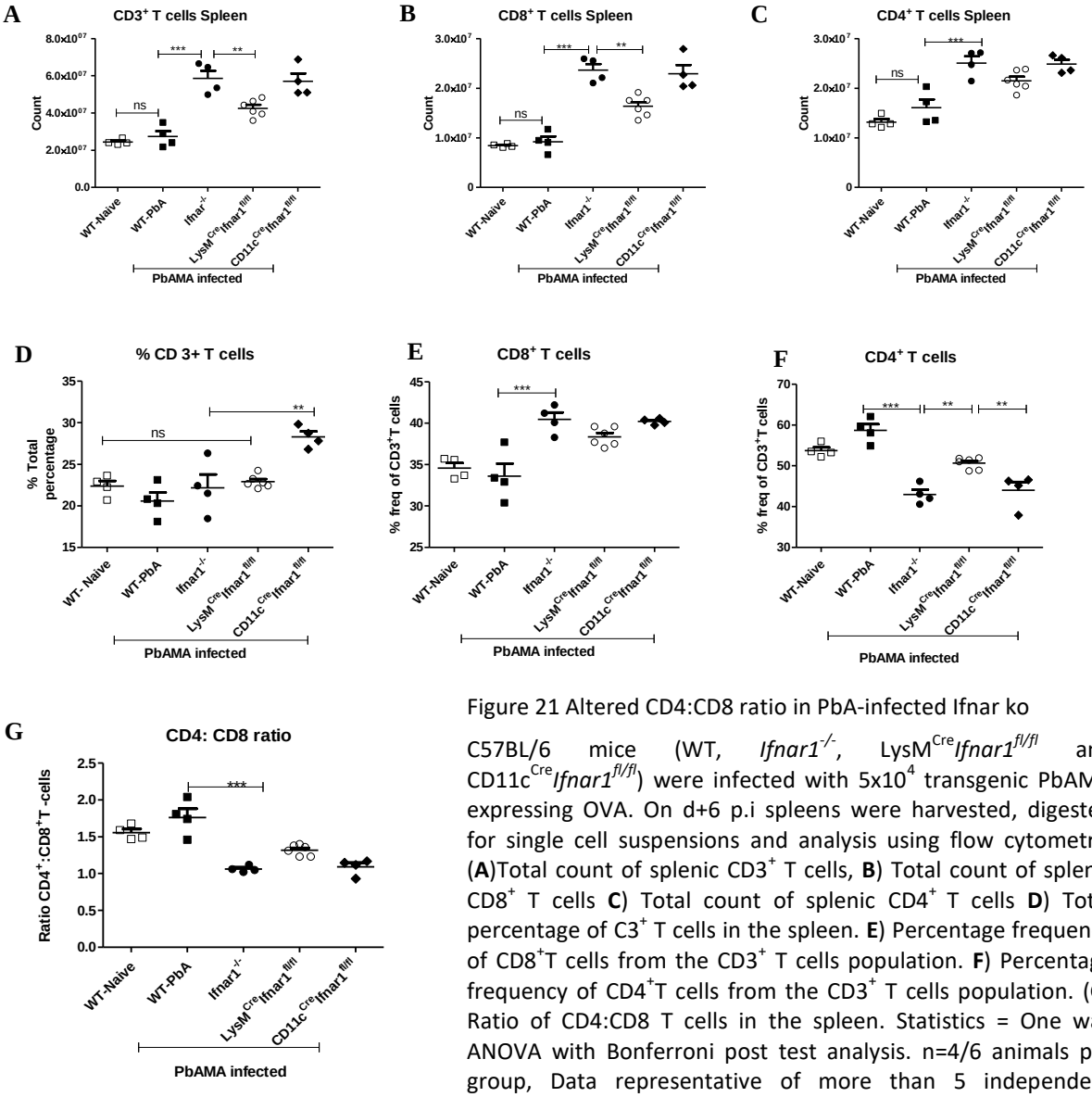

Figure 21 Altered CD4:CD8 ratio in PbA-infected Ifnar ko C57BL/6 mice (WT, *Ifnar1*$^{-/-}$, LysM^{Cre}*Ifnar1*$^{fl/fl}$ and CD11c^{Cre}*Ifnar1*$^{fl/fl}$) were infected with 5x10^4 transgenic PbAMA expressing OVA. On d+6 p.i spleens were harvested, digested for single cell suspensions and analysis using flow cytometry. (**A**)Total count of splenic CD3$^+$ T cells, **B**) Total count of splenic CD8$^+$ T cells **C**) Total count of splenic CD4$^+$ T cells **D**) Total percentage of C3$^+$ T cells in the spleen. **E**) Percentage frequency of CD8$^+$T cells from the CD3$^+$ T cells population. **F**) Percentage frequency of CD4$^+$T cells from the CD3$^+$ T cells population. (**G**) Ratio of CD4:CD8 T cells in the spleen. Statistics = One way ANOVA with Bonferroni post test analysis. n=4/6 animals per group, Data representative of more than 5 independent experiments.

The percentage of total T cells in the spleen were comparable among the naïve, infected WT, *Ifnar1*$^{-/-}$ and LysM^{Cre}*Ifnar1*$^{fl/fl}$ mice, however, CD11c^{Cre}*Ifnar1*$^{fl/fl}$ had a significant increase in their percentage of splenic T cells (Figure 21D). Most important, we observed a major switch in the frequency of CD8$^+$T cells and CD4$^+$T cells in the spleen of the infected Ifnar ko, with CD8$^+$T cells being the major population in their spleens and not CD4$^+$T cells (Figure 21 E-F). This increase in the total count and shift in frequency of CD8$^+$T cells, resulted in an altered CD4:CD8 *ratio* among the Ifnar ko (Figure 21G). Taken together, the altered CD4:CD8 ratio indicates either that the observed protection from ECM might be due to inefficient activation, or actively blocked emigration of CD8$^+$ T cells from the spleen after priming and proliferation.

3.2.6 Spleens of Ifnar ko mice contained high percentage of CXCR3^{+}CD8^{+}T cells

As we have demonstrated above, the cytotoxic activity and the priming of CD8^{+}T cells was apparently unimpaired in ECM negative PbA-infected Ifnar ko mice in comparison to ECM positive PbA-infected WT mice. However, we also observed accumulation of T cells in the spleens of Ifnar ko mice. We next addressed the question whether the retained T cells displayed a different phenotype to that of the equivalent T cells in the spleens of PbA-infected WT mice, which suffered from ECM. We therefore compared the expression of activation markers LFA-1α (CD11a), CD69, PD-1, CTLA-4 and intercellular adhesion molecule ICAM-1. We also examined for expression of chemokine receptors CCR5, CXCR3 and CCR7, which have been shown to have a role in the migration of T cells into the brain during ECM (Belnoue et al. 2003; Zhao et al. 2014; Van den Steen et al. 2008).

We observed increased expression of activation markers CD69, CD11a, ICAM-1, as well as of regulatory markers CTLA-4 and PD-1 on splenic CD8^{+}T cells in all PbA-infected animals in comparison to the naïve (Figure 22A-E). Expression of CD69, CD11a, ICAM-1 and CTLA-4 on splenic CD8^{+}T cells was equally elevated in the infected WT and infected ko mice (Figure 22A-D). Although the splenic CD8^{+} T cells from infected *Ifnar1*$^{-/-}$ had increased levels of PD-1 in comparison to the naïve mice, these levels were significantly lower than the infected WT mice and infected CD11c^{Cre}*Ifnar*$^{fl/fl}$ mice (Figure 22E). We observed a slight but non-significant increase in the percentage of CD8^{+}T cells expressing CCR5 in the spleens of infected WT mice in comparison to the naïve control mice, which ,as expected, did not express this inflammatory chemokine receptor (Figure 22F). The percentage of splenic CD8^{+}T cells expressing CCR5 was significantly higher among the infected Ifnar ko mice in comparison to the infected WT mice (Figure 22F). CXCR3 was strongly expressed only on CD8^{+}T cells of infected mice but not on CD8^{+}T cells of naive mice (Figure 22G). Importantly, we observed significantly elevated frequency of CXCR3^{+}CD8^{+}T cells in the spleens of the infected Ifnar ko mice, (16%$\pm$3 difference), in comparison to the infected WT mice (Figure 22G). The percentage of splenic CD8^{+}T expressing CCR7 was increased in samples from all the infected groups of mice in comparison to the naïve, although infected CD11c^{Cre}*Ifnar1*$^{fl/fl}$ had higher percentages in comparison to the other infected groups of mice (Figure 22H).

These data show that the CD8^{+} T cells from ECM negative ko mice expressed similar levels of activation markers as those of the infected WT, with the exception of PD1. Strikingly, PbA-infected ko mice contained more CD8^{+} T cells expressing the important chemokine receptors required for emigration from the spleen, suggesting the arrest or retention of these CD8^{+} T cells

in the spleens of the Ifnar ko mice was not due to the lack of activation or lack of expression of the chemotaxis receptors.

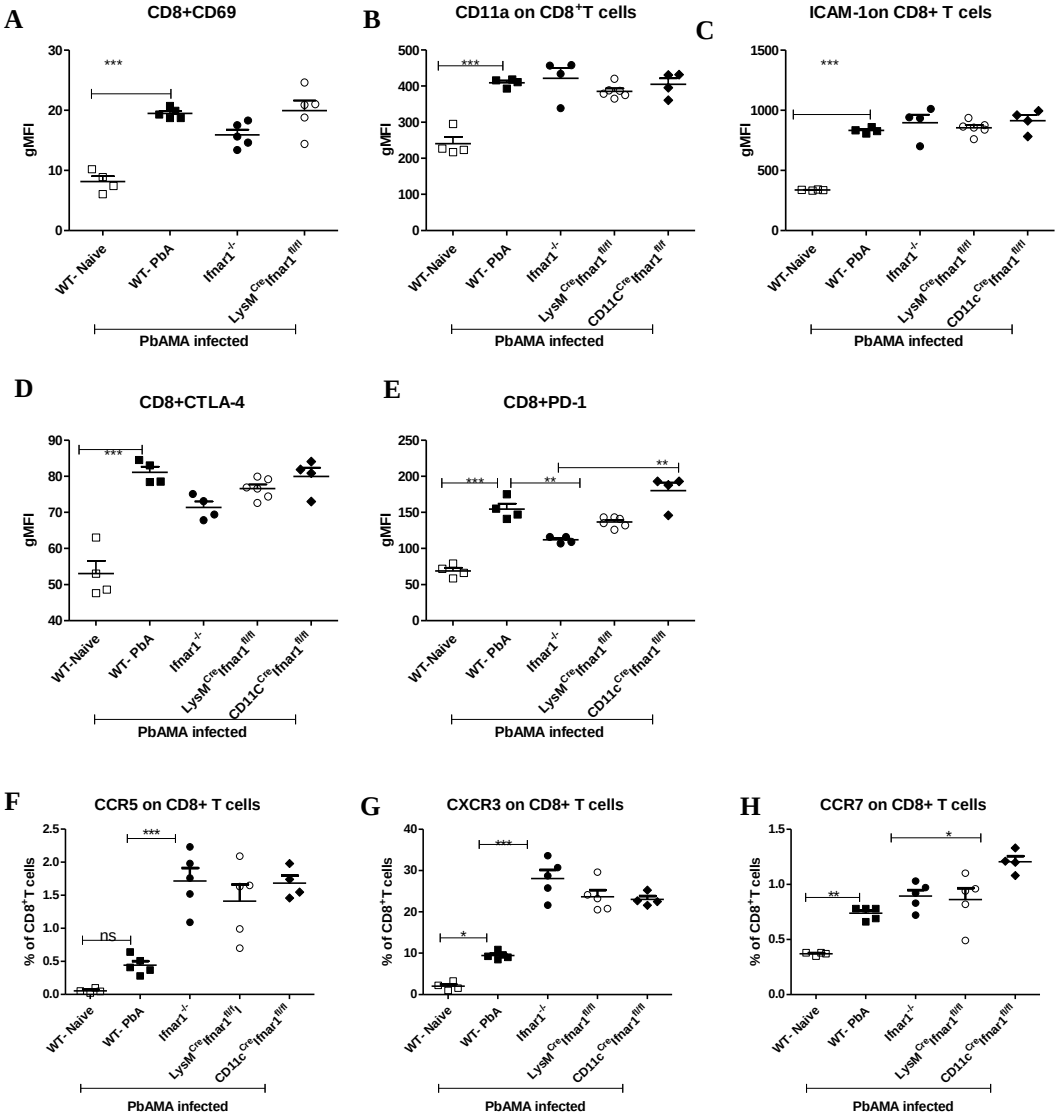

Figure 22 CD8$^+$ T cells of Ifnar ko display an activated status during PbAMA infection

C57BL/6 (WT, *Ifnar1*$^{-/-}$, LysM^{Cre}*Ifnar1*$^{fl/fl}$ and CD11c^{Cre}*Ifnar1*$^{fl/fl}$) mice were infected with 5x10^4 transgenic PbAMA expressing OVA, on d+6 p.i ,spleens were harvested, digested and single cell suspensions prepared. The cells were counted, stained and analysed using flow cytometry. (**A-E)** Expression of CD69, CD11a, ICAM-1, CTLA-4 and PD1 on CD8$^+$ T cells. (**F-G**) Percentages of splenic CD8$^+$T cells expressing CCR5, CXCR3 and CCR7. Statistics = One-way ANOVA with Bonferroni post test analysis. n=4/5 animals per group.

3.2.7 CD4$^+$T cells of Ifnar ko developed a similar Th-1 response as the WT

We further investigated if the protection from ECM in PbA-infected Ifnar ko mice we had observed was due to alteration in splenic CD4$^+$ T cells. As malaria is a T-helper 1 (Th-1) driven disease, we questioned whether the protection we had observed in the ECM protected mice was due to a shift of the subtype, from a Th-1 to either a regulatory or anti inflammatory CD4$^+$ T cell subtype in the splenic milieu, as mice deficient of the transcriptional factor T-bet have

been shown to be 70% protected from ECM (Oakley et al. 2013). We therefore analysed on day 6 p.i splenic $CD4^+CD3^+$ T cells for presence of the different $CD4^+$ T cell subsets, by analysing the expression of their phenotype driven transcription factors; T-bet for Th-1, GATA3 for Th-2, FoxP3 for T-regs and RoRγ for Th-17. We also analysed the expression pattern of activation markers, adhesion molecules chemokine receptors and cytotoxic granules on splenic $CD4^+$T cells, similar to the analysis of the $CD8^+$T cells described above.

We observed in all the PbA-infected mice an increased percentage of splenic $CD4^+$T cells displaying a Th-1 phenotype, characterised as $CD4^+$T cells expressing the transcription factor T-bet, $Tbet^+CD4^+CD3^+CD8^{neg}NK1.1^{neg}$ (Figure 23A & B). The percentage of $CD4^+$T cells expressing a Th-1 phenotype was significantly higher (~24%) among the infected WT mice in comparison to the naïve control mice that had only ~3% of their $CD4^+$ T cells expressing T-bet (Figure 23A & B). Importantly, we observed that the splenic $CD4^+$T cells of ECM-protected mice contained a clear Th-1 population, PbA-infected *Ifnar1*$^{-/-}$ mice had an average 20% more splenic $CD4^+$T cells expressing T-bet compared to the infected WT mice (Figure 23A & B). The percentage of splenic Th-1 cells in samples from the infected $LysM^{Cre}$*Ifnar1*$^{fl/fl}$ mice were comparable to the infected WT, and significantly lower than the infected *Ifnar1*$^{-/-}$ mice and $CD11c^{Cre}$*Ifnar1*$^{fl/fl}$ mice (Figure 23B). We observed an elevated splenic Th-1 population in infected $CD11c^{Cre}$*Ifnar1*$^{fl/fl}$ mice in comparison to the infected WT mice, however, the percentage were significantly lower than in the infected *Ifnar1*$^{-/-}$ mice (Figure 23B). The percentage of splenic $CD4^+$ T cells that expressed the transcription factor FoxP3, T-regs, were significantly reduced among all the infected groups of mice in comparison the naïve control mice (Figure 23A & C). The percentage of splenic $CD4^+$T that had differentiated into T-regs, were comparable among the infected WT, *Ifnar1*$^{-/-}$ and $CD11c^{Cre}$*Ifnar1*$^{fl/fl}$ mice, however, the infected $LysM^{Cre}$*Ifnar1*$^{fl/fl}$ mice had significantly higher percentages than the other infected groups of mice (Figure 23A & C). The percentage of splenic $CD4^+$ T cells expressing granzyme B was increased among all the infected groups of mice in comparison to the naïve, with the Ifnar ko having a significantly higher percentage of these cells in compared to the infected WT mice (Figure 23D). We did not detect any hints indicative for splenic Th-2 or Th-17 cells in samples from all the mice groups, through the analysis of their transcriptional factors GATA3 and RORγ T (data not shown).

Regarding the expression of activation or regulatory surface markers, we observed elevated expression of CD69, PD1and ICAM-1 on splenic $CD4^+$T-cells among all infected animals in comparison to the naïve (Figure 23E, F&G). Expression of CD69 on splenic $CD4^+$T cells in

samples from infected WT were comparable to the infected LysM^{Cre}*Ifnar1*$^{fl/fl}$ mice, but were higher than in the infected *Ifnar1*$^{-/-}$ mice (Figure 23 E). Even though all the infected groups of mice had elevated levels of PD1 and ICAM-1 on splenic CD4^{+}T cells, CD11c^{Cre}*Ifnar1*$^{fl/fl}$ mice had significantly higher levels than the other infected groups of mice (Figure 23F & G). Although, we observed increased expression of CTLA-4 on splenic CD4^{+}T cells of the infected WT mice, this was statistically insignificant in comparison to the levels on T cells of naïve and infected Ifnar ko mice (Figure 23H).

We did not observe any differences in the percentage of splenic CD4^{+}T cells expressing CCR5 and CCR7 between the naïve control and the infected WT mice (Figure 23I & J). The percentage of splenic CD4^{+}T cells expressing CCR5 was ~13% ($\pm$1) more in all the infected Ifnar ko mice in comparison to the infected WT mice (Figure 23I). The frequency of splenic CD4^{+}T cells expressing CCR7 were higher in the infected *Ifnar1*$^{-/-}$ mice in comparison to the naïve control and the other infected groups of mice (Figure 23J). In general, splenic CD4^{+}T cells in samples from the infected groups of mice expressed more CXCR3 in comparison to the T cells from naïve mice (Figure 23K). Importantly, infected *Ifnar1*$^{-/-}$ had the highest frequency of CXCR3^{+}CD4^{+}T cells in their spleen compared to the other infected mice, this increase was; ~20%x more than infected WT mice, ~8%x more than infected LysM^{Cre}*Ifnar1*$^{fl/fl}$ mice and ~9.5%x more than infected CD11c^{Cre}*Ifnar1*$^{fl/fl}$ mice (Figure 23K). Infected LysM^{Cre}*Ifnar1*$^{fl/fl}$ and CD11c^{Cre}*Ifnar1*$^{fl/fl}$ mice both contained more splenic CXCR3^{+}CD4^{+} T cells in comparison to the infected WT mice (Figure 23K).

Taken together, these results show that the lack of type I IFN receptor did not alter the development of a Th-1 phenotype associated with *Plasmodium* infection. Importantly, we observed an increase in the frequency of Th-1 cells as well as the increase of CD4^{+}CXCR3^{+} T cells in the spleens of *Ifnar1*$^{-/-}$. This data also indicate that the T-regs had no major role in the protection observed among the *Ifnar1*$^{-/-}$ as their levels were reduced. We also observed differences between LysM^{Cre}*Ifnar1*$^{fl/fl}$ and *Ifnar1*$^{-/-}$ in the composition of their splenic CD4^{+} T cells, although both groups had displayed the same phenotype during the analysis of their brains.

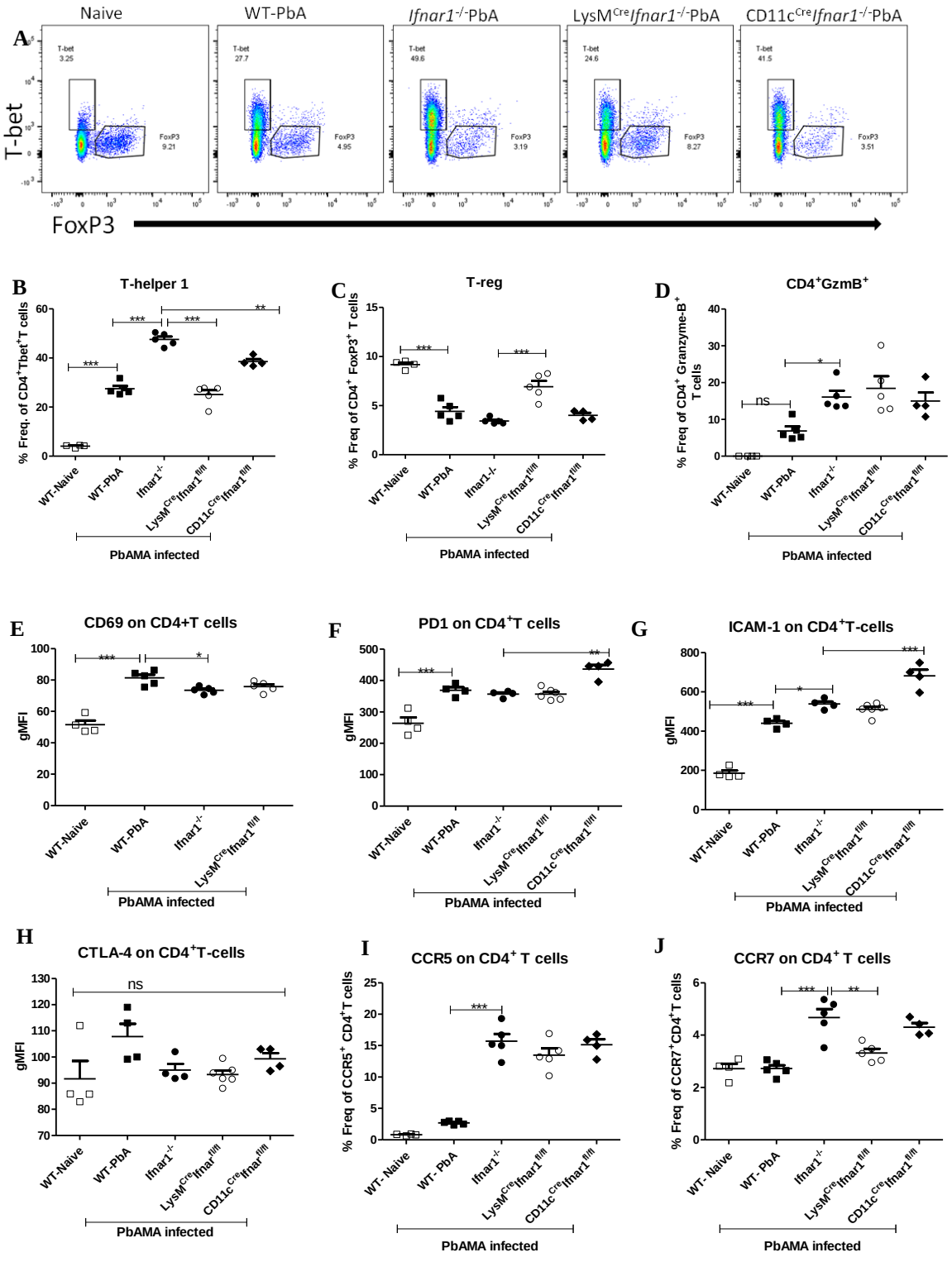
A
Naive
WT-PbA
Ifnar1-/-PbA
LysMCreIfnar1-/-PbA
CD11cCreIfnar1-/-PbA
T-bet
FoxP3
B
T-helper 1
% Freq. of CD4+Tbet+T cells
C
T-reg
% Freq of CD4+ FoxP3+ T cells
D
CD4+GzmB+
% Freq of CD4+ Granzyme-B+ T cells
E
CD69 on CD4+T cells
gMFI
F
PD1 on CD4+T cells
G
ICAM-1 on CD4+T-cells
H
CTLA-4 on CD4+T-cells
I
CCR5 on CD4+ T cells
% Freq of CCR5+ CD4+T cells
J
CCR7 on CD4+ T cells
% Freq of CCR7+CD4+T cells
WT-Naive
WT-PbA
Ifnar1-/-
LysMCreIfnar1fl/fl
CD11cCreIfnar1fl/fl
PbAMA infected
ns

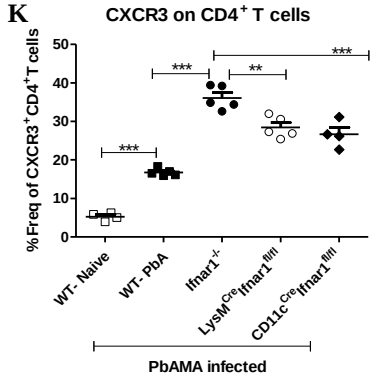

Figure 23 All infected mice express Th1 phenotype

C57BL/6 mice (WT, *Ifnar1*$^{-/-}$, LysM^{Cre}*Ifnar1*$^{fl/fl}$ and CD11c^{Cre}*Ifnar1*$^{fl/fl}$) mice were infected with 5x10^4 transgenic PbAMA iRBCs i.v. On d+6, spleens were harvested, digested, and single cell suspensions prepared. The cells were counted, stained and analysed using flow cytometry. **A)** Raw data from representative samples of every experimental group. **B**) Frequency of Th-1 cells (Tbet$^+$CD4$^+$CD3$^+$CD8^{neg}NK1.1^{neg}). **C**) Frequency of T-regs (FoxP3$^+$CD4$^+$CD3$^+$CD8^{neg}NK1.1^{neg}). **D**) Frequency of granzymeB$^+$CD4$^+$ Tbet^{neg}CD3$^+$CD8^{neg}NK1.1^{neg} T cells. (**E-H)** Expression level of CD69, PD-1, ICAM-1 and CTLA-4 on CD4$^+$T cells. (**I-K**) Frequency of CD4$^+$T cells expressing chemokine receptors; CCR5, CCR7 and CXCR3. Statistics= One-way ANOVA with Bonferroni post test analysis. n=4/5 animals per group.

3.2.8 Ifnar deficiency did not impair NK cell cytotoxicity

NK cells play an important role during innate immune response, as these lymphocytes kill and neutralize infected cells without requiring any priming from APCs. During *P. berghei* infection, splenic NK cells numbers decrease in the spleens of ECM susceptible mice (Hansen et al. 2007), the Hansen group hypothesised that these phenomenon could be due to high turnover or due to migration of these cells out of the spleen. Here, we quantified NK cells in the spleen and assessed their expression of granzyme-B in PbA-infected mice.

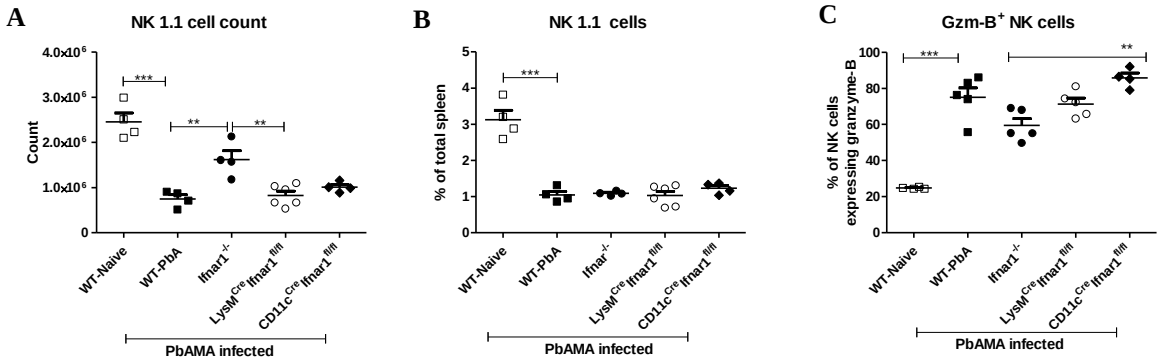

Figure 24 Ifnar deficiency does not impaire NK cytotoxicity

C57BL/6 (WT, *Ifnar1*$^{-/-}$, LysM^{Cre}*Ifnar1*$^{fl/fl}$ and CD11c^{Cre}*Ifnar1*$^{fl/fl}$) mice were infected with 5x10^4 PbAMA iRBc i.v. On d+6 p.i, spleens were harvested, digested, and single cell suspensions prepared. The cells were counted, stained and analysed using flow cytometry. (**A**) Total calculated number of NK cells in the spleen (**B**) Percentage of NK cells in the spleen (**C**) Frequency of NK cells expressing granzyme-B. Statistics= One-way ANOVA with Bonferroni post test analysis, n=4/5 animals per group.

We observed a significant decrease in the total number of splenic NK cells among the infected mice, with fold decreases of; 3.3x in infected WT, 1.5x in infected *Ifnar1*$^{-/-}$, 3x in infected LysM^{Cre}*Ifnar1*$^{fl/fl}$ and 2.4x in infected CD11c^{Cre}*Ifnar1*$^{fl/fl}$ mice, in comparison to the naïve mice (Figure 24A). PbA-infected *Ifnar1*$^{-/-}$ mice showed the least reduction in cell numbers, with the total counts being double those of infected WT and LysM^{Cre}*Ifnar1*$^{fl/fl}$, but not varying

significantly to that of CD11c^{Cre}*Ifnar1*$^{fl/fl}$ (Figure 24A). The decrease in NK cells in samples from the infected mice was also observed in the percentages of these cells in the spleen (Figure 24 B). We detected significant increase in the percentage of granzyme-B expression by NK cells in sample from all the infected groups of mice, in comparison to the naïve mice (Figure 24C). Taken together, these data shows that the lack of the Ifnar did not impair NK cytotoxicity.

3.2.9 Decreased percentage of splenic B cell in PbA-infected ko mice.

In immune response B cell can perform several functions; they can act as effector cells and produce antibodies or as APCs. As CD8^{+}T cell are the accepted effector cells during PbA infection, we analysed splenic B cell as APC. We analysed their expression of MHC class II, CD86 and ICAM-1.

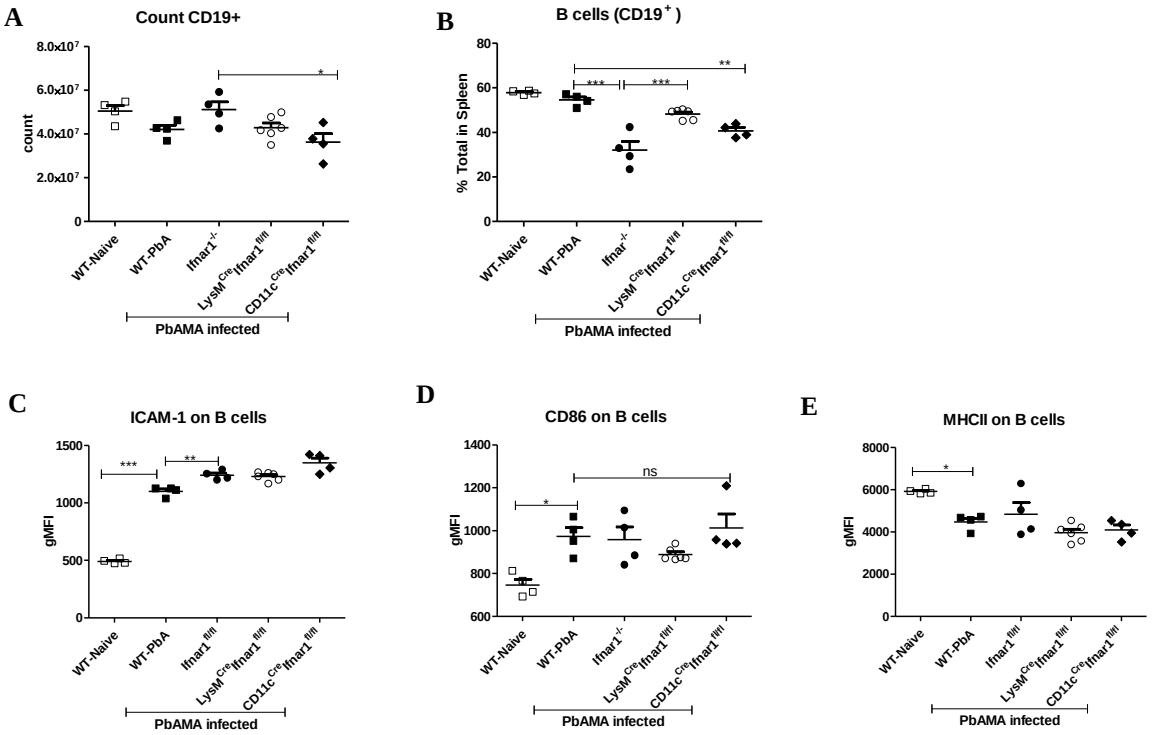

Figure 25 splenomegally on Ifnar ko resulted in difference in B cell counts and percentages

C57BL/6 mice (WT, *Ifnar1*$^{-/-}$, LysM^{Cre}*Ifnar1*$^{fl/fl}$ and CD11c^{Cre}*Ifnar1*$^{fl/fl}$) mice were infected with 5x10^{4} PbAMA iRBCs i.v. On d+6 spleens were harvested, digested, and single cell suspensions prepared. The cells were counted, stained and analysed using flow cytometry. **A**) Total count of B cells in the spleen analysed by expression of CD19 (**B**) Total percentage of B cells in the spleen (**C-E**) Expression levels of ICAM-1, CD86 and MHC class-II on B cells. Statistic= One-way ANOVA with Bonferroni post test analysis, n=4/5 animals per group.

We did not observe a difference in the total B cell count between the naïve, infected WT, *Ifnar1*$^{-/-}$ and LysM^{Cre}*Ifnar1*$^{fl/fl}$ mice, however, PbA-infected CD11c^{Cre}*Ifnar1*$^{fl/fl}$ had reduced counts in comparison to infected WT and *Ifnar1*$^{-/-}$ mice (Figure 25A). The total percentage of

splenic B cells was comparable between the infected WT and the naïve control mice (Figure 25B). Interestingly, and contrary to the counts, all infected Ifnar ko had decreased percentage of B cells in their spleen in comparison the naïve mice (Figure 25B). Infected *Ifnar1*$^{-/-}$ mice had the lowest B cell percentages in their spleen, with mean percentage decrease of 29% to the naïve and 23% to the infected WT mice (Figure 25B). The percentage of B cells in the spleens of infected LysM^{Cre}*Ifnar1*$^{fl/fl}$ mice was not significantly different to that of the infected WT mice, however in comparison to the infected *Ifnar1*$^{-/-}$ mice, they had 16% more cells (Figure 25B). While CD11c^{Cre}*Ifnar1*$^{fl/fl}$ had mean decrease of 18% and 14% to the naïve and infected WT mice, but they did not differ significantly to the infected *Ifnar1*$^{-/-}$ and LysM^{Cre}*Ifnar1*$^{fl/fl}$ mice (Figure 25B). Splenic B cells from all infected groups of mice showed an increased expression of ICAM-1 in comparison to those of the naïve mice, however, the levels were higher in the Ifnar ko in comparison to the infected WT mice (Figure 25C). The expression levels of CD86 on splenic B cells were increased in all the infected mice, although there was no statistical significance between cells from LysM^{Cre}*Ifnar1*$^{fl/fl}$ and those from naïve mice (Figure 25D). We observed reduced MHC class-II expression on splenic B cells from samples of all the infected groups of mice, although the values were decreased among the *Ifnar1*$^{-/-}$ mice, they were not statistically different to those of the naïve control mice (Figure 25E).

Taken together, these data show that the splenomegaly observed among the Ifnar ko lead to the difference in percentage and total count of B cells in the spleen and although there was a decreased total percentage of B cells, the total count remained high. The data show reduced expression of Ag presenting molecules but elevated expression of co-stimulatory molecules on B cells among all infected ko, but varying levels of expression.

3.2.10 *Ifnar1*$^{-/-}$ mice had increased amounts splenic conventional dendritic cells

DCs play a role in the innate immunity, but their most important role is to link the innate with the adoptive immune system. After they encounter the pathogen or its associated molecules, the DCs process and degrade them into peptides, and these are then presented via MHC molecules to naïve T cells. DCs expressing the peptide via MHC molecules, must also express co-stimulatory molecules in order to activate naïve T cells properly. DCs are classified as either plasmocytoid dendritic cells (pDCs) or conventional dendritic cells (cDCs). During infection with *Plasmodium berghei*, cDCs have been shown to induce CD4^{+} T cell activation (deWalick et al. 2007), deWalick also excluded any major role of pDCs in pathogenesis of ECM. Lundie et al. further showed that CD8α^{+}DCs are the major APCs to prime and induce proliferation of CD8^{+}T cells (Lundie et al. 2008).

We have already shown an unimpaired T cells response in the spleen of the Ifnar ko mice, since $CD8^+$T cells were able to recognise parasite derived peptides presented via MHC class-I (Figure 18). This ability of $CD8^+$T cell to recognise Ag indicates that there was efficient priming of the T cells by APCs. As DCs have already been shown to be key APCs during ECM, we investigated whether the lack of type I IFN signalling influenced the DC phenotype during PbAMA infection. We characterized splenic DCs, first as $CD11c^+$MHC class II^+CD3^- $CD19^-$ and then further into $CD8\alpha^+$ and $CD8\alpha^{neg}$ DCs. In these DC subsets, we looked for expression levels of co-stimulatory molecule CD86 and adhesion molecule ICAM-1, which are necessary for T cell activation.

We observed a non significant decrease in the total count of DCs in spleens of infected WT in comparison to the naïve control mice (Figure 26A). $LysM^{Cre}$*Ifnar1*$^{fl/fl}$ and $CD11c^{Cre}$*Ifnar1*$^{fl/fl}$ contained in their spleens more DCs in comparison to their appropriate naïve ko mice, however, the difference was statistically insignificant (Figure 26A). Splenic DCs count among infected $LysM^{Cre}$*Ifnar1*$^{fl/fl}$ and $CD11c^{Cre}$*Ifnar1*$^{fl/fl}$ were not significantly different to the infected WT mice (Figure 26A). Interestingly, infected *Ifnar1*$^{-/-}$ had a 3.4 ($\pm$0.3) fold increase in the total DCs count in comparison to naïve *Ifnar1*$^{-/-}$ mice, $LysM^{Cre}$*Ifnar1*$^{fl/fl}$ and $CD11c^{Cre}$*Ifnar1*$^{fl/fl}$ mice and a 10x fold increase in comparison to infected WT mice (Figure 26A). Frequencies of splenic DCs in infected WT mice were significantly reduced, with mean difference of 0.7% in comparison to naïve, infected $LysM^{Cre}$*Ifnar1*$^{fl/fl}$ and $CD11c^{Cre}$*Ifnar1*$^{fl/fl}$ mice (Figure 26D). The increase in total DCs calculation among infected *Ifnar1*$^{-/-}$ mice was also observed as percentages, which resulted in mean differences of 1.4% to naïve *Ifnar1*$^{-/-}$ mice, 2.7% to infected WT, ~1.8% to $LysM^{Cre}$*Ifnar1*$^{fl/fl}$ and $CD11c^{Cre}$*Ifnar1*$^{fl/fl}$ mice (Figure 26D).

The same trend indicating decreased cell count of $CD8\alpha^+$DCs was observed in the spleens of the infected WT, $LysM^{Cre}$*Ifnar1*$^{fl/fl}$ and $CD11c^{Cre}$*Ifnar1*$^{fl/fl}$ mice with significant differences to their respective naïve controls (Figure 26B). Unlike the other infected groups, PbA-infected *Ifnar1*$^{-/-}$ mice contained comparable levels of splenic $CD8\alpha^+$ DC to their naïve ko control, but differed in comparison to the other infected mice with 5.2x fold increase to infected WT, 2.8x to infected $LysM^{Cre}$*Ifnar1*$^{fl/fl}$ and 1.7x to $CD11c^{Cre}$*Ifnar1*$^{fl/fl}$ mice (Figure 26B).

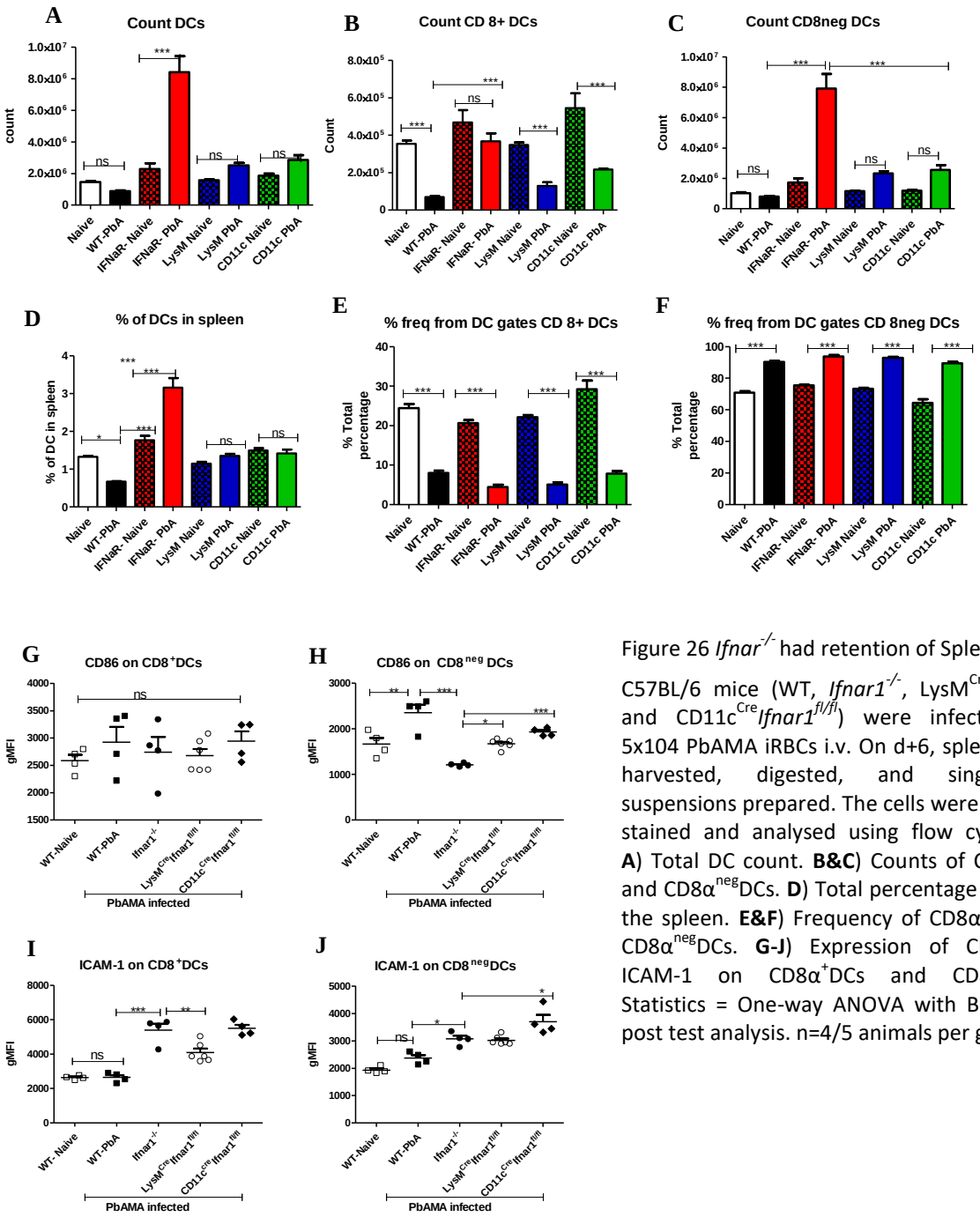

Figure 26 *Ifnar*$^{-/-}$ had retention of Splenic cDCs. C57BL/6 mice (WT, *Ifnar1*$^{-/-}$, LysM^{Cre}*Ifnar1*$^{fl/fl}$ and CD11c^{Cre}*Ifnar1*$^{fl/fl}$) were infected with 5x104 PbAMA iRBCs i.v. On d+6, spleens were harvested, digested, and single cell suspensions prepared. The cells were counted, stained and analysed using flow cytometry. **A**) Total DC count. **B&C**) Counts of CD8α^{+}DCs and CD8α^{neg}DCs. **D**) Total percentage of DCs in the spleen. **E&F**) Frequency of CD8α^{+}DCs and CD8α^{neg}DCs. **G-J**) Expression of CD86 and ICAM-1 on CD8α^{+}DCs and CD8α^{neg}DCs. Statistics = One-way ANOVA with Bonferroni post test analysis. n=4/5 animals per group.

Moreover, the infected *Ifnar1*$^{-/-}$ mice had an increase in the total number of CD8α^{neg}DCs in their spleens in comparison to the other infected groups, with 4.6x fold increase to naïve *Ifnar1*$^{-/-}$, 10x to infected WT, 3.2 (±0.2)x to infected LysM^{Cre}*Ifnar1*$^{fl/fl}$ and CD11c^{Cre}*Ifnar1*$^{fl/fl}$ mice (Figure 26C). Surprisingly, frequencies of CD8α^{+} DCs, were comparable and displayed an average reduction of ~17% (±2) in all the infected groups in comparison to their respective naïve groups (Figure 26 E). The decrease in the frequency of CD8α^{+}DCs resulted in an increase in the frequency of CD8α^{neg} DCs in all the infected animals (Figure 26F).

We did not observe any significant difference in the expression levels of CD86 on splenic $CD8\alpha^{+}$DCs between the naïve and the infected mice (Figure 26G). There was an increase in the expression of CD86 on $CD8\alpha^{neg}$DCs in spleen samples of the infected WT mice in comparison to those of the naïve and the Ifnar ko mice, we observed the least expression of CD86 on $CD8\alpha^{neg}$DCs among the infected *Ifnar1*$^{-/-}$ mice (Figure 26H). We did not observe an increase in ICAM-1 expression on either population of splenic DCs of the infected WT in comparison to those samples from the naïve (Figure 26 I&J). In contrast, splenic DCs from Ifnar ko mice showed a significant increase in their ICAM-1 expression levels by both $CD8\alpha^{+}$ DC and $CD8\alpha^{neg}$DC in comparison to the naïve and infected WT mice, with $CD11c^{Cre}$*Ifnar1*$^{fl/fl}$ having the highest ICAM-1 expression on $CD8\alpha^{neg}$DCs (Figure 26 I&J). These data show retention of DCs in the spleens of *Ifnar1*$^{-/-}$ mice, resulting in an increase of the frequency of these cells in the spleen.

3.2.11 Macrophages of *Ifnar1*$^{-/-}$ acquired an alternative activated phenotype

During infection with *Plasmodium* parasites, splenic macrophages are among the first cells to come into contact with the parasite, this occurs during the process of clearing infected red blood cells. We next analysed the myeloid cells populations and addressed the question as to whether there was also retention of these cells in the spleens of ECM protected *Ifnar1*$^{-/-}$ and $LysM^{Cre}$*Ifnar1*$^{fl/fl}$, and if so, whether the phenotype of these cells differed to that of infected WT. We characterized myeloid cells into neutrophils ($Ly6G^{hi}CD11b^{hi}Ly6C^{int}F4/80^{neg}$), monocytes ($Ly6C^{hi}CD11b^{hi}F4/80^{+}Ly6G^{neg}$) and alternative activated macrophages (Relm-$\alpha^{hi}F4/80^{hi}CD11b^{hi}Ly6C^{int}Ly6G^{int}$).

We observed a significant decrease in the total percentage of splenic $CD11b^{+}$ population in samples of PbA-infected WT, $LysM^{Cre}$*Ifnar1*$^{fl/fl}$ and $CD11c^{Cre}$*Ifnar1*$^{fl/fl}$ mice in comparison to the naïve control mice (Figure 27C). Importantly, infected *Ifnar1*$^{-/-}$ mice had double the amount of splenic $CD11b^{+}$ cells in their samples in comparison to the other infected mice groups (Figure 27C). Although the infected WT, $LysM^{Cre}$*Ifnar1*$^{fl/fl}$ and $CD11c^{Cre}$*Ifnar1*$^{fl/fl}$ mice had decreased percentages of $CD11b^{+}$ cells in their samples, the cell counts were comparable to the naïve mice (Figure 27D). Infected *Ifnar1*$^{-/-}$ mice continued to have substantial increase in the cell counts when compared to other groups, with fold increase of 2.7x to naïve, 3.1x to infected WT, 1.7x to infected $LysM^{Cre}$*Ifnar1*$^{fl/fl}$ and 2.2x to infected $CD11c^{Cre}$*Ifnar1*$^{fl/fl}$ mice (Figure 27D).

We further characterised / differentiated the $CD11b^{+}$ population into inflammatory monocytes, macrophages and neutrophils. We gated the $CD11b^{+}$ population as either F4/80 vs Relm-α or

Ly6C vs Ly6G. To confirm that these were three distinct populations, we next gated $CD11b^{+}$ as F4/80 vs Ly6G and overlaid with populations that were $Ly6C^{hi}Ly6G^{neg}$ (inflammatory monocytes) $F4/80^{hi}Relm^{hi}$ (macrophages) and $Ly6G^{hi}Ly6C^{int}$ (neutrophils) (Figure 27A&B). More than 85% of the $Ly6C^{hi}Ly6G^{neg}$ population expressed $CCR2^{+}$ hence confirming this population as inflammatory monocytes. The splenic $CD11b^{+}$ population of the infected WT mice contained an average of 40.5% $Ly6C^{hi}$ inflammatory monocytes, this increase was more than double the percentage in the naïve mice (Figure 27E). PbA infected *Ifnar1*$^{-/-}$ and LysM^{Cre}*Ifnar1*$^{fl/fl}$ mice had comparable percentages of $Ly6C^{hi}$ inflammatory monocytes to those of the naïve mice, while CD11c^{Cre}*Ifnar*$^{fl/fl}$ mice had ~15% more cells in comparison to the naïve (Figure 27E). Interestingly, this observation changed when we analysed total count of $Ly6C^{hi}$ inflammatory monocytes, with the highest increase being observed only in samples from the infected *Ifnar1*$^{-/-}$ mice, whilst the samples from infected WT, LysM^{Cre}*Ifnar1*$^{fl/fl}$ and CD11c^{Cre}*Ifnar1*$^{fl/fl}$ mice were comparable to those of the naïve (Figure 27H).

We observed a significant increase in frequency of neutrophils among the infected LysM^{Cre}*Ifnar1*$^{fl/fl}$ mice with a means difference of 25% to naive, 23% to infected WT, 24% to infected *Ifnar1*$^{-/-}$ and 17% to CD11c^{Cre}*Ifnar1*$^{fl/fl}$ (Figure 27 F). However, when we calculated the total neutrophil count, the increase was observed also among the infected *Ifnar1*$^{-/-}$ mice, but not in the infected WT and CD11c^{Cre}*Ifnar1*$^{fl/fl}$ mice which had counts comparable to the naïve (Figure 27 I). Unexpectedly and interestingly, we observed a significant amount of alternative activated macrophages (AAM) in spleen samples from infected *Ifnar1*$^{-/-}$ and a small population in samples from infected LysM^{Cre}*Ifnar1*$^{fl/fl}$ (Figure 27G). These AAM accounted for approximately 11%($\pm$2) and 5% of the $CD11b^{+}$ population in the spleens of infected *Ifnar1*$^{-/-}$ and LysM^{Cre}*Ifnar1*$^{fl/fl}$ mice, respectively, but made up less than 2% in spleen samples from infected WT and CD11c^{Cre}*Ifnar1*$^{fl/fl}$ mice (Figure 27G). This increase in the AAM population was also observed as total counts in samples from infected *Ifnar1*$^{-/-}$ mice, the infected WT and CD11c^{Cre}*Ifnar1*$^{fl/fl}$ mice almost completely lacked these cell populations (Figure 27J). Although the naive control and infected LysM^{Cre}*Ifnar1*$^{fl/fl}$ mice contained some AAM population in their spleens, the counts were significantly lower than those observed in samples from *Ifnar1*$^{-/-}$ mice (Figure 27J).

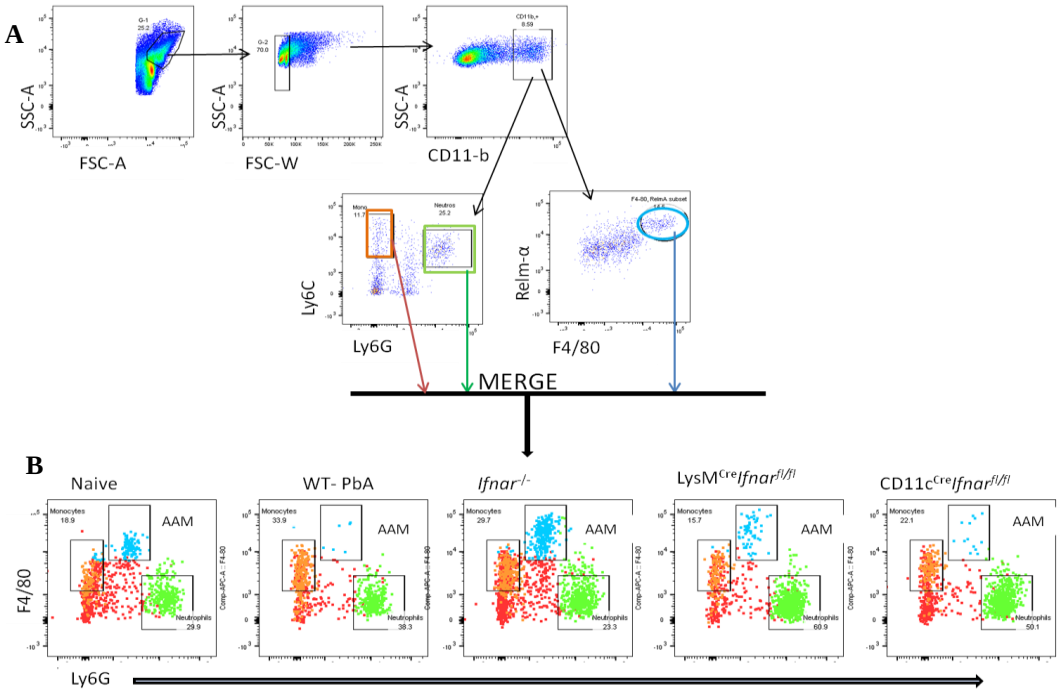

AAM (**F4/80^{hi}Relm-alpha^{hi}CD11b^{hi}Ly6C^{low}Ly6G^{int}**), **Monocytes** (**Ly6C^{hi}CD11b^{+}Ly6G^{neg}F4/80^{int}**)
Neutrophils (**Ly6G^{hi}Ly6C^{int}CD11b^{+}F4/80^{neg}**)

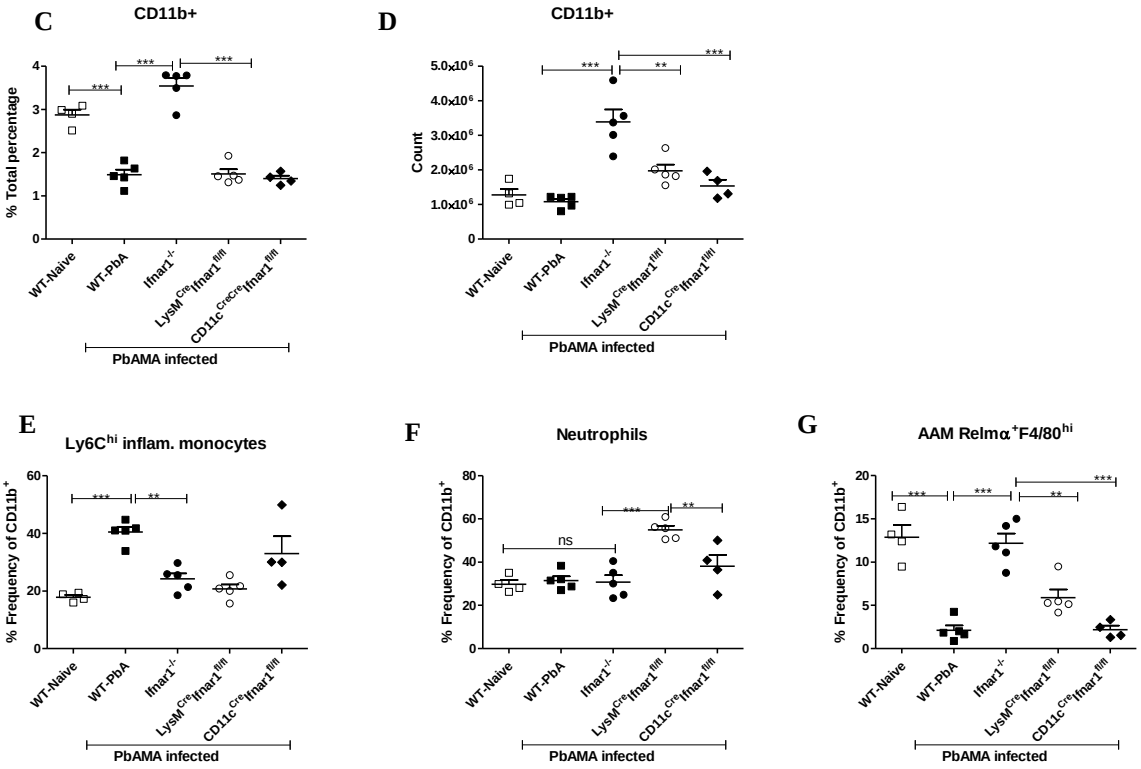

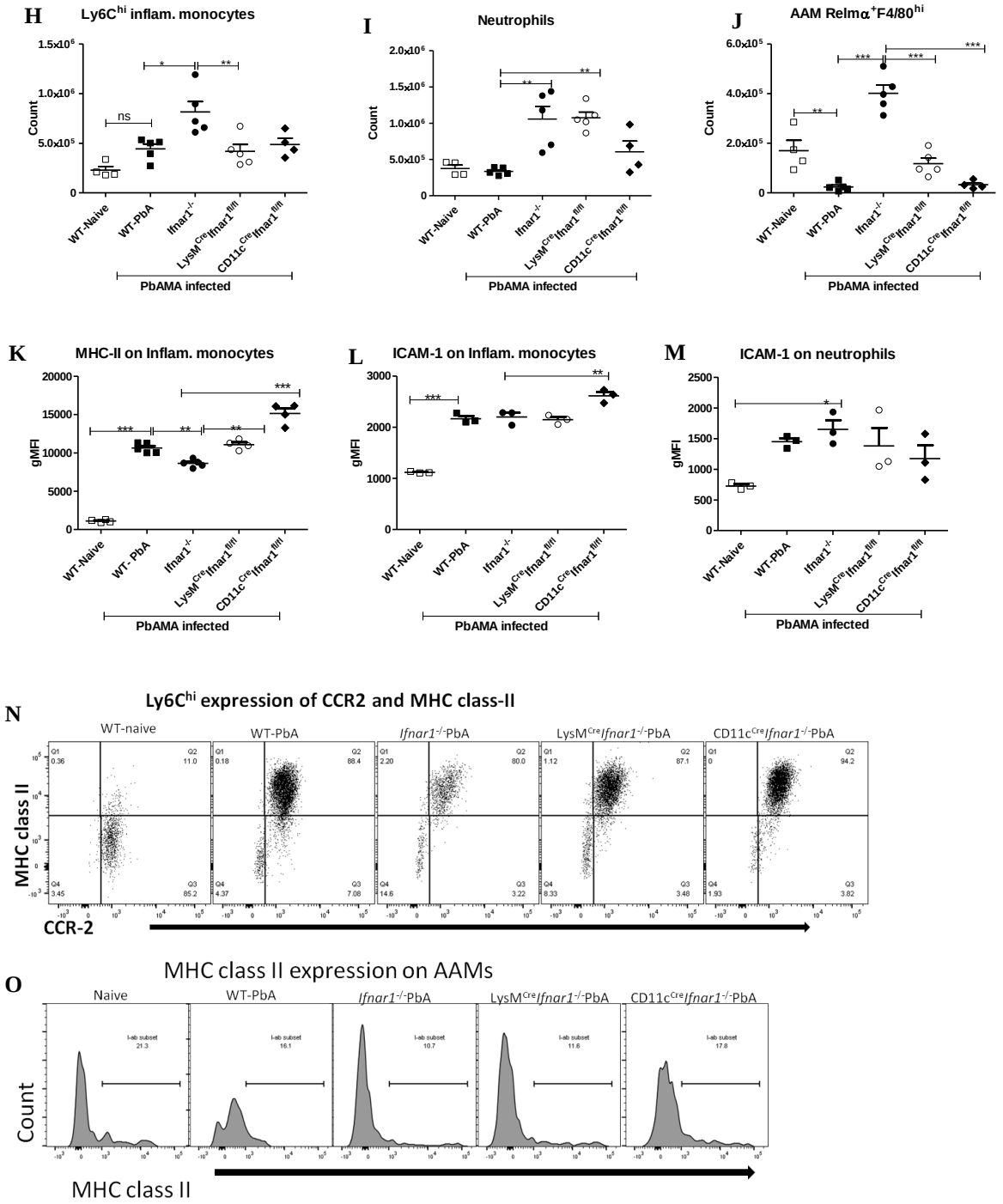

Figure 27 Ifnar ko mice contained alternative activated macrophages in their spleens

C57BL/6 mice (WT, *Ifnar1*$^{-/-}$, LysM^{Cre}*Ifnar1*$^{fl/fl}$ and CD11c^{Cre}*Ifnar1*$^{fl/fl}$) mice were infected with 5x10^4 PbA iRBCs i.v. On d+6, spleens were harvested, digested and single cell suspensions prepared. The cells were counted, stained and analysed using flow cytometry. (**A**) Example of how cells were gated for selection of desired population (**B**) Raw data with overlayed groups to confirm distinct populations (**C**) Percentage of CD11b^{hi} cells in the spleen **(D)** Total splenic CD11b^{hi} count. (**E-G**) Frequency of splenic monocytes, neutrophils and AAM from CD11b^{hi} cells (**H-I**) Total count of splenic inflammatory mononocytes, neutrophils and AAM. (**K-L**) Expression of MHC class-II and ICAM-1 on monocytes. (**M**) Expression of ICAM-1 on neutrophils. (**N**) Representative raw data on expression of MHC-II and CCR2 on inflammatory monocytes. (**O**) Histogram expression of MHC-II on AAM. n=4/5 animals per group, statistics= One-way ANOVA with Bonferroni post test.

Expression of MHC class II molecules on Ly6C^{hi} inflammatory monocytes was increased only in samples from PbA infected mice but not in samples from the naïve mice. The expression level of MHC class II molecules on Ly6C^{hi} inflammatory monocytes in samples from infected *Ifnar1*$^{-/-}$ mice were slightly lower in comparison to the other infected groups of mice (Figure 27K&N). The expression levels of ICAM-1 on splenic monocytes were increased in samples from all the infected mice in comparison to the naïve, with the expression levels being comparable between infected WT, *Ifnar1*$^{-/-}$ and LysM^{Cre}*Ifnar1*$^{fl/fl}$ mice (Figure 27 L). However, samples from infected CD11c^{Cre}*Ifnar1*$^{fl/fl}$ mice had higher expression levels of ICAM-1 on inflammatory monocytes in comparison to samples from the other groups of mice (Figure 27 L). Expression of ICAM-1 on neutrophils was increased in splenic samples from infected *Ifnar1*$^{-/-}$ mice in comparison to the naïve, however, the values were comparable to the other infected mice, the infected WT and the other ko did not differ significantly to the naïve (Figure 27 M). We observed very low expression level of MHC-II on AAM from all the groups of mice (Figure 27 O).

Taken together, our data show that PbA-infection of complete Ifnar ko mice resulted in the induction of macrophages that were polarized to an alternative activated phenotype, while the presence of the IFN receptor in the infected WT mice resulted in high number of inflammatory monocytes in the spleen, that we had correlated with ECM pathology before (Schumak et al., 2015). Thus, the presence of AAM and decreased presence of Ly6C^{hi} inflammatory monocytes in the spleens of infected *Ifnar1*$^{-/-}$ could be a factor contributing to the protection of these mice from ECM.

3.2.11.1 Up-regulation of M2a genes in splenic myeloid cells from Ifnar1$^{-/-}$ *mice*

During infection, macrophages can be polarized to either classically activated macrophages (CAM) or alternative activated macrophages (AAM), depending on the cytokine signal received or type of infection. These macrophage phenotypes are commonly referred to as M1 for CAM and M2 for AAM, the terms was coined by Mills et al., after observations from macrophages derived from mice that display Th-1 or Th-2 phenotypes (Mills et al. 2000). When those macrophages were exposed to the same stimuli, they activated different arginine pathways resulting in nitric oxide (NO) production for Th-1 and ornithine in Th-2 mouse strains (Mills et al. 2000). Other stimuli like TNF have been now shown to be able to stimulate an M1 phenotype. M2 activation can be induced by several stimulus like IL-4, IL-13, IL-10, TGF-β, fungal and parasitic infections (Rőszer 2015), however their activation is not limited to these factors. The M2 are further categorised into sub groups M2a-2d, depending on stimuli,

genes expressed, cytokines and chemokines produced (Rőszer 2015; Martinez & Gordon 2014). As we had observed significant increase in the presence of Relmα^{hi} F4/80^{hi} CD11b^{hi} population among *Ifnar1*$^{-/-}$ mice and some among LysM^{Cre}*Ifnar1*$^{fl/fl}$ mice, we next wanted to confirm further if these were M2 macrophages. We enriched CD11b^{+} splenocytes using MACs sorting and isolated cDNA from these cells, then we analysed the mRNA for the expression of hallmark genes associated with M2 phenotype, *arginase-1, Ym-1*and *Fizz//Relm-α,* (Mills et al. 2000; Raes et al. 2002). We also analysed the expression of cytokines *TNF, iNOS* (for M1) and *IL-10* (for M2).

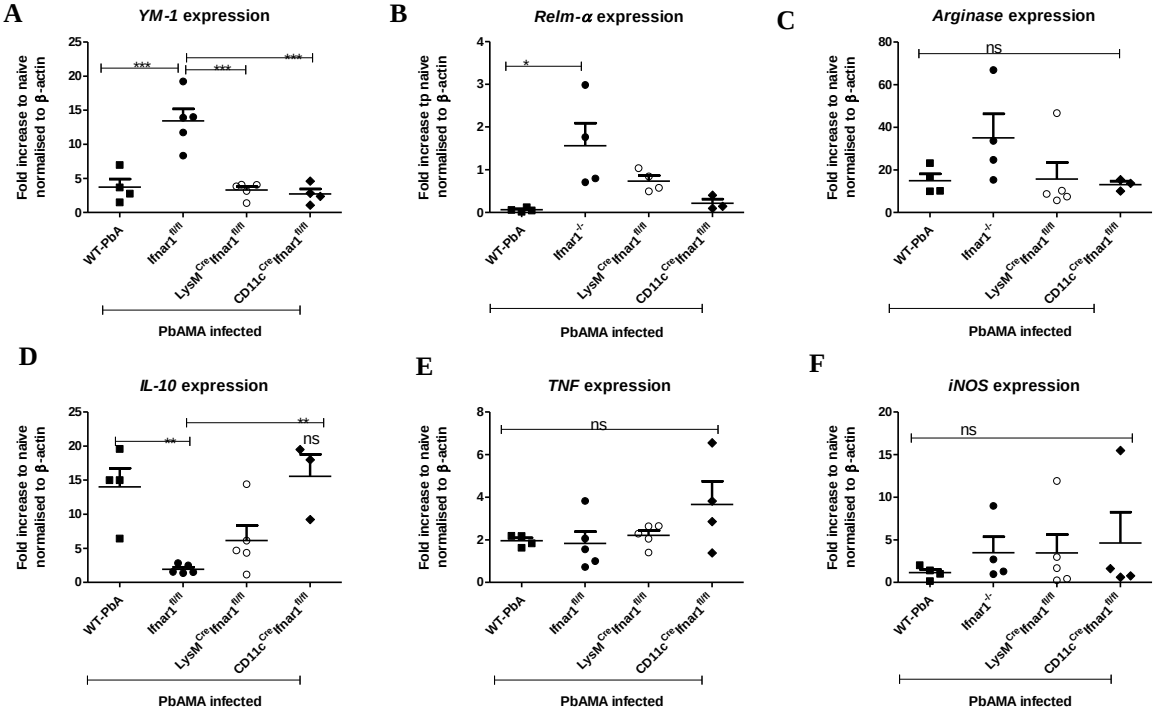

Calculation of fold change (Pfaffl *etal* 2001)

$$\text{Fold change (normalized)} = \frac{(\mathbf{E}p-target)^{\Delta CT-target}}{(\mathbf{E}p\ housekeeping)^{\ \Delta CT-housekeeping}}$$

$C_{T\text{-target}}=(C_{\text{T Naïve}}-C_{\text{T-PbAMA infected}})$

$C_{\text{T-housekeeping}}=(C_{\text{T naïve housekeeping}}-C_{\text{T-housekeeping PbAMA infected}})$

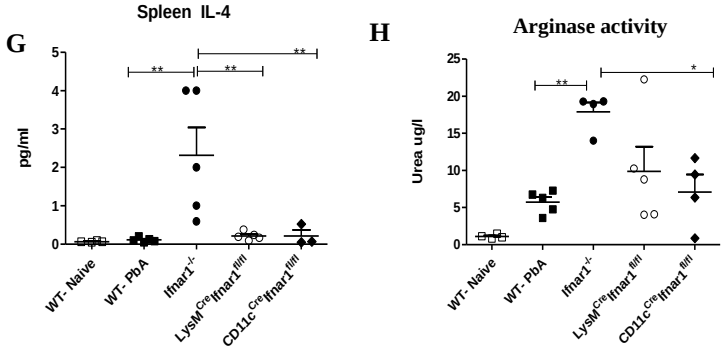

Figure 28 *Ifnar1*$^{-/-}$ show an M2a phenotype

C57BL/6 (WT, *Ifnar1*$^{-/-}$, LysM^{Cre}*Ifnar1*$^{fl/fl}$ and CD11c^{Cre}*Ifnar1*$^{fl/fl}$) mice were infected with 5x10^{4} PbA iRBC i.v. On d+6, Single cell suspensions prepared. The cells were counted and 4x10^{7} spleen cells were incubated with anti CD11b magnetic beads for 15 mins then sorted using MACs sorter. From the sorted CD11b^{+}, cDNA was prepared as described in methods and mRNA expressions measured. (**A-F**) Expression level of *YM-1, Relmα/Fizz, Arg-1, IL-10, TNF and iNOS.* (**G**) Production of IL-4 measured from splenocytes by ELISA. (**H**) Arginase activity (1x10^{6} CD11b^{+} cells were lysed and supernatants used to measure levels of arginase production). Statistics = One-way ANOVA with Bonferroni post test analysis. n=3/4/5 animals per group.

We normalised each sample to β-actin then calculated expression levels as fold increase against naïve as described by Pfaffl et al. (Pfaffl 2001). In agreement with our earlier observation, we observed in splenic CD11b^{+} sorted samples from *Ifnar1*$^{-/-}$ high expression of the hallmark genes indicative of M2a macrophages.

Expression levels of *Ym-1* and *Relm-α/Fizz* were significantly up-regulated in samples from infected Ifnar1$^{-/-}$ mice (Figure 28A-B). Expression of *YM-1* was 10 fold higher in samples from *Ifnar1*$^{-/-}$ in comparison to those from WT, LysM^{Cre}*Ifnar1*$^{fl/fl}$ and CD11c^{Cre}*Ifnar1*$^{fl/fl}$ mice (Figure 28A). While *Relm-α/Fizz* expression was completely lacking by the myeloid cells from infected WT and CD11c^{Cre}*Ifnar1*$^{fl/fl}$ mice, we detected a slight increase but non-significant in the samples from LysM^{Cre}*Ifnar1*$^{fl/fl}$ mice (Figure 28B). We observed an increase in *Arg-1* expression in the splenic CD11b^{+} cells from infected *Ifnar1*$^{-/-}$ mice, however, this increase was not statistically significant in comparison to the other infected group (Figure 28C). Strikingly, we did not observe any increased expression of M2a genes in samples from infected LysM^{Cre}*Ifnar1*$^{fl/fl}$ mice (Figure 28A-C). Although we had measured significant levels of IL-10 in splenocyte cultures of infected *Ifnar1*$^{-/-}$ and LysM^{Cre}*Ifnar1*$^{fl/fl}$ mice, the mRNA expression levels of IL-10 in CD11b^{+} cells were decreased in comparison to infected WT and CD11c^{Cre}*Ifnar1*$^{fl/fl}$ mice (Figure 28D). We did not observe any difference in the expression of TNF and iNOS levels among all groups of infected mice (Figure 28E&F). Expression of mannose receptor (CD206) on Relm-α^{hi}F480^{hi}CD11b^{+} cells was very low with only a slight increase in samples from *Ifnar1*$^{-/-}$ mice (data not shown). Secretion of the cytokine IL-4 has been shown to stimulate M2 macrophage genes. Here, increased levels of IL-4 were only detected in supernatants of splenocytes of infected *Ifnar1*$^{-/-}$ mice (Figure 28G). We detected not only upregulated expression levels of *arg-1* gene among the infected *Ifnar1*$^{-/-}$ mice, but the Macs sorted CD11b^{+} cells from infected *Ifnar1*$^{-/-}$ showed also a high protein production of arginase-1, analysed by conversion of arginine to urea (Figure 28H).

Taken together, our data demonstrate the phenotype of altered macrophages in infected *Ifnar1*$^{-/-}$ mice, meeting the description of an M2a phenotype in contrast to the classical M1 found in WT C57BL/6 that develop ECM upon PbA infection. Although the LysM^{Cre}*Ifnar1*$^{fl/fl}$ mice were protected from ECM, their macrophages did not polarize to an M2a phenotype, however, they could have another M2 phenotype.

3.2.11.2 Type I IFN signalling controlled expression of CCL3/ MIP1α

During infections, macrophage and other cells secrete chemokines that have a role in chemotaxis and recruitment of cells to organs of inflammation. We analysed the production of inflammatory chemokines CCL2, CCL3 and CCL5 by spleen cells of PbAMA-infected mice.

We measured significantly increased level of CCL2 on spleen samples from infected WT mice in comparison to the naïve control; although the infected Ifnar ko mice had reduced CCL2 levels in comparison to the infected WT, this difference was not statistically significant (Figure 29A). The levels of CCL3/MIP1α was significantly reduced among the infected *Ifnar1*$^{-/-}$ and CD11c^{Cre}*Ifnar1*$^{fl/fl}$ mice in comparison to both the naïve and the infected WT, while infected LysM^{Cre}*Ifnar1*$^{fl/fl}$ mice were comparable to all the groups (Figure 29B). In contrast to the observation in the brain, where we measured high levels of CCL5/Rantes from the infected WT mice, the spleen samples of infected WT produced significantly lower amounts of CCL5/Rantes in comparison to samples from the the naïve control, infected *Ifnar1*$^{-/-}$ and infected LysM^{Cre}*Ifnar1*$^{fl/fl}$ mice (Figure 29C). The production levels of CCL5/Rantes, was decreased in samples from infected CD11c^{Cre}*Ifnar1*$^{fl/fl}$ mice in comparison to the naïve mice, but was comparable to the other infected groups of mice (Figure 29C).

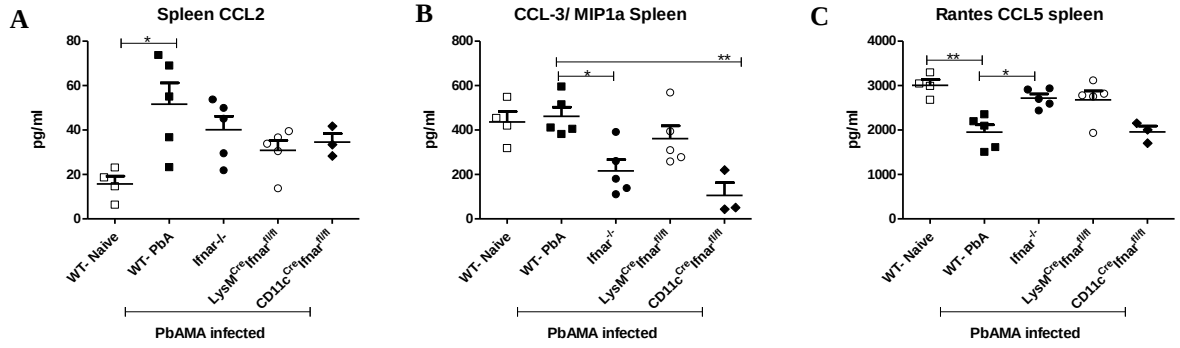

Figure 29 Ifnar ko mice had reduced levels of CCL3 in their spleens

C57BL/6 mice (WT, *Ifnar1*$^{-/-}$, LysM^{Cre}*Ifnar1*$^{fl/fl}$ and CD11c^{Cre}*Ifnar1*$^{fl/fl}$) were infected with 5x10^4 PbAMA iRBCs i.v. On d+6, spleens were harvested, digested, and single cell suspensions prepared. The cells were counted and 1x10^6 cells were plated in triplicates and cultured over night. ELISAs were performed from the supernatants as described in methods. **A-C**) Production of CCL2, CCL3 and CCL5 in the spleen. Statistics= One-way ANOVA with Bonferroni post test analysis, n=4/5 animals per group.

Taken together, these data show varying levels of inflammatory chemokines in the spleens of the infected mice, with reduced levels of CCL3 in the spleen samples of the infected Ifnar ko and less CCL5 in the spleens of WT mice, this may be due to the cells that secrete it, mostly CD8$^+$T cells, having left the spleen to migrate into the brain where the levels were higher.

3.2.12 Splenic CD11b+ cells from WT were able to restore pathology

We next addressed the question whether $CD11b^+$ from infected WT mice would be able to restore ECM susceptibility. Thus, we infected 20 WT mice and 20 $LysM^{Cre}Ifnar1^{fl/fl}$ mice and isolated on d+3p.i. splenic $CD11b^+$ cells from 10 of infected WT mice, which were then adoptively transferred into 10 of the infected $LysM^{Cre}Ifnar1^{fl/fl}$ mice in order to create 4 different groups, including all controls. The schematic Figure 30 A shows the outline of the experiment.

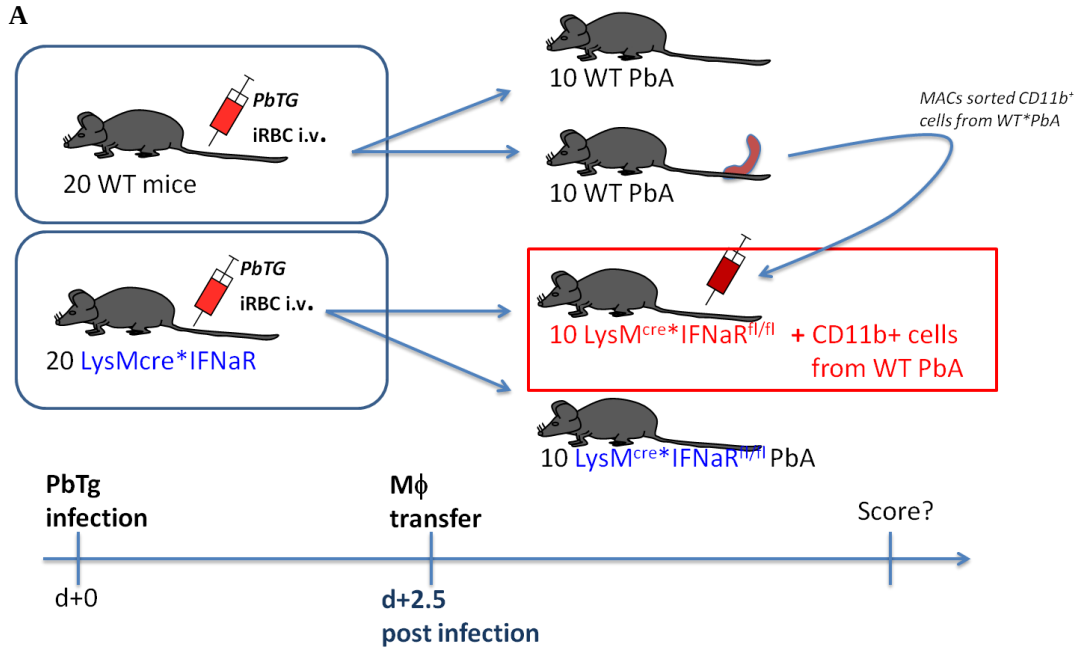

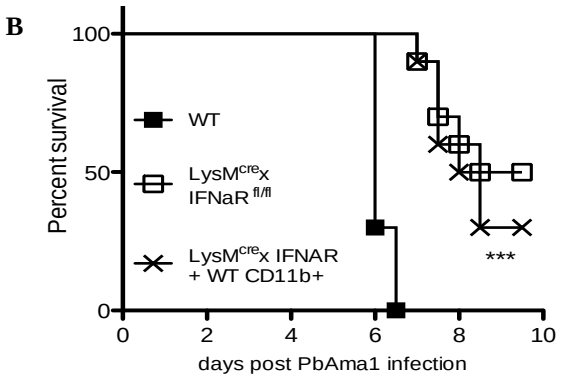

Figure 30 $CD11b^+$ cells restored ECM pathology

20 WT mice and 20 $LysM^{Cre}Ifnar1^{fl/fl}$ mice were infected i.v. with $5x10e^4$ iRBC of PbAMA. On day 3 p.i., $CD11b^+$ splenocytes were MACS-purified from 10 PbA-infected WT mice, were pooled and transferred i.v. into 10 infected $LysM^{Cre}$ $Ifnar1^{fl/fl}$ mice (1 donor/1 recipient). All mice were monitored for survival. Statistics = Kaplan-Meier survival and log-rank Test. n=10 in the final groups.

The infected WT mice served as positive control for ECM and they all developed ECM with 100% death by day 7; in contrast, 50% of the PbA-infected $LysM^{Cre}Ifnar^{fl/fl}$ control group remained ECM free (Figure 30 B). Importantly, those $LysM^{Cre}Ifnar1^{fl/fl}$ mice that had received $CD11b^+$ splenocytes from PbA-infected WT donors, developed ECM features with 1 day delay resulting in a death rate of 70% within the ECM period (day 6-9 p.i.). Thus, the transfer of WT macrophages was able to restore type I IFN signaling via $CD11b^+$ cells and boosted the onset of ECM.

3.2.13 Summary of the spleen results

Taken together, our data demonstrate a crucial role of type I IFN signalling in ECM development. However, type I IFN signalling was dispensable in development of CTL responses in the periphery. But importantly, we detected in ECM protected mice the presence of alternatively activated macrophages, that were different from the classical M1 found in C57BL/6, since they could be identified as M2 in the *Ifnar1*$^{-/-}$ mice upon PbA infection. Furthermore, PbA-infected Ifnar ko contained elevated numbers of immune effector cells in their spleen, predominantly CD8 T cells. Thus, our results also strongly indicated retention of T cells, DCs and CD11b^{+} population in the spleens of Ifnar ko mice, which might contribute to the protection from T-cell dependent brain inflammation in ECM.

3.3 High infective parasite dose of PbA mimics Malaria tolerance and prevents ECM in susceptible B6 mice

In endemic malaria zones, school children and adults have been found to have high parasitemia without development of either clinical symptoms or severe disease; apparently, repeated infections sustain a continuous antigen load, thus the high parasitemia affords them a form of tolerance. Primary data from the lab have indicated that WT mice infected with $1x10^7$ iRBCs (=high dose) were highly protected from ECM, this protection was shown to be mediated via IL-10 as *IL-10*$^{-/-}$ mice infected with $1x10^7$ iRBCs succumbed to ECM (Data Beatrix Schumak). We therefore further analysed the high dose protected mice to understand how the protection was mediated, we questioned whether there were differences in the infiltration of cells into the brain or whether there was a difference in the generation of parasite specific CTL responses in the spleen.

3.3.1 High dose tolerance mice had infiltration of CD8$^+$ T cells into their brain

We infected WT mice with the already established dose of $5x10^4$ iRBC and another group of WT as well as *IL-10*$^{-/-}$ with $1x10^7$ iRBC to confirm the ECM protection in the malaria tolerance model and its dependence on IL-10. Thus, we first analysed the ECM outcome and then the brains of mice for the infiltration of immune cells from the periphery. As described, the WT mice infected with the elevated dose were significantly protected from ECM in comparison to low dose infected littermates, whereas this protection was absent in *IL-10*$^{-/-}$ infected with $1x10^7$ iRBC, indicated by a low score (Figure 31A). However, the cell counts from brain-enriched leukocytes did not differ significantly between the different experimental groups (Figure 31B), so the reduced cell count in ECM negative high dose infected mice remained a trend. Next, we characterised brain-associated cells from the periphery via flow cytometry (shown in schematic Figure 7A).

We analysed the infiltration of effector CD8$^+$ T cell and CD4$^+$ T cells into the brains of the high dose mice and compared them with the ECM positive low dose infected WT mice and high dose infected *IL-10*$^{-/-}$ mice. We observed high frequencies of peripheral immune cells as stained by CD45 in the brain tissue of all the infected mice in comparison to the naive mice (Figure 31 C). Surprisingly, we detected a high percentage of T cells, particularly CD8$^+$ T cells in brain samples of the high dose infected WT and *IL-10*$^{-/-}$ mice in comparison to the low dose infected WT mice (Figure 31D&E). The high dose infected WT mice had elevated frequencies

of CD8^{+}T cell in their brain samples with a mean increase of 30% in comparison to the naïve control and 13% in comparison to the low dose infected WT mice (Figure 31 E).

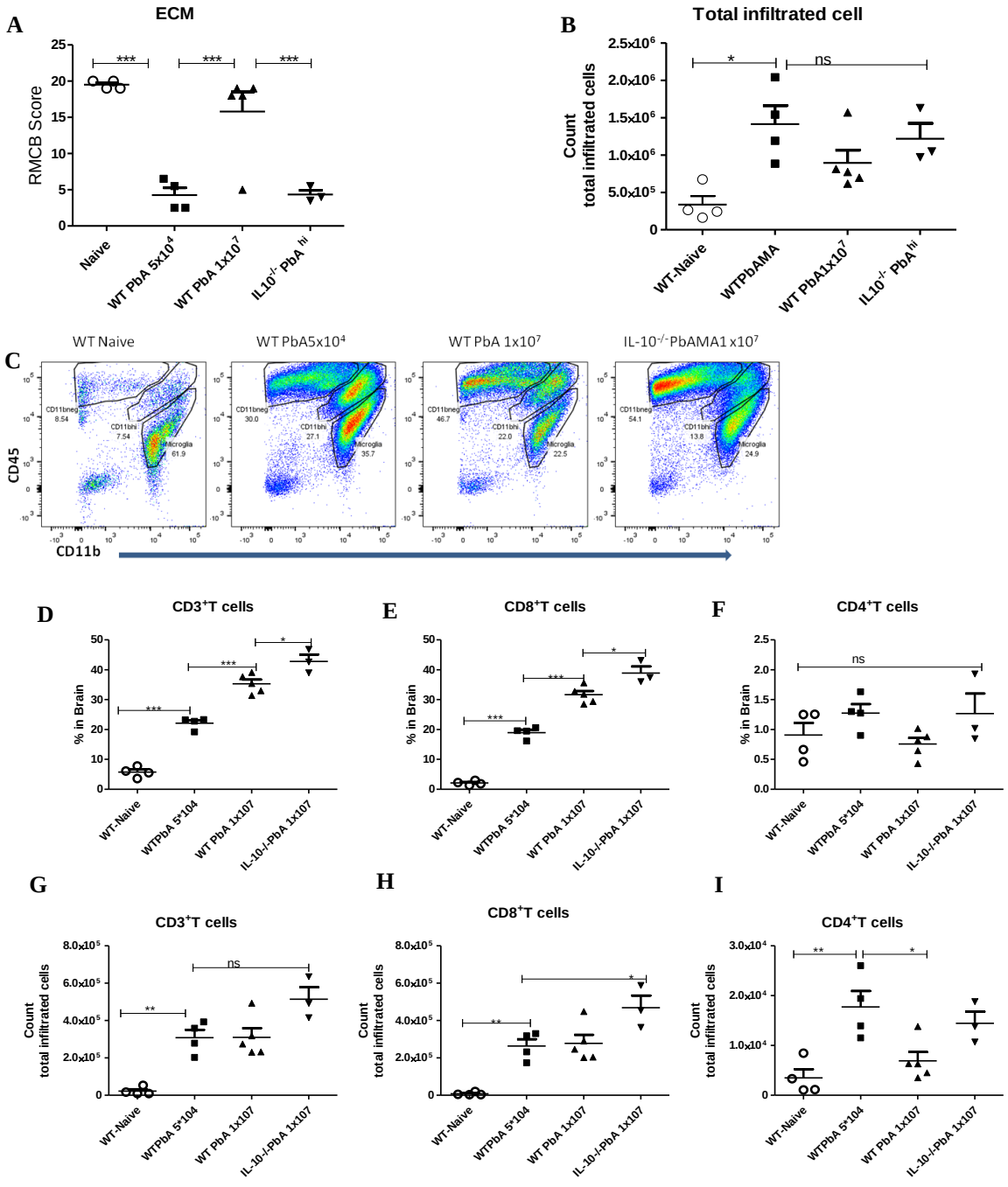

Figure 31 High levels of CD8^{+} T cells in the brain of Malaria tolerance mice without ECM

C57/BL6 WT mice were infected with 5x10^{4} and 1x10^{7}, IL-10$^{-/-}$ mice with 1x10^{7} iRBCs i.v, on d+6, mice were perfused and brains harvested, digested, and single cell suspensions prepared. The cells were counted, stained and analysed using flow cytometry. **A**) ECM score calculated using RMBCS (**B**) Total count of brain infiltrated cells. **C**) Raw data from representative samples from every experimental group showing the gating to discriminate CD45^{hi} cell. **D-F**) Percentages of infiltrated CD3^{+}, CD8^{+} and CD4^{+} T cells in the brain. **G-I**) Cell counts of infiltrated CD3^{+}, CD8^{+} and CD4^{+} T cells in the brain. Statistical analysis = One-way ANOVA with Bonferroni's post test. n=3/4/5 animals per group.

In comparison, the brain samples of high dose infected *IL-10*$^{-/-}$ mice revealed the highest infiltration of CD8^{+} T cells, which was 8% more than in the samples from the high dose infected WT mice (Figure 31 E). We observed comparable percentages of CD4^{+}T cells in brain samples of the naïve and the infected groups of mice (Figure 31 F). We also observed increased total T cell counts in brain samples of all PbA infected mice in comparison to the naïve control mice (Figure 31 G). The CD8^{+} T cell count was significantly elevated in brain samples of high dose infected *IL-10*$^{-/-}$ mice in comparison to the other infected mice groups (Figure 31 H). Unlike in the percentage values of CD4^{+}T cells, which were comparable among all the animal groups, the total cell counts were significantly higher in the low dose infected WT mice in comparison to the other infected mice (Figure 31 F&I). Taken together, these data indicates the presence of immune cell in the brains of ECM protected high dose infected WT mice, however, FACS analysis does not allow to determine if these cells had passed the BBB and were arrested in the brain or just present in the circulation and not able to pass the BBB.

3.3.2 High dose mice contained inflammatory monocytes in brain tissue

We next analysed whether mononuclear cells had infiltrated into the brains of the high dose infected WT mice. As earlier mentioned, inflammatory monocytes have been shown to contribute to ECM pathology (Schumak et al. 2015). The mononuclear cells were gated according to their expression of CD11b and CD45 (illustrated in schematic Figure 15A).

Here, we observed increased frequencies of CD11b^{hi} cells from the periphery in the brains of low dose infected WT and high dose infected WT in comparison to the naïve, although this difference was statistically insignificant (Figure 32A). We observed an increased frequency of Ly6C^{hi} inflammatory monocytes in brain samples of both low dose and high dose infected mice in comparison to the naïve (Figure 32B). We did not observe significant difference in the frequency of Ly6C^{hi} inflammatory monocytes in brain samples of both high dose infected WT and *IL-10*$^{-/-}$ mice in comparison to the low dose infected WT mice (Figure 32B). The frequency of neutrophils in brain was reduced in samples from all PbA infected mice in comparison to the naïve control mice, however, when we considered cell counts, the low dose infected WT mice had higher but non-significant values (Figure 32C&F). We also observed significantly elevated cell count of CD11b^{hi} and Ly6C^{hi} inflammatory monocytes in brain samples of low dose infected WT in comparison to the naïve (Figure 32D &E). Although there were lower counts of CD11b^{hi} and Ly6C^{hi} inflammatory monocytes in brain samples from the high dose infected WT in comparison to the low dose infected WT mice, these differences were not statistically significant (Figure 32D &E). Brain samples of high dose infected *IL-10*$^{-/-}$ mice were

comparable to both the low dose and high dose infected WT mice (Figure 32D-F). In conclusion, although we observed with FACS Ly6C^{hi} inflammatory monocytes in brain samples of the high dose infected WT tolerance model, these mice were still protected from ECM.

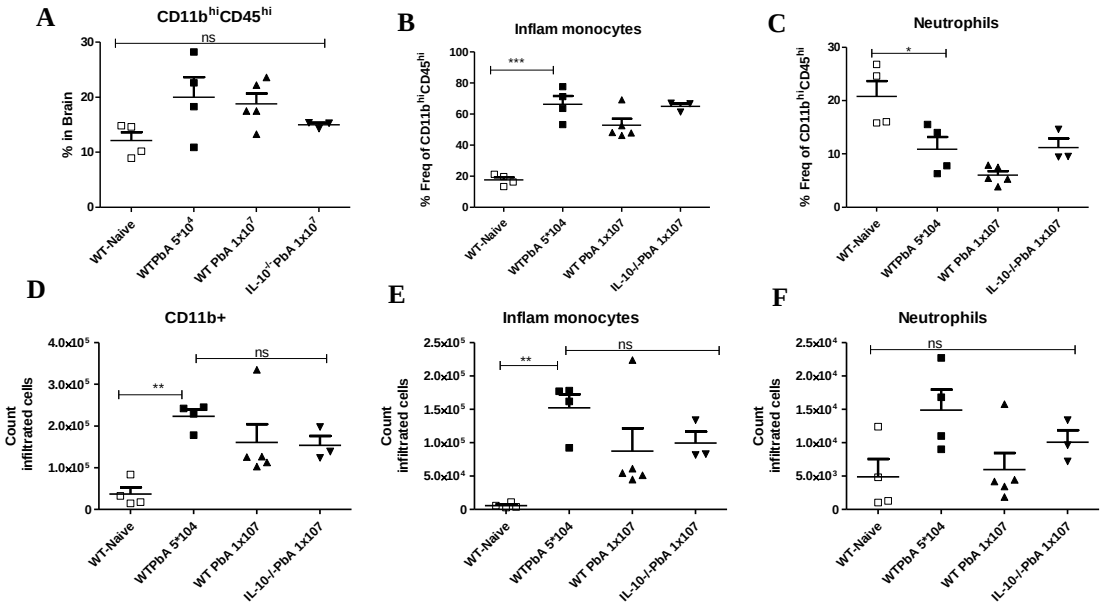

Figure 32 inflam. monocytes in brains of mice from the malaria tolerance group despite absence of ECM

C57/BL6 WT mice were infected with 5x10^4 and 1x10^7, IL-10$^{-/-}$ mice with 1x10^7 PbA iRBCs i.v. On d+6, mice were perfused and brains harvested, digested, and single cell suspensions prepared. The cells were counted, stained and analysed using flow cytometry. **A**) Percentage of brain infiltrated CD11b^{hi}CD45^{hi} cells. (**B**) Freq. of CD11b^{hi}CD45^{hi} that are inflam. monocytes. **C**) Freq. of CD11b^{hi}CD45^{hi} that are Neutrophil. **D-F**) Total cell counts of infiltrated CD11b^{+}, inflam. monocytes and neutrophils in the brain. Statistical analysis= One-way ANOVA with Bonferroni post test. n=3/4/5 animals per group.

3.3.3 The high parasite load resulted in dampened inflammatory response without impairing the Ag specific response

As we had observed that WT mice infected with high dose of PbA were protected from ECM, but still presented peripheral immune cells in their brains (even if it was not clear whether these cells had passed the BBB or not). We questioned whether this protection from ECM was due an impaired immune response in the spleen. We therefore analysed the effector CD8^{+}T cells in the spleens of the Malaria-tolerized mice for the ability to recognise and kill target cells presenting parasite specific MSP-1 Ag as described in the section with the Ifnar ko,(page 44). Briefly, mice were infected with appropriate doses of transgenic PbAMA expressing ovalbumin. On day 5p.i. and 6 p.i. We performed an in vivo kill to calculate the specific cytolytic activity of peptide-specific T cells that were generated in immunized animals, but not in non-immune naïve control mice.

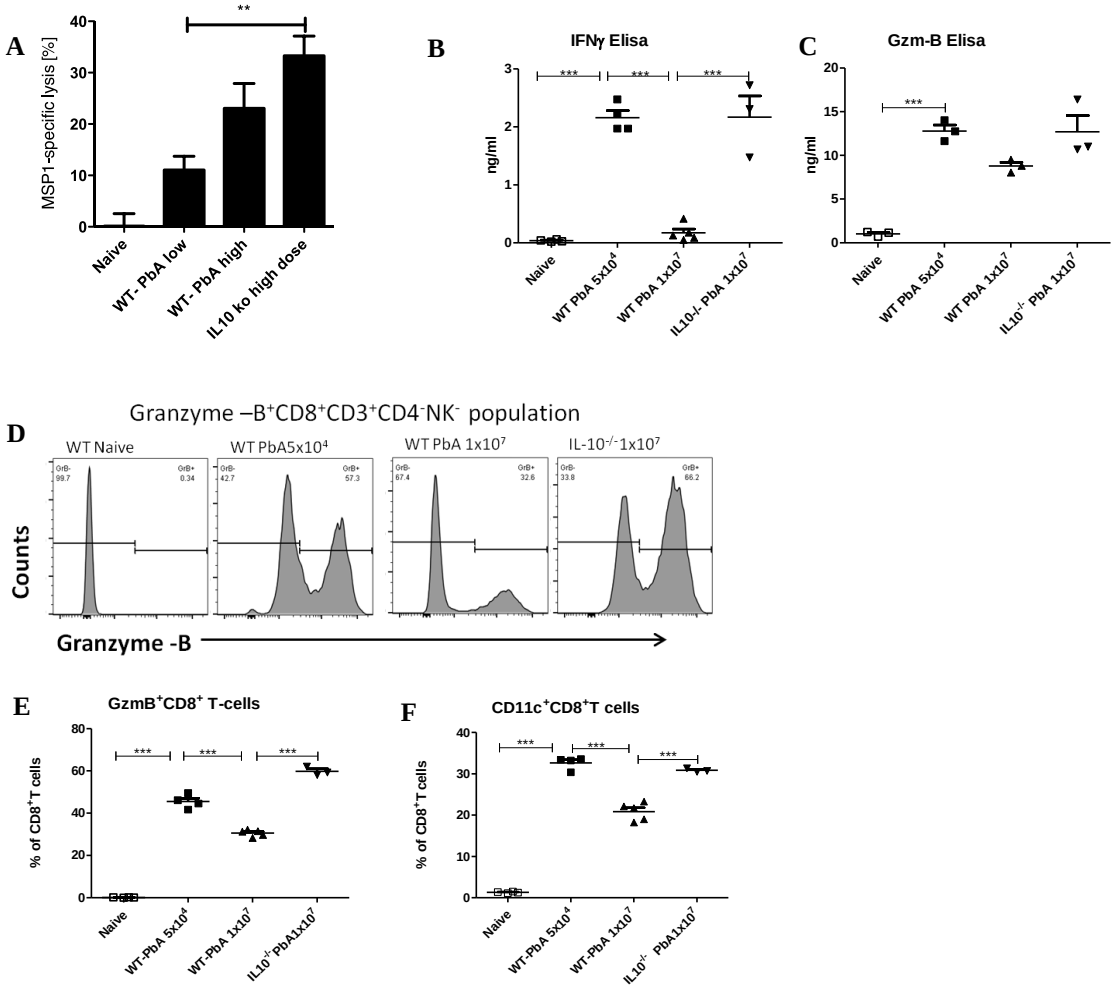

Figure 33 IL-10 damped inflammatory response in *Malaria tolerance but did not alter Ag specific kill*

C57/BL6 WT mice were infected with $5x10^4$ and $1x10^7$, IL-$10^{-/-}$ mice with $1x10^7$ PbA iRBCs i.v. On d+6, mice were perfused, spleens were digested and single cell suspensions prepared. The cells were counted, stained and analysed using flow cytometry. For Elisa $1x10^6$ cells were plated in triplicates and cultured overnight at 37^0C, the next day supernatants were taken and ELISA performed as described in methods. (**A**) Analysis of antigen-specific CTL activity in the spleen. (**B&C**) Production of IFNγ and granzyme B measured by ELISA (**D**) Histogram showing the expression levels of grazyme B on $CD8^+$ T cells. **E&F**) Frequency of $CD8^+$T cells expressing granzyme B and CD11c. Statistics =One-way ANOVA with Bonferroni post test. n=3/5 animals per group.

Here, we observed that the high dose infected WT mice were able to recognise and mount a parasite specific CTL response against the target cells presenting the MSP-1 peptide, with high dose infected *IL-10*$^{-/-}$ mice demonstrating the highest kill (Figure 33A). Most importantly, despite the ability to specifically lyse Ag, we observed a complete lack of IFNγ production in spleens of high dose infected WT mice that were protected from ECM in comparison to the low dose infected WT and high dose infected *IL-10*$^{-/-}$ mice, which both suffered from ECM (Figure 33B). Interestingly, splenic $CD8^+$ T cells from the high dose infected WT mice showed in addition reduced granzyme B expression, which was ~14.5% lower in comparison to both low dose infected WT and high dose infected *IL-10*$^{-/-}$ mice. Also, we measured significantly

lower amounts of granzyme-B in supernatants from spleen cell of high dose infected WT mice in comparison to the ECM positive low dose infected WT and high dose infected *IL-10*$^{-/-}$ mice (Figure 33C-E). In parallel to diminished granzyme-B levels, we also observed ~10% less splenic CD11c^{+}CD8^{+} T cell in samples from high dose infected WT mice in comparison to the other PbA infected mice (Figure 33F). As expected, the corresponding splenocytes from naïve control mice produced neither IFNγ nor granzyme-B nor contained any antigen activated CD8^{+}T cells (Figure 33B-F).

Taken together, these data demonstrated the role of the elevated parasite dose in suppression of detrimental effector molecules that are crucial for ECM, even if a basic CTL response was still detectable. Furthermore, the lack of IL-10 resulted in the production of the inflammatory cytokine IFNγ, whereas high-dose infected WT mice that had successful induced malaria tolerance benefited from dampening inflammation without affecting the Ag specific CTL response.

3.3.4 Malaria tolerance mice contained an unaltered CD4:CD8 ratio in the spleen

Above, we had observed in the ECM-protected Ifnar ko mice splenomegaly and an altered CD4:CD8 ratio in the spleen, resulting from a retention of CD8 T cells. Here, we also compared the spleen weights, total cell counts and CD4^{+} T cells/ CD8^{+} T cells composition between the high dose PbA infected and the low dose infected mice.

We did not observe a difference in the total spleen cell counts in samples from the low dose infected WT in comparison to the naïve control and the high dose infected *IL-10*$^{-/-}$ mice (Figure 34 A). However, the high dose infected WT mice had significantly elevated spleen cells count in comparison to the naïve and the high dose infected *IL-10*$^{-/-}$ mice with ~1.46 fold increase to both groups (Figure 34 A). Despite the comparable spleen cell numbers between the low dose infected WT mice and the naïve control mice, the spleens of the low dose infected WT mice weighed ~56mg more than those of the naïve control (Figure 34 B). The spleen weights of the low dose and high dose infected WT mice were comparable (Figure 34 B).

We observed less CD3^{+}T-cells in the spleens of low and high dose infected WT mice when compared to the naïve control mice, however, this difference was not statistically significant (Figure 34C). The percentage of CD8^{+} splenic T cells were comparable in samples from the naïve, low dose infected WT and high dose infected WT mice, however, high dose infected *IL-10*$^{-/-}$ mice had a significant increase in this population in their samples (Figure 34D). The frequency of CD4^{+} T cells in spleen samples from high dose and low dose infected WT mice

were comparable to the naive, however, the high dose infected *IL-10*$^{-/-}$ mice had a significant decrease in this population in comparison to the other groups of mice (Figure 34D).

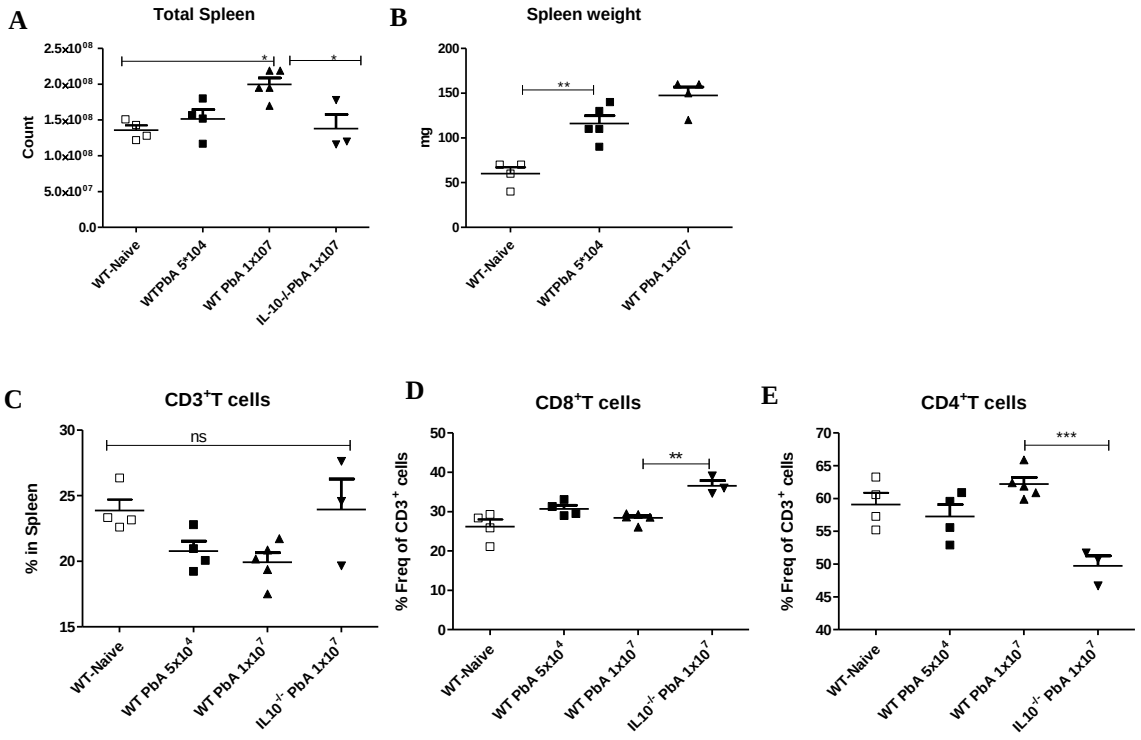

Figure 34 IL-10 ko high dose have high CD8$^+$ T cells in their spleens

C57/BL6 WT mice were infected with 5x10^4 and 1x10^7, *IL-10*$^{-/-}$ mice with 1x10^7 PbA iRBCs i.v. On d+6, mice were perfused, spleens weighed, then digested and single cell suspensions prepared. The cells were counted, stained and analysed using flow cytometry. **A**) Total spleen cells count (**B**) Weight of the spleens. **C**) Percentage of CD3$^+$T cell populations in the spleen (**D&E**) Frequency of CD8$^+$ T cells and CD4$^+$ T cells. Statistics= One-way ANOVA with Bonferroni post test. n=3/4/5 animals per group.

Taken together, these data show that the infected WT mice of the so-called malaria tolerance model group presented in general splenomegaly, but contained a comparable composition of splenic T cell populations as the low dose ECM positive mice.

3.3.5 High dose infection suppressed the development of a Th-1 phenotype

As ECM is a Th-1 driven disease, we next analysed, whether the protection from ECM that we had observed among the high-dose infected mice was mediated by regulatory T cells (T reg). We therefore analyse the different CD4$^+$ T cell subsets by staining their transcriptional factors; T-bet for Th-1, FoxP-3 for T regs, GATA3 for Th-2 and ROR-γt for Th-17. From the FoxP3^{neg}Tbet^{neg}CD4$^+$ T cells, we evaluated the expression of granzyme B.

We observed an increased frequency of CD4$^+$T cells expressing T-bet in spleen samples from the low dose infected WT in comparison to the naïve control mice, importantly, the high dose

infected WT mice had ~11% less T-bet expressing $CD4^+$T cells in their spleen samples in comparison to the low dose infected WT mice (Figure 35 A&B).

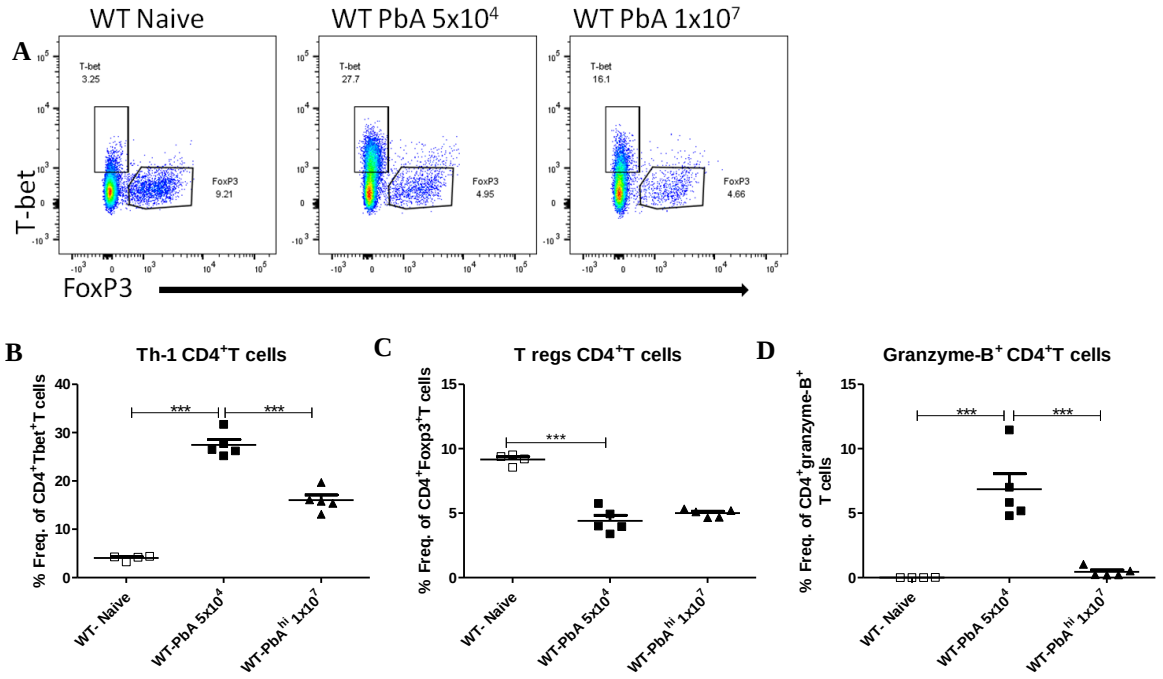

Figure 35 High parasite dose partially suppressed Th-1 response

C57/BL6 WT mice were infected with $5x10^4$ and $1x10^7$ PbA iRBCs i.v. On d+6, mice were perfused and brains harvested, digested, and single cell suspensions prepared. The cells were counted, stained and analysed using flow cytometry. (**A**) Raw data from representative samples from every experimental group (**B**) Frequency of $CD4^+$T cells expressing T-bet. (**C**) Frequency of $CD4^+$T cells expressing FoxP3. (**D**) Frequency of $CD4^+Tbet^{neg}FoxP3^{neg}CD8^{neg}NK^{neg}$ expressing granzyme-B. Statistics = One-way ANOVA with Bonferroni's Multiple post test. n=4/5 animals per group.

Furthermore, the percentage of FoxP3 expressing splenic $CD4^+$ T cells was reduced, in samples from both low and high dose infected WT mice in comparison to the naïve mice (Figure 35A&C). The high dose infected WT mice completely lacked the presence of granzyme B expressing $CD4^+$T cells in their spleen, therefore being comparable to the naïve mice, unlike the low dose infected WT mice that contained ~6% granzymeB^+ $CD4^+$ T cells in their spleens (Figure 35 D). We did not detect any Th-2 or Th-17 cells in the spleen samples of all the mice (data not shown). Taken together, this data show that in the high-dose-induced tolerance mice the Th-1 response was suppressed to some extent, and the expression of granzyme-B by $CD4^+$ T cell in the spleen completely blocked. This data also indicate that T-regs might just have a minor role in the protection observed in the tolerance mice model.

3.3.6 NK cells from high dose mice produced significantly less granzyme B

We next analysed splenic NK cells during the high dose infection to see the impact of the high parasite dose on this cell population and possible source of further effector molecules. We

observed a significant decrease in the percentage of NK cells in the spleen samples from all infected groups in comparison to the naïve mice. The percentage of NK cells among the high dose infected WT mice was reduced in comparison to the low dose infected WT but was comparable to the high dose infected *IL-10*$^{-/-}$ mice (Figure 36A).

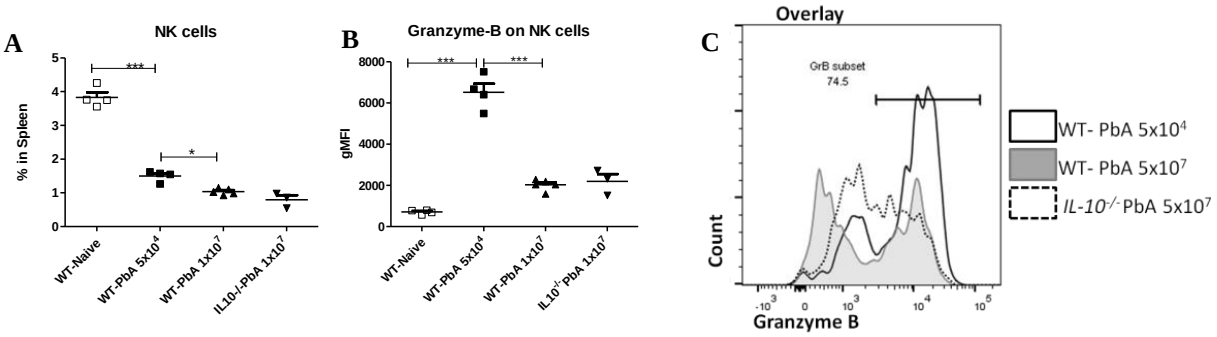

Figure 36 PbA high dose affects granzyme-B expression by NK cells

C57/BL6 WT mice were infected with 5x10^4 and 1x10^7, *IL-10*$^{-/-}$ mice with 1x10^7 PbA iRBCs i.v. On d+6, mice were perfused and spleens harvested, digested, and single cell suspensions prepared. The cells were counted, stained and analysed using flow cytometry. (**A**) Percentage of NK cells in the spleen. (**B**) Expression level of granzyme-B by NK cells as gMFI. (**C**) Histogram overlay of expression of granzyme B by NK cells. Statistics= One-way ANOVA with Bonferroni post test. n=3/4/5 animals per group.

Interestingly, we also observed significantly reduced expression levels of granzyme B in splenic NK cells from high dose infected WT mice, in comparison to the low dose infected WT mice (Figure 36B &C). The high dose infected *IL-10*$^{-/-}$ mice also had reduced expression of granzyme B in their spleen in comparison to the low dose infected WT mice (Figure 36B &C). Taken together, this data support the impact of high doses of PbA infection in suppression of the important effector molecule granzyme- B by splenic NK cells.

3.3.7 Infection with high dose of parasites resulted in decreased B cells in the spleen

We next analysed the influence of the high dose parasite load on splenic B cells and DC populations, as we had mentioned earlier that DCs are the key APCs during ECM with a key role in priming effector T cells (Lundie et al. 2008; deWalick et al. 2007). Here, we observed a significant decrease in the percentage of splenic CD19$^+$ B cell in samples from high dose infected WT mice in comparison to the low dose infected WT and high dose infected *IL-10*$^{-/-}$ mice (Figure 37A). The population of splenic CD11c$^+$ DCs was significantly reduced in samples from all the infected groups in comparison to the naïve mice (Figure 37 B). We did not pursue these groups of cells any further.

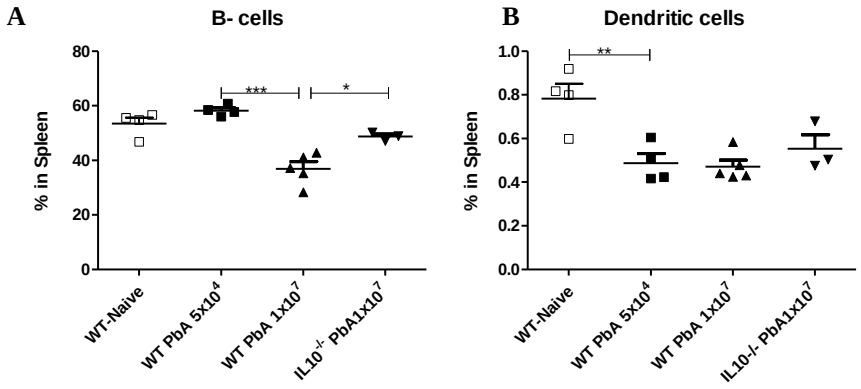

Figure 37 High parasite load resulted in decreased amount of splenic B cells

C57/BL6 WT mice were infected with $5x10^4$ and $1x10^7$, IL-$10^{-/-}$ mice with $1x10^7$ PbA iRBCs i.v. On d+6, mice were perfused and spleens harvested, digested, and single cell suspensions prepared. The cells were counted, stained and analysed using flow cytometry. (**A**) Percentage of B cells in the spleen (**B**) Percentage of DCs in the spleen. Statistics= One-way ANOVA with Bonferroni post test. n=3/4/5 animals per group.

3.3.8 Comparable IL-10, IL6 and TNF in the spleens of the ECM protected mice

We further compared the levels of cytokines and chemokine in the spleen of the malaria tolerance group of mice in comparison to the ECM susceptible WT mice. Surprisingly, the protected mice infected with high dose parasite load had comparable levels of chemokines and cytokines to the low dose infected WT mice despite the different disease outcome.

The levels of IL-10, IL-6 and CCL3 did not differ significantly between the naïve and the PbA infected WT mice (Figure 38A, B&E). Also unexpected was the increased level of TNF measured in supernatants from splenocytes of the high dose infected WT mice, this increase was comparable to the low dose infected WT mice, but significantly higher than the naïve control mice (Figure 38C). We measured low amounts of CCL2 in supernatants from spleen cells of high dose infected WT in comparison to low dose infected WT mice, the high dose had values comparable to the naïve control mice (Figure 38D), whereas CCL3 and CCL5 did not differ significantly between the two groups of infected mice (Figure 38E& F). Taken together, these data show that tolerance occurred in the high dose infected mice, in spite of the high TNF levels in the spleen, which may have been counteracted by a regulatory mediator.

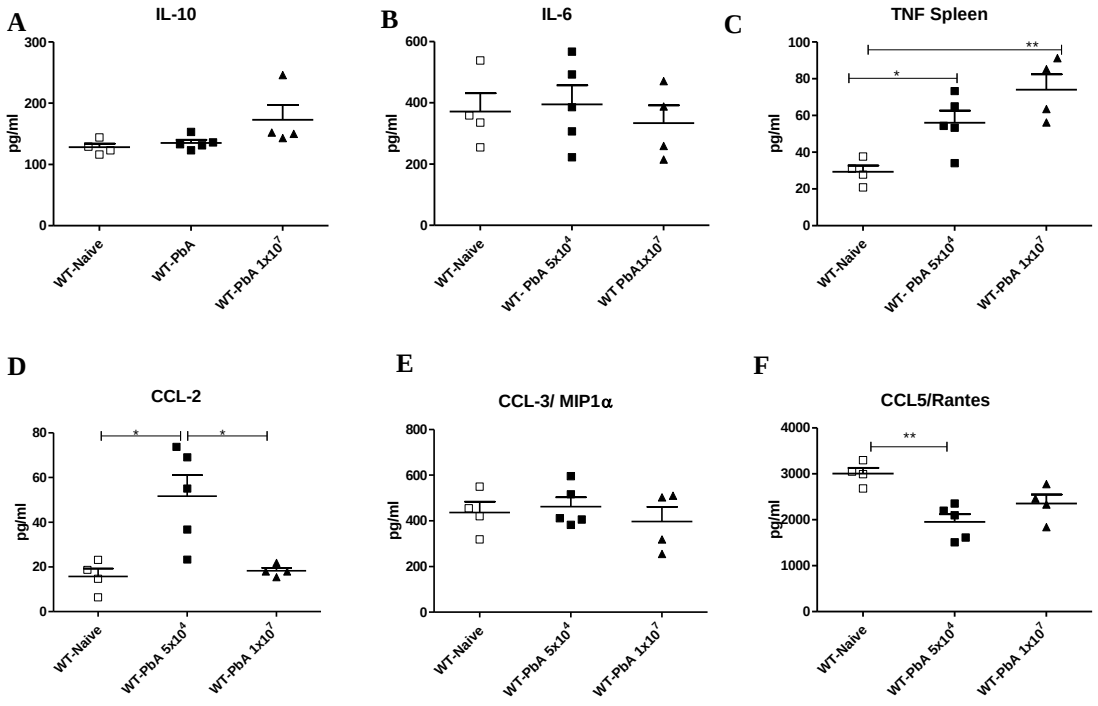

Figure 38 Protected high dose infected WT mice produced high levels of TNF in their spleen

C57/BL6 WT mice were infected with $5x10^4$ and $1x10^7$ PbA iRBCs i.v. On d+6, mice were perfused, spleens harvested, digested, and single cell suspensions prepared. The cells were counted and $1x10^6$ cells plated in triplicates in 96 well plates, the cultures were then incubated for 24hrs at 37^0C. Supernatants were collected and ELISA performed as described in methods. (**A-C**) Production of cytokines IL-10, IL-6 and TNF in the spleen. (**D-E**) Production of chemokines of CCL3/MIP-1α and CCL5/Rantes in the spleen. Statistics= One-way ANOVA with Bonferroni post test. n=4/5 animals per group.

3.3.9 High parasite loads partially suppressed the expression of MHC class II on Ly6C^{hi}CCR2^{+} inflammatory monocytes in the spleen

We have shown the predominant presence of AAMs in splenic samples of ECM protected *Ifnar1*$^{-/-}$ mice (Figure 27). As we did not observe any increase in the T-regs population in the high dose infected mice, we next questioned whether the tolerance observed in the high dose infection might be also here driven by AAMs. We analysed for the presence of AAM, inflammatory monocytes and neutrophils. As described above (Figure 27), we gated first for CD11b^{hi} cells and from this population we selected Relmα^{hi}F480^{hi} and Ly6Chi vs Ly6G, and then overlayed the populations to confirm they were different populations.

We observed a reduction in the percentage of CD11b^{hi} cells in the spleen samples of both low and high dose infected WT mice in comparison to the naïve control mice (Figure 39 B).

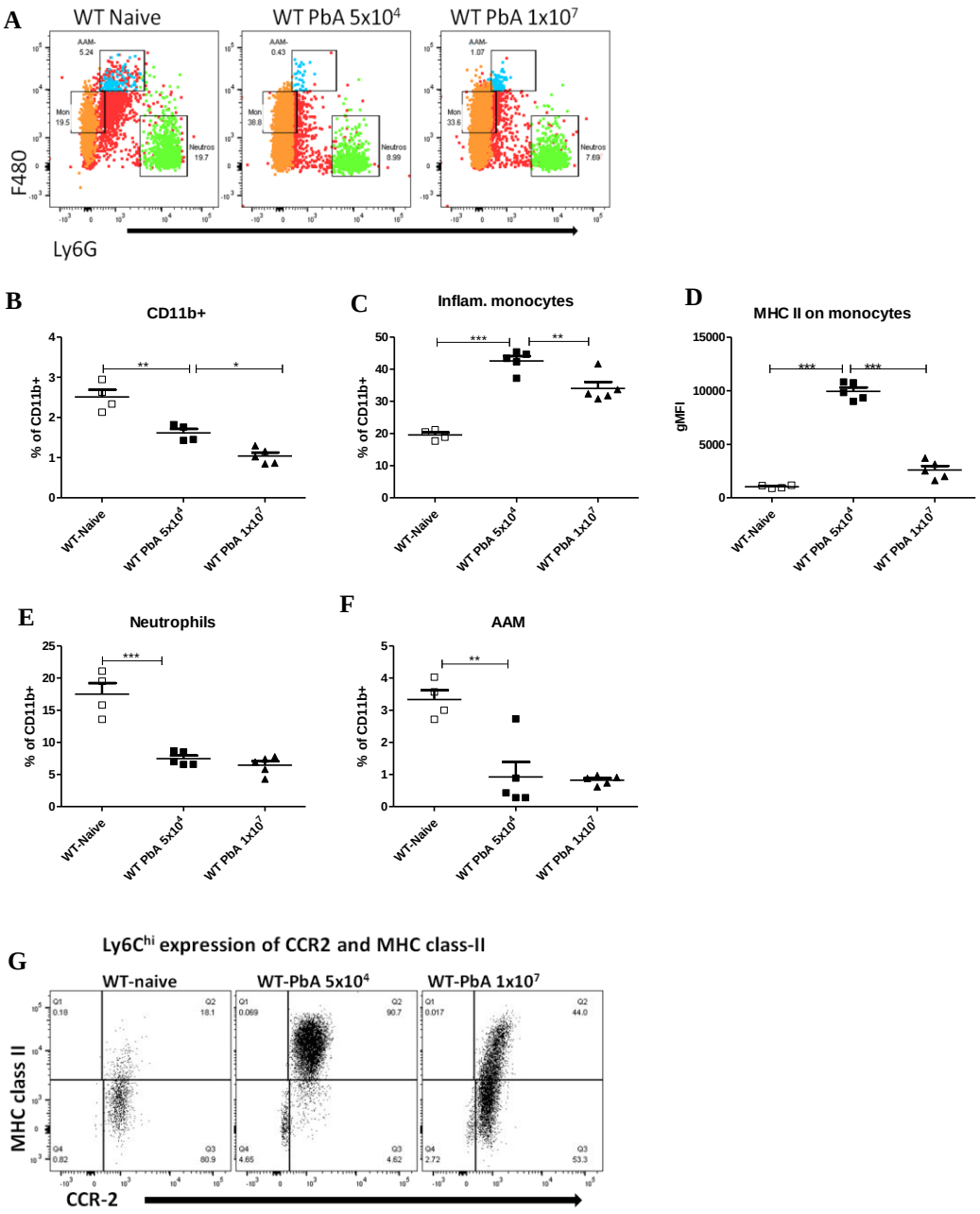

Figure 39 Tolerance mice model did not contain AAM

C57/BL6 WT mice were infected with $5x10^4$ and $1x10^7$ PbA-iRBCs i.v. On d+6, mice were perfused, spleens harvested and single cell suspensions prepared. The cells were counted, stained and analysed using flow cytometry **A)** Raw Facs data from representative samples from each experimental groups. **B)** Percentage of $CD11b^{hi}$ in the spleen. **C)** Percentage of inflam. monocytes. **D**) Expression of MHC calss II on Inflam. monocytes. **E & F)** Frequency of neutrophils and alternative activated macrophages from $CD11b^+$ cells. Statistics= One-way ANOVA with Bonferroni post test. n=4/5 animals per group.

The low dose infected WT mice had significantly more $CD11b^+$ cell that were identified as $Ly6C^{hi}CCR2^+$ inflammatory monocytes in comparison to the naive and the high dose infected WT (Figure 39C). Although we observed an increased percentage of $Ly6C^{hi}CCR2^+$ inflammatory monocytes that had been associated with pathology, in spleen samples of high dose infected WT mice in comparison to the naïve control, this population was significantly

smaller (~9% less) than in the low dose infected WT mice (Figure 39C). Importantly, we measured lower levels of expression of MHC class II on Ly6C^{hi}CCR2^{+} inflammatory monocytes in spleen samples from high dose PbA infected mice in comparison to the low dose infected mice (Figure 39D&G). The percentage of neutrophils was significantly reduced in samples from both low and high dose infected WT in comparison to samples from naïve control mice (Figure 39E**)**. Unlike in the infected *Ifnar1*$^{-/-}$ mice (Figure 27G), the CD11b^{hi} populations of both the low dose infected WT mice and the high dose infected WT mice contained very low populations of AAMs (Figure 39F). Taken together, our data show that the mice infected with high parasite dose contained less inflammatory monocytes which expressed strongly reduced levels of MHC class II, however, tolerance induction and protection could not be attributed to AAM here.

3.3.10 Protection of the high dose infected mice was dependent on IL-10 production by myeloid cells

Results from previous lab experiments showed that protection of the high dose infected mice was dependent on IL-10. We have also shown that this protection was apparently not dominantly driven by T-regs. We therefore investigated whether the protection was mediated by macrophages, since we had observed in the ECM protected Ifnar ko mice a specific relevance of this cell population. We performed a survival analysis using LysM^{cre}*IL-10*$^{fl/fl}$ mice, which lacked specifically the production of IL-10 by LysM^{+} cells.

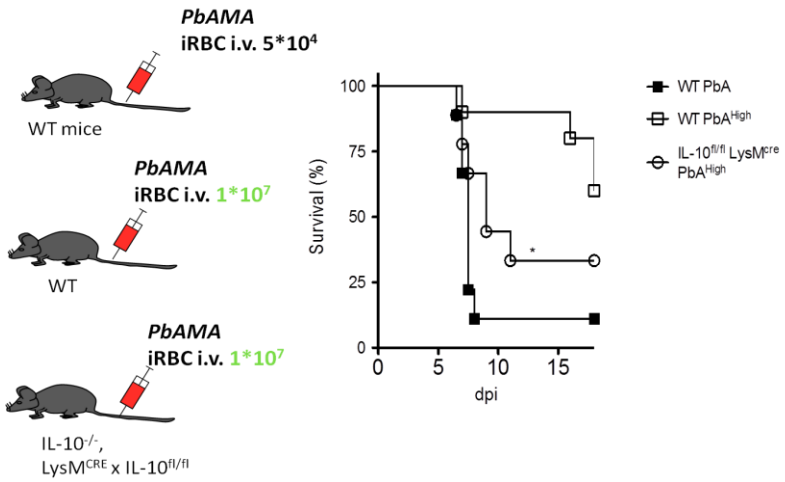

Figure 40 protection in the tolerance model is mediated by macrophages

C57/BL6 and LysM^{Cre}*IL-10*$^{fl/fl}$ mice were infected with 5x10^{4} and 1x10^{7} iRBCs i.v. They were then monitored from d+5 p.i for survival. n=8 animals per group. Statistics=mLog-rank (Mantel-Cox) Test.

.

As expected, 90% of the low dose infected WT mice developed ECM and died by day 7 p.i, while 90% of the high dose infected WT mice survived past the ECM phase, importantly only 25% of the mice lacking IL-10 on LysM expressing cells survived past the ECM phase (Figure 40). Mice that survived past the ECM phase developed high parasitemia and anemia and were

sacrificed. This data demonstrated the role LysM expressing cells in production of IL-10 that promoted tolerance during the high dose infection.

Summary; our results demonstrated the role of IL-10 produced by macrophages in providing tolerance during high dose infection. The tolerance model was characterized by complete lack of production of pro-inflammatory cytokine IFNγ and reduced granzyme B production by NK cells. However, the capacity to recognise and lyse antigen presenting target cells was not impaired in mice infected with an elevated dose of parasites. Furthermore, we confirmed an essential role of IL-10 in immune regulation during PbA infection and point out that myeloid cells, – in particular $LysM^{pos}$ cells /$CD11b^{pos}$ cells – had a key role in balancing the immune responses towards inflammation (which can result in ECM) or immune regulation, thereby preventing immune damage.

4 Discussion

Malaria has been regarded as a disease of poverty as it is predominantly found in developing countries. And although cerebral malaria (CM) in children can be successfully treated, it still impacts the "disability-adjusted life years" (DALYs), meaning lost years, and has lasting impact on the cognitive development of the children (Idro et al. 2010). CM is multifactorial, and murine models have made it easier to study different factors. The contribution of immune cells, parasites load in the brain, cytokines and chemokines are continuously being included or excluded in their contribution of CM pathology with the help of experimental models. Using murine models of CM, we demonstrate here the non-redundant role of inflammatory type I IFN signalling via myeloid cells in the pathogenesis of ECM. Ifnar ko mice were protected from ECM and lacked brain inflammation. However, they were able to generate parasite-specific CTL responses in the periphery, although these were attenuated and paralleled by the co-presence of alternatively activated macrophages and IL-10, which apparently dominated the immune responses. We also examined a model for malaria tolerance, which was induced upon infection with an elevated dose of *Plasmodium* parasites and characterized by reduced production of IFNγ and observed that IL-10 plays a role in tolerance.

The role of type I IFNs in diseases can be compared to the head and tail of a coin, depending on the disease the outcome can be beneficial or detrimental. Type I IFNs are beneficial in infectious diseases for controlling viral infections and as therapy for Hepatitis B and C (González-Navajas et al. 2012). In auto-immune diseases, IFN-β is used as therapy for relapsing-remitting multiple sclerosis through reduction of inflammation and episodes of relapse (González-Navajas et al. 2012). In contrast to the benefits shown in viral infections and multiple sclerosis, type IFN production and signalling during malaria has been shown to be detrimental to the host. The crucial role of type I IFN production and signalling in *Plasmodium* infection cannot be underestimated, as the parasite and its by-products, GPI, heme, and parasite DNA, trigger the production of type I IFNs via different sensing pathways (Sharma et al. 2011; Gazzinelli et al. 2014). These produced type I IFNs then signal via the single heterodimeric receptor IFNaR1& IFNaR2.

Here we observed enhanced survival in mice lacking Ifnar during PbA infection, this is in agreement with what has been shown before (Ball et al. 2013; Palomo et al. 2013; Sharma et al. 2011; Haque et al. 2011). We also show that the protection from ECM occurred independently of parasitemia, an observation also shown by Ball et al. using the *Ifnar1*$^{-/-}$ mice (Ball et al. 2013). However, Haque et al. showed reduced parasitemia among the ECM-protected *Ifnar1*$^{-/-}$

mice (Haque et al. 2011), this difference could be attributed to either genetic differences in parasites or mice.

Here, we have gone a step further in our experiments to clearly demonstrate, that the lack of the receptor on myeloid cells, specifically the LysM+ population - limiting this to macrophages - was crucial in mediating the pathology, while the lack of the receptor on cDCs was dispensable. We further propose a mechanism through which the lack of the Ifnar on all cells and on myeloid cells mediates the protection against ECM.

4.1 Type I IFN signalling via Ifnar on myeloid has a role in pathogenesis of ECM.

In our results we observed protection from brain inflammation in mice lacking Ifnar on all cells or specifically on myeloid cells. Both groups had a stable BBB, few immune cells from the periphery present in their brains and low inflammatory mediators in their brains. In contrast, mice deficient of the Ifnar only on cDCs developed ECM, had high presence of immune cells from the periphery and inflammatory mediators in their brains, and although they showed a stable BBB, this was mostly attributed to the one day delay in ECM that we observed in their survival. Since most of the PbA infected WT mice develop neurological symptoms on d+6p.i and die shortly after, at the time point of our experiments, PbA infected CD11c^{Cre}*Ifnar1*$^{fl/fl}$ mice still showed a stable BBB.

ECM has been strongly linked to effector CD8^{+}T cells primed in the spleen that infiltrate into the brain and cause pathology via release of granzyme B and perforin (Lundie et al. 2008; Nitcheu et al. 2003; Haque et al. 2011). Expression of CD11c on CD8^{+}T cells was shown to be a marker of activation, priming and cytotoxicity during PbA infection (Zhao et al. 2014; Tamura et al. 2011). We have shown in our results that mice that lacked the Ifnar specifically on myeloid cells or on all cells had low numbers of CD8^{+} T cells present in their brains. It was therefore crucial to observe, that the few CD8^{+} T cells from the periphery present in the brains of the protected mice expressed similar levels of cytotoxicity and activation as those of the ECM positive mice. This was demonstrated by expression of granzyme B and CD11c by CD8^{+}T cells isolated from the brains, hence showing that these cells were as cytotoxic and activated as the T cells that were from the ECM positive mice. However, what differed was the total amount of these cells present in the brain and we could not rule out by FACS analysis, whether these T cells in ECM negative mice really had passed the blood brain barrier, which was shown to be intact. Furthermore, the protected mice had lower amounts of parasites in

their brains and for pathology to occur it was shown that there has to be a substantial amount of parasite load in the brain (Howland et al. 2013; Baptista et al. 2010). Although we observed some variation in the levels of expression of ICAM-1 and CCR2 on $CD8^+$ T cells, we presume that these did not have a role in the ECM protection, as ko mice of CCR2 and ICAM-1 were shown to be susceptible to malaria (Belnoue et al. 2003; Ramos et al. 2013). Therefore, we can conclude that the low amount of effector $CD8^+$T cells, coupled with low parasite antigen in the brain, contributed to protection from ECM observed in mice that lacked the Ifnar specifically on myeloid cell or on all cells.

Inflammatory monocytes are the second largest cell population that infiltrates into the brains of mice that develop ECM. Increased amounts of $Ly6C^{hi}$ inflammatory monocytes have been found in the brains of ECM positive mice and were shown to have a role in the recruitment of efffector T cells as their depletion resulted in decreased $CD8^+$T cells in the brains (Pai et al. 2014; Schumak et al. 2015). We show that signalling of type I IFNs via myeloid cells was required for the infiltration of $Ly6C^{hi}$ inflammatory monocytes from the periphery into the brain. The lack of Ifnar resulted in significantly lower amounts of $Ly6C^{hi}$ inflammatory monocytes in the brain, which proved to be beneficial for the mice as there was little or no TNF being produced, which would have contributed to creating an inflammatory environment. We presume that $Ly6C^{hi}$ inflammatory monocytes were the main source of TNF found in the brains of the ECM positive WT and $CD11c^{Cre}$*Ifnar1*$^{fl/fl}$ mice. We cannot however completely rule out that other brain infiltrated cells or resident cells were also producing TNF, however $Ly6C^{hi}$ inflammatory monocytes have been shown to be the major producers of TNF in mice model for intracerebral hemorrhage (Hammond et al. 2014) and contact dermatitis (Chong et al. 2014). As $Ly6C^{hi}$ inflammatory monocytes have been shown to have a role in the recruitment of $CD8^+$T cells into the brain (Schumak et al. 2015), their absence in the brain could be a contributing factor to the low number of $CD8^+$T cells in the samples from the ECM protected mice.

The influence of type I IFN signalling in recruitment of cells into the brains was not only limited to $CD8^+$T cell and inflammatory monocytes, in the absence of Ifnar, $CD4^+$ T cells, NK cells and $CD8\alpha^+$DCs were also reduced. NK cells were shown to infiltrate into the brains of ECM positive mice and were suggested to contribute to the recruitment of $CD8^+$ T cells into the brain (Hansen et al. 2007).

Chemokine ligands and their receptors have roles in homeostasis and migration of immune cells to sites of inflammation. In PbA infection, chemokine receptors CXCR3 and CCR5 were

shown to be necessary for recruitment of effector $CD8^+$T cells into the brains during ECM (Campanella et al. 2008; Belnoue et al. 2003). With brain samples of mice that developed ECM containing elevated levels of their chemokine ligands CCL3/MIP1α, CCL5/ Rantes, CXCL9 and CXCL10 (Campanella et al. 2008; Van den Steen et al. 2008; Belnoue et al. 2003).

In our results we have shown that the ECM protected mice had low amounts of inflammatory chemokines CCL3 and CCL5 in their brains. This observation matched the low amount of peripheral immune cells in the brains of these mice. The lack of CCL3/ MIP1α could be as a result of low inflammatory monocytes in the brains of these ECM protected mice. Although microglia are also possible producers of these chemokines (Kohno et al. 2014), we presume that in the case of ECM, the infiltrated inflammatory monocytes are the main producers, as we observed lack of CCL3/ MIP1α only in mice that had low amounts of inflammatory monocytes in their brains. CCL5 is produced by activated T cells, macrophages and monocytes among other cells (Aldinucci & Colombatti 2014), its low levels could be associated with the low numbers of either of these cells in the brain of the ECM protected mice. These two chemokine (CCL3 and CCL5) are ligands for CCR5 and although they were lacking, some of the $CD8^+$ T cells that had infiltrated into the brains of the ECM protected *Ifnar1*$^{-/-}$ and LysM^{Cre}*Ifnar1*$^{fl/fl}$ were expressing CCR5. However, the majority of the $CCR5^+CD8^+$ T cells were co-expressing CCR7 and therefore these cells might have still been recruited via ligands for CCR7, furthermore CCR5 binds to CCL4 /MIP-1β which was not analysed. CXCR3 was expressed by the $CD8^+$T cells found in the brains of the protected Ifnar ko mice, we however suggest to analyse for the expression of CXCL9 and CXCL10/IP-10, which are both ligands for CXCR3 and linked to recruitment and migration of cells to the brain during ECM (Campanella et al. 2008). Thus, we conclude that during PbA infection, type I IFN signalling is apparently involved in recruitment of immune cells from the periphery into the brain, which secrete inflammatory cytokines and chemokines resulting in recruitment of more cells, until the cell-threshold required for pathology is attained.

4.2 Antigen specific response is un-impaired in ECM negative Ifnar ko

In priming of T cells, three signals are required, signal I is provided by interaction of MHC molecule presenting antigen and the T cell receptor, signal two is provided by the interaction of co-stimulatory molecules and the third signal by cytokines. Either IL-12 or type I IFNs provide the necessary signal 3 required for activation of $CD8^+$ T cells (Curtsinger et al. 2005). Published studies on the role of Ifnar during PbA infection showed partial but high survival,

intact BBB and reduced infiltration of cells into the brain (Palomo et al. 2013; Ball et al. 2013), however, it has not yet been shown whether protection observed occurred due to altered generation of effector $CD8^+$ T cells in the spleen. As the activation of the effector $CD8^+$ T cell occurs in the spleen before the emigration of these cells to the brain, it is paramount to show whether these cells are well primed and able to mount a parasite specific response.

We show for the first time, to our knowledge, the CTL activity of antigen-specific $CD8^+$T cells in Ifnar deficient mice during PbA-infection. In our results, we have clearly demonstrated that $CD8^+$ T cells of Ifnar ko mice were able to recognise both parasite specific endogenous antigen and transgenic Ova antigen and mount specific CTL response. We have also shown that the spleens of the Ifnar ko mice contained elevated numbers of cytotoxic granzyme-B^+CD8^+ T cell and expressed activation marker CD1lc on their surface. We further confirmed that granzyme-B was not only expressed but was equally released. We conclude that the protection from ECM was not due to generally impaired or inefficient Ag priming or CTL responses in the spleen, since the proof of their specific function strongly imply their existence.

Cerebral malaria is a T hepher-1(Th-1)-driven disease marked by high production of inflammatory cytokines IFNγ and TNF (Hunt & Grau 2003). Mice genetically deficient of Th-1 transcriptional factor T-bet are highly protected (70%) from ECM (Oakley et al. 2013). Here we have clearly detected in all the infected Ifnar deficient groups of mice the presence of Th-1 cells ($Tbet^+CD4^+$) in their spleens. Moreover, we have measured unimpaired production of Th-1 cytokines IFNγ and TNF in the spleen samples of these protected mice. However, as we observed comparable IFNγ production between the WT and infected ko mice, we did not analyse for specific cell production. We therefore cannot conclusively say which cells were the producer, as IFNγ is produced by several cells during PbA infection; $CD4^+$T cell (Villegas-Mendez et al. 2012), $CD8^+$ T (Zhao et al. 2014; Howland et al. 2013; Schumak et al. 2015), NK cells cells (Hansen et al. 2007). Strikingly, despite the presence of Th-1 cells and IFNγ, the Ifnar ko mice had concomitantly high levels of anti-inflammatory cytokine IL-10. We concluded that the high IL-10 levels could have contributed to control of the inflammation and could be one of the reason of the subsequent protection observed among the Ifnar ko. We presume that T-regs did not play a major role in the protection observed in *Ifnar1*$^{-/-}$ mice as these mice showed a similar reduction of this population as that observed among the ECM positive mice. However, we cannot completely rule out T-regs as contributors to the protection among the LysM^{Cre}*Ifnar1*$^{fl/fl}$ mice as we see that they contained more T-regs than infected WT, *Ifnar1*$^{-/-}$ and CD11c^{Cre}*Ifnar1*$^{fl/fl}$ mice. Thus, we conclude that during PbA infection type I IFN

signalling is dispensable in the development of, CTL response, Th-1 response and their related inflammatory mediators in the periphery and also confirming that the protection was not mediated by lack of or alteration of Th-1 response.

What is crucial during any infection is the ability and capacity of APCs to recognise foreign Ag, process it and effectively present it to T cells, initiating pathogen specific immune response. As we observed efficient functions of cytotoxic $CD8^+$ T cells, thereby implying proper priming as well as Th-1 cell in the spleens of all the infected mice groups, we presumed unimpaired DCs function. During *Plasmodium* infection, cDCs were shown to prime and activate $CD4^+$ T cells and $CD8^+$ T-cells, with $CD8\alpha^+$DCs priming $CD8^+$ T cells, while $CD8\alpha^{neg}$DCs and/or $CD4^+$DCs priming $CD4^+$T cell (Sponaas et al. 2006; deWalick et al. 2007; Lundie et al. 2008; Piva et al. 2012). The phenomena of decreasing frequencies of $CD8\alpha^+$ DCs in the spleen that we observed in our results, has also been observed during infection with *P. chabaudi* and was attributed to increased cell death by apoptosis (Sponaas et al. 2006). Although we observed varying expression of co-stimulatory molecules on cDCs between the ko and the WT, we presume that these differences did not play a critical role in Ag presentation. However, this is worth looking into in future experimens. Current experiments from our labs indicate that BMDCs from infected *Ifnar1*$^{-/-}$ were indeed impaired in priming $CD8^+$T cells, resulting in low production of IFNγ by antigen-specific T cells (Master's thesis Johanna Scheunemann). In view of this, more detailed ex *vivo* assays need to be performed. In our experiments we analysed B cells as APCs and not as effector cells, as so far no effector role during ECM could be attributed to this cell type (Belnoue et al. 2002). In the full Ifnar ko mice, we observed decreased percentages but increased total numbers of B cell, this difference was due to the observed splenomegaly, however, we did not pursue this population any further.

4.3 Type I IFN signalling was required for the emigration of effector cells from the spleen into the brain

Whilst we demonstrated here that the cytotoxic functions of effector $CD8^+$T cells were unimpaired, we also showed that the protection we observed was due to lack of cells infiltrating into the brain. This was apparently due to arrest/ retention of these in the spleens, contributing to the observed marked splenomegaly. Although we detected an increase in total cell numbers in all the cell population among the Ifnar ko, we considered that retention/ arrest of $CD8^+$T cells occurred as the increase in this population resulted in alteration of the

CD4:CD8 ratio in the spleen and it is well-accepted that $CD8^+$ T cells are primed in the spleen and emigrate to the brain to cause pathology in PbA-infected WT mice.

Migration of T cells out of the priming site is dependent on chemokines, chemokine receptors, intergrins, activation marker CD69, adhesion molecules and sphingosine 1-phosphate receptor type 1($S1P_1$) among other signals (Sheridan & Lefrançois 2011). As $CD8^+$T cells are the main effector cells, it was surprising to observe that the retained cells had a phenotype comparable to that of the infected WT. We confirmed that the retained cells were activated, Ag specific and cytotoxic. Secondly, we ruled out the possibility that the retention was mediated by differences in the $CD8^+$T cell phenotype, as we observed comparable expression of activation markers (ICAM-1, CD11a and CTLA-4) among the $CD8^+$T cells of the WT. We also confirmed the expression of the chemokine receptors CCR5 and CXCR3, which have been shown to be important for the recruitment of T cells from the spleen into the brain during ECM (Belnoue et al. 2003; Van den Steen et al. 2008). Moreover the mice that lacked the type I IFN receptor had more $CXCR3^+CD8^+$ T cells and $CCR5^+CD8^+$ T cells in their spleen in comparison to the infected WT mice. Importantly, the antigen specificity of these $CD8^+$T cells, expression of cytotoxic granules granzyme B, increased expression of activation markers; ICAM-1, CD11a, CTLA-4 and increased expression of chemokine receptors CXCR3, CCR5 and CCR7 strongly indicate that these cells in the spleens of the ECM protected mice were competent and might have been capable of causing pathology if they had emigrated from the spleen into the brain.

We therefore conclude that during PbA infection, type I IFN signalling on myeloid cells has a role in providing the crucial signal for the emigration of effector $CD8^+$T cells from the spleen into the brain, and in the absence of the receptor, cells are retained/arrested in the spleen. Preliminary data of spleen immunohistochemistry indicated increase in size of the white pulp among the infected *Ifnar1*$^{-/-}$ mice in comparison to the infected WT (Bachelor thesis Sarah Helow). More studies need to done to confirm whether this is active retention or the signal to emigrate is missing.

4.4 Type I IFN signalling on macrophages and inflammatory monocytes is required for emigration of cells from the spleen during PbA infection.

We show in our results a significant increase in the $CD11b^+$ populations only among infected *Ifnar1*$^{-/-}$ mice, with significant increase in both counts and percentages. When we analysed the composition of the $CD11b^+$ population, we observed low percentages of $Ly6C^{hi}CCR2^+$ inflammatory monocytes in the spleen of the mice deficient of Ifnar on all cells and specifically

on myeloid cells, however cDCs Ifnar ko mice had higher percentages of these cells. Inflammatory monocytes are recruited to sites of infection and contribute to the adoptive immune response (Shi & Pamer 2011). Recruitment of inflammatory monocytes to the site of inflammation is dependent but not limited to chemokines, chemokine receptors and adhesion molecules; CCL2, CCL3, CCL5, CCR2, CCR5, ICAM-1 and VCAM-1 (Shi and Pamer 2011). In *P. chabaudi* infection, $Ly6C^{hi}$ monocytes recruited to the spleen were shown to have a role in parasite control (Sponaas et al. 2009).

Although we observed lower percentages of $Ly6C^{hi}CCR2^{+}$ inflammatory monocytes in spleen samples of *Ifnar1*$^{-/-}$ and $LysM^{Cre}$*Ifnar1*$^{fl/fl}$, the amounts of CCL2 were comparable to the infected WT mice. Moreover, type IFN signalling via Ifnar was shown not to be required for the recruitment of inflammatory monocytes into the spleen during *L. monocytogenes* infection (Jia et al. 2009). One possible explanation of the low numbers of inflammatory monocytes in the spleens of the ECM protected mice could be that these cells are recruited to the spleen in form of monocyte precursor cells, but differentiate into suppressive macrophages subsets, resulting in an increase of the alternatively activated macrophages (AAM) that were observed among the Ifnar ko mice and which was a major finding of this thesis.

The presence of AAMs in the spleens of PbA-infected *Ifnar1*$^{-/-}$ mice has not been shown before. This was also the first time that we observed a major difference in the composition of immune effector cells between the mice lacking Ifnar specifically on myeloid cell and the complete ko. The presence of AAM was completely unexpected due to two major reasons; first, ECM is a T-helper 1 driven disease and macrophages of WT C57BL/6 mice under inflammatory conditions are polarized to M-1 classical activated macrophages (Mills et al. 2000). Secondly, considering that PbA-infection is an inflammatory disease, and the fact that we measured increased levels of M1 polarizing cytokines TNF and IFNγ in their spleens, we expected that the macrophages should ideally acquire an M1 phenotype. AAM are classified into M2a, 2b, 2c and 2d subclasses depending on the present stimulating signal, expressed genes, secreted cytokine and chemokines (Rőszer 2015). PbA-infected *Ifnar1*$^{-/-}$ mice had an M2a phenotype, demonstrated by the up-regulation of M2a hallmark genes *Relmα/Fizz1*, *YM-1*, *arg-1* and and also functional protein = arginase-1 production by $CD11b^{+}$ Cells. We also measured IL-4 production only among the *Ifnar1*$^{-/-}$ mice, which is correlated to with M2a phenotype. We did not investigate the source of the IL-4, however, we can rule out the Th-2 cells, as we did not detect presence of these cells in the spleen. One possible producer of the measured IL-4 could be type 2 lymphoid cells (ILC2), since it was recently shown that ECM

susceptible mice treated with recombinant IL-33 presented an ILC2 population capable of IL-4, IL-5 and IL-13 production that polarized macrophages to AAM and resulted in ECM protection (Besnard et al. 2015). Furthermore, eosinophils can also contribute to maintain AAMs as shown in the adipose tissue by production of IL-4 (Wu et al. 2011).

During parasitic infections, M2a macrophages are found mostly in helminth infection and have a role in tissue healing and controlling inflammation (Kreider et al. 2007). The presence of AAM and the production of high volumes of arginase-1, Relm-α and IL-10 are apparently beneficial to the PbA infected mice *Ifnar1*$^{-/-}$ mice, as these molecules have been shown to promote healing and suppress T cell activity (Murray & Wynn 2011; Rőszer 2015). Adoptive transfer of M2 macrophages into NOD mice was shown to prevent development of type I diabetes (Parsa et al. 2012). These M2 macrophages could therefore provide a balanced or neutralizing milieu and contribute to the observed protection of the PbA-infected mice from ECM.

M1 macrophages and Th-1 cells can crosstalk via chemokines, cytokines and other signals, which then drive the disease to an inflammatory outcome. The Th-1 driven inflammatory cells and cytotoxic CD8^{+} T cells in the infected WT are continuously receiving M1 signals to exit the spleen and proceed to the brain. However, in the *Ifnar1*$^{-/-}$ there are apparently mixed signals sent, with M2 macrophages providing anti-inflammatory signals associated with Th-2 to Th-1 cells, which could be resulting in the retention/arrest of the effector cells in the spleen.

The lack of M2a macrophages and low inflammatory monocytes in the spleens of the LysM^{Cre}*Ifnar1*$^{fl/fl}$ could have been due to a possibly different milieu resulting in polarized macrophages of another M2 (?) macrophage subtype. One possibility could be the M2d macrophage subtype, as we observed high levels of IL-6 as early as d+2 after infection, since IL-6 was shown to polarize macrophages to a M2d phenotype (Rőszer 2015). However, this is speculation and more experiments are needed to determine whether these cells had a different M2 phenotype, or whether they developed into regulatory macrophages (Mregs) or myeloid derived suppressor cells (MDSC). Mregs produce high levels of IL-10 and are immuno-suppressive, they do not upregulate the M2a markers, YM1, Relmα nor do they produce arginase-1 (Fleming & Mosser 2011). MDSC are also immunosuppressive, they produce high amounts of IL-10, monocyte derived MDSC express iNOS while granulocyte derived MDSC produce arginase-1 (Talmadge & Gabrilovich 2013). Nonetheless, whether it is the presence of M2, Mreg or MDSC, these cells are probably all playing a role in retention/arrest of effector cells from entering the brain and causing severe form of disease. The immunosuppressive

macrophages might have contributed to the expansion of T-regs populations observed in the spleen of these mice which was higher than in the other infected mice but lower than the naive. M2 macrophages were shown to contribute to expansion of T-regs in mice treated with recombinant IL-33 (Besnard et al. 2015). As a proof of concept, we were able to restore ECM susceptibility by the adoptive transfer of $CD11b^{+}$ cells from PbA-infected WT mice into PbA-infected $LysM^{Cre}$*Ifnar1*$^{fl/fl}$ mice. By transferring these cells, we restored the required inflammatory signalling and inflammatory milieu required to drive the disease to an ECM outcome, confirming their central position in the pathology.

4.5 Hypothesis of role of type I IFN signalling in ECM pathogenesis

In viral infections, type I IFN signalling on myeloid cells was shown to have a protective role against murine coronavirus and West Nile virus (Cervantes-Barragan et al. 2009; Pinto et al. 2014). Not only is the type I IFN receptor on myeloid cells required for protection during virus infection, a protective role during experimental autoimmune encephalomyelitis (EAE) was demonstrated in the mouse model for multiple sclerosis (Prinz et al. 2008). Furthermore, in West Nile viral infection, type I IFN signalling was shown to have a role in maintaining the integrity of the BBB (Pinto et al. 2014; Daniels et al. 2014). However, here we have demonstrated a detrimental role of type I IFN signalling on myeloid cells during PbA infection.

It has been shown that type I IFN regulates CCL3/MIP1α production, which recruits NK cells to site of inflammation, these NK then produce CXCL9 at the site of infection (Salazar-Mather et al. 2002). NK cells are involved in recruitment of T cells into the brain in a CXCR3 dependant manner resulting in ECM (Hansen et al. 2007) while $Ly6C^{hi}$ inflammatory monocytes infiltrate into the brains earlier than other leukocytes (Pais & Chatterjee 2005; Pai et al. 2014), and had a role of recruitment of $CD8^{+}$T cells, $CD4^{+}$ T cells and NK cells (Schumak et al. 2015; Pai et al. 2014). In view of this, we hypothesize that one possibility by which the type I IFN signalling contributes to ECM pathology is by signalling via the Ifnar on the inflammatory monocytes and macrophages, resulting in the release of inflammatory cytokines, chemokines and other signals that probably enable the $Ly6C^{hi}$ inflammatory monocytes to emigrate from the spleen into the brain. In the brain they release TNF, CCL3/MIP1α and other inflammatory mediators, which facilitates the recruitment of other leukocytes such as effector $CD8^{+}$ T cells into the brain, resulting in ECM pathology. In absence of the receptor, the required inflammatory signal from monocytes and macrophages is missing, polarizing these cells an immunosuppressive phenotype and resulting in retention of cells in the spleen.

4.6 Malaria tolerance is driven by IL-10 via suppression of inflammatory responses

In malaria endemic areas, older children and adults develop a form of natural acquired immunity to the disease, in which they are infected but do not develop severe forms of malaria (Langhorne et al. 2008). Using the ECM susceptible C57BL/6 WT mice, a malaria tolerance model was developed in our lab where mice were protected from ECM after infection with very high loads of parasites. The high parasite load resulted in dampening the immune response and in protection of mice from the deadly ECM outcome. Interestingly we found in the brain tissue of these experimentally infected mice the presence of $CD8^+$T cells, $Ly6C^{hi}$ inflammatory monocytes and other leukocytes. Strikingly, these mice were protected from ECM and did not develop neurological symptoms. Importantly, these mice were able to recognise parasite specific antigen and lyse the cell in their spleens but showed strongly impaired IFNγ production.

The presence of $CD8^+$T cells in the brain was shown to not necessarily result to pathology, as non-ECM *Pb* NK65 infected mice also contain T cells but do not develop ECM (Shaw et al. 2015). However, the behaviour of the T cells and whether they get arrested determines whether ECM will develop (Shaw et al. 2015). In future experiments it would be an idea to observe how the few cells that we observed in the brains of the ECM protected mice interact with the endothelial cells by use of intravital microscopy (IVM). Through the use of IVM several insights have been described in the literature including; $Ly6C^{hi}$ inflammatory monocytes are among the first cells to infiltrate the brain (Pai et al. 2014), perivascular arrest of $CD8^+$ T cells occurred only in ECM positive mice (Shaw et al. 2015) and how the destruction of BBB occurred (Zhao et al. 2014; Hoffmann et al. 2016).

In this tolerance model we also show how the parasite manipulated the host immune system, by completely blocking the production of IFNγ. The role of IFNγ has been shown to be required for ECM to develop, this was been demonstrated by its neutralization (Grau et al. 1989) and by receptor ko mice (Amani et al. 2000; Belnoue et al. 2008). Here we show that the high parasite dose was able to completely block IFNγ production and also partially suppress the Th-1 cell response, resulting in infected mice containing low amounts of T-bet expressing cells in their spleens, moreover, the expression of granzyme B by $CD4^+$T cells was completely abrogated. Granzyme-B production by $CD8^+$ T cells and NK cells were also significantly reduced in comparison to the low dose mice.

The high parasite load also resulted in suppressed expression of MHC class II of Ly6C^{hi} inflammatory monocytes in the spleen, thereby indicating altered presentation capabilities. In Toxoplasmosis, inflammatory monocytes were shown to enhance Th-1 responses (Dunay et al. 2008). Therefore, this low expression of MHC class II on Ly6C^{hi} inflammatory monocytes might have reduced their ability to prime CD4^{+}T cells and hence the reduction in the Th-1 population. Furthermore, we showed that the observed protection required IL-10 produced by myeloid cells and probably not by T-regs. We conclude that during high dose of infection, the parasite is successfully able to manipulate the host response by completely blocking IFNγ production and partially suppressing Th-1 response in the spleen. One possibility is that during high dose infection, the myeloid cells in the spleen are somehow stunned due to overwhelming PRR signalling and are unable to drive the disease to the inflammatory state required for ECM, instead produce IL-10 which creates a suppressive milieu. We were able to rule out the involvement of M2 macrophages in the suppressive phenotype acquired here, however more experiments need to be performed to determine whether other suppressive macrophage subpopulations were involved.

4.7 Conclusion and relevance

Taken together, the genetic ablation of a strong pro-inflammatory signalling pathway was sufficient to prevent brain inflammation, whereas parasite-specific immune responses in the periphery were un-impaired. Also in the malaria tolerance model, brain inflammation was attenuated, while peripheral immune responses were still generated. Hence, we were demonstrating two examples of successful immune regulation, one by the host and the second by the parasite. We would recommend more experiments to be done to establish whether the effector cells are actively retained in the spleen or the signal to emigrate is missing, and to try and establish what is that crucial signal required by these cells to exit the spleen. Analysis of the brain by histology and intravital microscopy would also be helpful in future experiments.

The results from African children living in endemic areas have already provided evidence on the benefits of lacking type I IFN signalling, as the mutation of IFNaR resulted in their protection from severe forms of malaria (Aucan et al. 2003; Ball et al. 2013). To extrapolate from this mutations and our results, we would propose further investigation on cell specific blocking of the IFNaR and only temporarily, limiting it to the period of the disease as a way of preventing severe form of malaria. From our results we would also propose using of drugs that drive macrophages to suppressive phenotype also only during the disease phase.

5 References

Aldinucci, D. & Colombatti, A., 2014. The Inflammatory Chemokine CCL5 and Cancer Progression. *Mediators of Inflammation*, 2014, pp.1–12.

Amani, V. et al., 2000. Involvement of IFN-gamma receptor-medicated signaling in pathology and anti-malarial immunity induced by Plasmodium berghei infection. *European journal of immunology*, 30(6), pp.1646–55.

Amante, F.H. et al., 2007. A Role for Natural Regulatory T Cells in the Pathogenesis of Experimental Cerebral Malaria. *The American Journal of Pathology*, 171(2), pp.548–559.

Amino, R. et al., 2006. Quantitative imaging of Plasmodium transmission from mosquito to mammal. *Nature medicine*, 12(2), pp.220–4.

Aucan, C. et al., 2003. Interferon-alpha receptor-1 (IFNAR1) variants are associated with protection against cerebral malaria in the Gambia. *Genes and immunity*, 4(4), pp.275–82.

Ball, E.A. et al., 2013. IFNAR1 controls progression to cerebral malaria in children and CD8+ T cell brain pathology in Plasmodium berghei-infected mice. *Journal of immunology (Baltimore, Md. : 1950)*, 190(10), pp.5118–27.

Baptista, F.G. et al., 2010. Accumulation of Plasmodium berghei-infected red blood cells in the brain is crucial for the development of cerebral malaria in mice. *Infection and Immunity*, 78(9), pp.4033–4039.

Belnoue, E., Kayibanda, M., et al., 2003. CCR5 deficiency decreases susceptibility to experimental cerebral malaria. *Blood*, 101(11), pp.4253–9.

Belnoue, E., Costa, F.T.M., et al., 2003. Chemokine Receptor CCR2 Is Not Essential for the Development of Experimental Cerebral Malaria. *Infection and Immunity*, 71(6), pp.3648–3651.

Belnoue, E. et al., 2008. Control of pathogenic CD8+ T cell migration to the brain by IFN-gamma during experimental cerebral malaria. *Parasite immunology*, 30(10), pp.544–53.

Belnoue, E. et al., 2002. On the pathogenic role of brain-sequestered alphabeta CD8+ T cells in experimental cerebral malaria. *Journal of immunology (Baltimore, Md. : 1950)*, 169(11), pp.6369–75.

Besnard, A.G. et al., 2015. IL-33-Mediated Protection against Experimental Cerebral Malaria Is Linked to Induction of Type 2 Innate Lymphoid Cells, M2 Macrophages and Regulatory T Cells. *PLoS Pathogens*, 11(2), pp.1–21.

Campanella, G.S. V et al., 2008. Chemokine receptor CXCR3 and its ligands CXCL9 and CXCL10 are required for the development of murine cerebral malaria. *Proceedings of the National Academy of Sciences*, 105(12), pp.4814–4819.

Carroll, R.W. et al., 2010. A rapid murine coma and behavior scale for quantitative assessment of murine cerebral malaria. *PloS one*, 5(10), pp.1–12.

Caton, M.L., Smith-Raska, M.R. & Reizis, B., 2007. Notch-RBP-J signaling controls the homeostasis of CD8- dendritic cells in the spleen. *The Journal of experimental medicine*, 204(7), pp.1653–1664.

Cervantes-Barragan, L. et al., 2009. Type I IFN-Mediated Protection of Macrophages and Dendritic Cells Secures Control of Murine Coronavirus Infection. *The Journal of Immunology*, 182(2), pp.1099–1106.

Chávez-Galán, L. et al., 2015. Much More than M1 and M2 Macrophages, There are also CD169(+) and TCR(+) Macrophages. *Frontiers in immunology*, 6(May), p.263.

Chong, S.Z. et al., 2014. CD8 T cells regulate allergic contact dermatitis by modulating CCR2-dependent TNF/iNOS-expressing Ly6C+ CD11b+ monocytic cells. *The Journal of investigative dermatology*, 134(3), pp.666–76.

Clausen, B.E. et al., 1999. Conditional gene targeting in macrophages and granulocytes using LysMcre mice. *Transgenic Research*, 8(4), pp.265–277.

Coban, C. et al., 2007. Pathological role of Toll-like receptor signaling in cerebral malaria. *International immunology*, 19(1), pp.67–79.

Couper, K.N., Blount, D.G. & Riley, E.M., 2008. IL-10: The Master Regulator of Immunity to Infection. *The Journal of Immunology*, 180(9), pp.5771–5777.

Cunnington, A.J., Riley, E.M. & Walther, M., 2013. Stuck in a rut? Reconsidering the role of parasite sequestration in severe malaria syndromes. *Trends in Parasitology*.

Curtsinger, J.M. et al., 2005. Type I IFNs provide a third signal to CD8 T cells to stimulate clonal expansion and differentiation. *Journal of immunology (Baltimore, Md. : 1950)*, 174(8), pp.4465–9.

Daniels, B.P. et al., 2014. Viral Pathogen-Associated Molecular Patterns Regulate Blood-Brain Barrier Integrity via Competing Innate Cytokine Signals. *mBio*, 5(5), pp.e01476-14-e01476-14.

Davies, L.C. et al., 2013. Tissue-resident macrophages. *Nature immunology*, 14(10), pp.986–95.

deWalick, S. et al., 2007. Cutting edge: conventional dendritic cells are the critical APC required for the induction of experimental cerebral malaria. *Journal of immunology (Baltimore, Md. : 1950)*, 178(10), pp.6033–7.

Dunay, I.R. et al., 2008. Gr1+ Inflammatory Monocytes Are Required for Mucosal Resistance to the Pathogen Toxoplasma gondii. *Immunity*, 29(2), pp.306–317.

Dunay, I.R., Fuchs, A. & Sibley, L.D., 2010. Inflammatory monocytes but not neutrophils are necessary to control infection with Toxoplasma gondii in mice. *Infection and immunity*, 78(4), pp.1564–70.

Engwerda, C.R. et al., 2002. Locally up-regulated lymphotoxin alpha, not systemic tumor necrosis factor alpha, is the principle mediator of murine cerebral malaria. *The Journal of experimental medicine*, 195(10), pp.1371–7.

Fleming, B.D. & Mosser, D.M., 2011. Regulatory macrophages: setting the threshold for therapy. *European journal of immunology*, 41(9), pp.2498–502.

Franken, L., Schiwon, M. & Kurts, C., 2016. Macrophages: Sentinels and regulators of the immune system. *Cellular Microbiology*, 18(4), pp.475–487.

Gachot, B. & Ringwald, P., 2014. Severe malaria. *Tropical medicine & international health : TM & IH*, 19 Suppl 1(3), pp.7–131.

Gazzinelli, R.T. et al., 2014. Innate sensing of malaria parasites. *Nature Reviews Immunology*, 14(11), pp.744–757.

Ginhoux, F. et al., 2010. Fate mapping analysis reveals that adult microglia derive from primitive macrophages. *Science (New York, N.Y.)*, 330(6005), pp.841–5.

González-Navajas, J.M. et al., 2012. Immunomodulatory functions of type I interferons. *Nature reviews. Immunology*, 12(2), pp.125–35.

Grau, G.E. et al., 1989. Monoclonal antibody against interferon gamma can prevent experimental cerebral malaria and its associated overproduction of tumor necrosis factor. *Proceedings of the National Academy of Sciences of the United States of America*, 86(14), pp.5572–4.

Grau, G.E. et al., 1987. Tumor necrosis factor (cachectin) as an essential mediator in murine cerebral malaria. *Science (New York, N.Y.)*, 237(4819), pp.1210–2.

Guiyedi, V. et al., 2015. Asymptomatic Plasmodium falciparum infection in children is associated with increased auto-antibody production, high IL-10 plasma levels and antibodies to merozoite surface protein 3. *Malaria journal*, 14, p.162.

Hammond, M.D. et al., 2014. CCR2+Ly6Chi Inflammatory Monocyte Recruitment Exacerbates Acute Disability Following Intracerebral Hemorrhage. *The Journal of neuroscience : the official journal*

of the Society for Neuroscience, 34(11), pp.3901–9.

Hansen, D.S. et al., 2007. NK cells stimulate recruitment of CXCR3+ T cells to the brain during Plasmodium berghei-mediated cerebral malaria. *Journal of immunology (Baltimore, Md. : 1950)*, 178(9), pp.5779–88.

Haque, A. et al., 2010. Cd4+ natural regulatory t cells prevent experimental cerebral malaria via CTLA-4 when expanded in vivo. *PLoS Pathogens*, 6(12).

Haque, A., Best, S.E., et al., 2011. Granzyme B expression by CD8+ T cells is required for the development of experimental cerebral malaria. *Journal of immunology (Baltimore, Md. : 1950)*, 186(11), pp.6148–56.

Haque, A., Best, S.E., et al., 2011. Type I interferons suppress $CD4^+$ T-cell-dependent parasite control during blood-stage Plasmodium infection. *European journal of immunology*, 41(9), pp.2688–98.

Hervas-Stubbs, S. et al., 2011. Direct effects of type I interferons on cells of the immune system. *Clinical cancer research : an official journal of the American Association for Cancer Research*, 17(9), pp.2619–27.

Hoffmann, A. et al., 2016. Experimental Cerebral Malaria Spreads along the Rostral Migratory Stream K. B. Seydel, ed. *PLOS Pathogens*, 12(3), p.e1005470.

Howland, S.W. et al., 2013. Brain microvessel cross-presentation is a hallmark of experimental cerebral malaria. *EMBO Molecular Medicine*, 5(7), pp.916–931.

Hunt, N.H. & Grau, G.E., 2003. Cytokines: accelerators and brakes in the pathogenesis of cerebral malaria. *Trends in Immunology*, 24(9), pp.491–499.

Idro, R. et al., 2010. Cerebral malaria: Mechanisms of brain injury and strategies for improved neurocognitive outcome. *Pediatric Research*, 68(4), pp.267–274.

Ishida, H. et al., 2010. Development of experimental cerebral malaria is independent of IL-23 and IL-17. *Biochemical and biophysical research communications*, 402(4), pp.790–5.

Jia, T. et al., 2009. MyD88 and Type I interferon receptor-mediated chemokine induction and monocyte recruitment during Listeria monocytogenes infection. *Journal of immunology (Baltimore, Md. : 1950)*, 183(2), pp.1271–8.

Kohno, H. et al., 2014. CCL3 Production by Microglial Cells Modulates Disease Severity in Murine Models of Retinal Degeneration. *The Journal of Immunology*, 192(8), pp.3816–3827.

Kreider, T. et al., 2007. Alternatively activated macrophages in helminth infections. *Current opinion in immunology*, 19(4), pp.448–53.

Langhorne, J. et al., 2008. Immunity to malaria: more questions than answers. *Nature immunology*, 9(7), pp.725–732.

Liehl, P. et al., 2014. Host-cell sensors for Plasmodium activate innate immunity against liver-stage infection. *Nature medicine*, 20(1), pp.47–53.

Lundie, R.J. et al., 2008. Blood-stage Plasmodium infection induces CD8+ T lymphocytes to parasite-expressed antigens, largely regulated by CD8alpha+ dendritic cells. *Proceedings of the National Academy of Sciences of the United States of America*, 105(38), pp.14509–14.

Martinez, F.O. & Gordon, S., 2014. The M1 and M2 paradigm of macrophage activation: time for reassessment. *F1000prime reports*, 6(March), p.13.

McNab, F. et al., 2015. Type I interferons in infectious disease. *Nat Rev Immunol*, 15(2), pp.87–103.

Mebius, R.E. & Kraal, G., 2005. Structure and function of the spleen. *Nature Reviews Immunology*, 5(8), pp.606–616.

Mills, C.D. et al., 2000. M-1/M-2 macrophages and the Th1/Th2 paradigm. *Journal of immunology (Baltimore, Md. : 1950)*, 164(12), pp.6166–73.

Mulder, R., Banete, A. & Basta, S., 2014. Spleen-derived macrophages are readily polarized into

classically activated (M1) or alternatively activated (M2) states. *Immunobiology*, 219(10), pp.737–45.

Murphy K. et al. 2012. *Janeway's Immunobiology*. 8th edition. Garland Science, London and New York.

Murray, P.J. & Wynn, T.A., 2011. Protective and pathogenic functions of macrophage subsets. *Nature reviews. Immunology*, 11(11), pp.723–37.

Nitcheu, J. et al., 2003. Perforin-dependent brain-infiltrating cytotoxic CD8+ T lymphocytes mediate experimental cerebral malaria pathogenesis. *Journal of immunology (Baltimore, Md. : 1950)*, 170(4), pp.2221–8.

Oakley, M.S. et al., 2013. The Transcription Factor T-bet Regulates Parasitemia and Promotes Pathogenesis during Plasmodium berghei ANKA Murine Malaria. *The Journal of Immunology*, 191(9), pp.4699–4708.

Othoro, C. et al., 1999. A low interleukin-10 tumor necrosis factor-alpha ratio is associated with malaria anemia in children residing in a holoendemic malaria region in western Kenya. *The Journal of infectious diseases*, 179(1), pp.279–282.

Pai, S. et al., 2014. Real-Time Imaging Reveals the Dynamics of Leukocyte Behaviour during Experimental Cerebral Malaria Pathogenesis. *PLoS Pathogens*, 10(7).

Pais, T.F. & Chatterjee, S., 2005. Brain macrophage activation in murine cerebral malaria precedes accumulation of leukocytes and CD8+ T cell proliferation. *Journal of neuroimmunology*, 163(1–2), pp.73–83.

Palomo, J. et al., 2013. Type I interferons contribute to experimental cerebral malaria development in response to sporozoite or blood-stage Plasmodium berghei ANKA. *European journal of immunology*, 43(10), pp.2683–95.

Parroche, P. et al., 2007. Malaria hemozoin is immunologically inert but radically enhances innate responses by presenting malaria DNA to Toll-like receptor 9. *Pnas*, 104(6), pp.1919–1924.

Parsa, R. et al., 2012. Adoptive transfer of immunomodulatory M2 macrophages prevents type 1 diabetes in NOD mice. *Diabetes*, 61(11), pp.2881–92.

Pfaffl, M.W., 2001. A new mathematical model for relative quantification in real-time RT-PCR. *Nucleic acids research*, 29(9), p.e45.

Pinto, A.K. et al., 2014. Deficient IFN signaling by myeloid cells leads to MAVS-dependent virus-induced sepsis. *PLoS pathogens*, 10(4), p.e1004086.

Piva, L. et al., 2012. Cutting edge: Clec9A+ dendritic cells mediate the development of experimental cerebral malaria. *Journal of immunology (Baltimore, Md. : 1950)*, 189(3), pp.1128–32.

Platanias, L.C., 2005. Mechanisms of type-I- and type-II-interferon-mediated signalling. *Nature reviews. Immunology*, 5(5), pp.375–86.

Prinz, M. et al., 2008. Distinct and nonredundant in vivo functions of IFNAR on myeloid cells limit autoimmunity in the central nervous system. *Immunity*, 28(5), pp.675–86.

Raes, G. et al., 2002. Differential expression of FIZZ1 and Ym1 in alternatively versus classically activated macrophages. *Journal of leukocyte biology*, 71(4), pp.597–602.

Ramos, T.N. et al., 2013. Experimental cerebral malaria develops independently of endothelial expression of intercellular adhesion molecule-1 (icam-1). *The Journal of biological chemistry*, 288(16), pp.10962–6.

Randall, L.M. et al., 2008. Cutting Edge: Selective Blockade of LIGHT-Lymphotoxin {beta} Receptor Signaling Protects Mice from Experimental Cerebral Malaria Caused by Plasmodium berghei ANKA. *J. Immunol.*, 181(11), pp.7458–7462.

Rénia, L. et al., 2006. Pathogenic T cells in cerebral malaria. *International journal for parasitology*, 36(5), pp.547–54.

Rőszer, T., 2015. Understanding the Mysterious M2 Macrophage through Activation Markers and

Effector Mechanisms. *Mediators of Inflammation*, 2015, pp.1–16.

Salazar-Mather, T.P., Lewis, C.A. & Biron, C.A., 2002. Type I interferons regulate inflammatory cell trafficking and macrophage inflammatory protein 1alpha delivery to the liver. *The Journal of clinical investigation*, 110(3), pp.321–30.

Saraiva, M. & O'Garra, A., 2010. The regulation of IL-10 production by immune cells. *Nature reviews. Immunology*, 10(3), pp.170–81.

Schofield, L. & Grau, G.E., 2005. Immunological processes in malaria pathogenesis. *Nature reviews. Immunology*, 5(9), pp.722–35.

Schofield, L. & Hackett, F., 1993. Signal transduction in host cells by a glycosylphosphatidylinositol toxin of malaria parasites. *The Journal of experimental medicine*, 177(1), pp.145–53.

Schumak, B. et al., 2015. Specific depletion of Ly6C(hi) inflammatory monocytes prevents immunopathology in experimental cerebral malaria. *PloS one*, 10(4), p.e0124080.

Sedger, L.M. & McDermott, M.F., 2014. TNF and TNF-receptors: From mediators of cell death and inflammation to therapeutic giants - past, present and future. *Cytokine and Growth Factor Reviews*, 25(4), pp.453–472.

Sharma, S. et al., 2011. Innate immune recognition of an AT-rich stem-loop DNA motif in the Plasmodium falciparum genome. *Immunity*, 35(2), pp.194–207.

Shaw, T.N. et al., 2015. Perivascular Arrest of CD8+ T Cells Is a Signature of Experimental Cerebral Malaria. *PLoS Pathogens*, 11(11), pp.1–33.

Sheridan, B.S. & Lefrançois, L., 2011. Regional and mucosal memory T cells. *Nature immunology*, 12(6), pp.485–91.

Shi, C. & Pamer, E.G., 2011. Monocyte recruitment during infection and inflammation. *Nature reviews. Immunology*, 11(11), pp.762–74.

Sponaas, A. et al., 2006. Malaria infection changes the ability of splenic dendritic cell populations to stimulate antigen-specific T cells. *The Journal of experimental medicine*, 203(6), pp.1427–33.

Sponaas, A.M. et al., 2009. Migrating monocytes recruited to the spleen play an important role in control of blood stage malaria. *Blood*, 114(27), pp.5522–5531.

Van den Steen, P.E. et al., 2008. CXCR3 determines strain susceptibility to murine cerebral malaria by mediating T lymphocyte migration toward IFN-γ-induced chemokines. *European Journal of Immunology*, 38(4), pp.1082–1095.

Stevenson, M.M. & Riley, E.M., 2004. Innate immunity to malaria. *Nature reviews. Immunology*, 4(3), pp.169–80.

Storm, J. & Craig, A.G., 2014. Pathogenesis of cerebral malaria--inflammation and cytoadherence. *Frontiers in cellular and infection microbiology*, 4(July), p.100.

Swain, S.L., McKinstry, K.K. & Strutt, T.M., 2012. Expanding roles for $CD4^+$ T cells in immunity to viruses. *Nature reviews. Immunology*, 12(2), pp.136–48.

Talmadge, J.E. & Gabrilovich, D.I., 2013. History of myeloid-derived suppressor cells. *Nature reviews. Cancer*, 13(10), pp.739–52.

Tamura, T. et al., 2011. Prevention of experimental cerebral malaria by Flt3 ligand during infection with Plasmodium berghei ANKA. *Infection and Immunity*, 79(10), pp.3947–3956.

Villegas-Mendez, A. et al., 2012. IFN- -Producing CD4+ T Cells Promote Experimental Cerebral Malaria by Modulating CD8+ T Cell Accumulation within the Brain. *The Journal of Immunology*, 189(2), pp.968–979.

White, N.J., 2014. Malaria. In *Manson's Tropical Diseases*. Elsevier Ltd, pp. 532–600.

White, N.J. et al., 2014. Malaria. *Lancet (London, England)*, 383(9918), pp.723–35.

Wilson, N.O. et al., 2010. Elevated Levels of IL-10 and G-CSF Associated with Asymptomatic Malaria in Pregnant Women. *Infectious Diseases in Obstetrics and Gynecology*, 2010, pp.1–7.

Winzeler, E.A., 2008. Malaria research in the post-genomic era. *Nature*, 455(7214), pp.751–756.

World Health Org. Malaria Fact sheet http://www.who.int/malaria/media/world-malaria-day-2016/en/.

Wu, D. et al., 2011. Eosinophils Sustain Adipose Alternatively Activated Macrophages Associated with Glucose Homeostasis. *Science*, 332(6026), pp.243–247.

Yadava, A. et al., 1996. Trafficking of Plasmodium chabaudi adami-infected erythrocytes within the mouse spleen. *Proceedings of the National Academy of Sciences of the United States of America*, 93(10), pp.4595–9.

Yañez, D.M. et al., 1996. Participation of lymphocyte subpopulations in the pathogenesis of experimental murine cerebral malaria. *Journal of immunology (Baltimore, Md. : 1950)*, 157(4), pp.1620–1624.

Zhao, H. et al., 2014. Olfactory plays a key role in spatiotemporal pathogenesis of cerebral malaria. *Cell Host and Microbe*, 15(5), pp.551–563.

Zhu, J. et al., 2011. Proinflammatory responses by glycosylphosphatidylinositols (GPIs) of Plasmodium falciparum are mainly mediated through the recognition of TLR2/TLR1. *Experimental parasitology*, 128(3), pp.205–11.

Acknowledgement

I would like to sincerely thank my supervisor and director of the institute Prof. Dr. Med. Achim Hörauf, for giving the opportunity to do my PhD in his institute and for the support.

I would like to thank Prof. Dr. Sven Burgdorf for accepting to be my second supervisor.

I would like to thank Dr. habil. Gerhild van Echten-Deckert and Prof. Dr. Michael Rapoport, for accepting to be members of my examination committee.

I would like to thank Dr. Beatrix Schumak, for her guidance and support during my thesis and for taking the time to mentor me.

I am grateful to the Deutscher Akademischer Austauschdienst (DAAD) for the scholarship during my study period here in Germany.

I want to appreciate my family for support; my mum, Vugutsa Korir Tagi, my sisters Jepkemboi, Laura and Chelangat, my brothers Davies Pokot , Dickens and Allan K. Tagi. All members of my big family and relatives!!

The Late Kipkorir Samuel Tagi for believing.

Thanks to my friends;- Peter for being a nice Pokot, Janina Küpper for being my second brain in the mornings, Mariana and all other doctoral buddies. Last but not least, thanks to all the members of AG. Schumak and members of IMMIP for support and friendship.

I thank God for this far he has brought me!